

**DESIGN AND BEHAVIOR OF A MID-RISE  
CROSS-LAMINATED TIMBER BUILDING**

BY  
CONOR LENON

A thesis submitted to the Faculty and Board of Trustees of the Colorado School of Mines in partial fulfillment of the requirements for the degree of Master of Science (Civil and Environmental Engineering)

Golden, Colorado

Date \_\_\_\_\_

Signed: \_\_\_\_\_

Conor Lenon

Signed: \_\_\_\_\_

Dr Shiling Pei  
Thesis Advisor

Golden, Colorado

Date \_\_\_\_\_

Signed: \_\_\_\_\_

Dr. John McCray  
Head Department of Civil and  
Environmental Engineering

## **ABSTRACT**

Cross-Laminated Timber (CLT) is a new engineered wood material that was introduced in the past decade as a promising candidate to build structures over 10 stories. So far, a handful of tall CLT buildings have been built in low seismic regions around the world. Full-scaled seismic shaking table tests revealed the vulnerability of this building type when resisting seismically-induced overturning. This study proposes a new analysis and design approach for developing overturning resistance for platform CLT buildings. New structural detailing is proposed to alter the moment-resisting mechanism and enable coupled action through the floor system. The method is applied to the design of a 12-story CLT building, which was evaluated numerically to assess the conservativeness of the design through system level finite element model simulations. Key words: Cross-Laminated Timber building, seismic design, Overturning, anchor tie down system

## TABLE OF CONTENTS

ABSTRACT .....	iii
LIST OF FIGURES.....	v
LIST OF TABLES.....	vii
ACKNOWLEDGEMENTS.....	ix
CHAPTER 1 HISTORY AND LITERATURE REVIEW.....	1
CHAPTER 2 THESIS APPROACH OVERVIEW.....	9
CHAPTER 3 CLT DESIGN APPROACH .....	12
3.1 Floor Sizing for Bending . . . . .	12
3.2 Floor Sizing for Vibration . . . . .	13
3.3 Wall Sizing for Vertical Loads . . . . .	14
3.4 Wall Sizing for Perpendicular to Grain Compression . . . . .	15
3.5 Wall Sizing for Fire . . . . .	15
3.6 Wall Bracket Selection for Shear Resistance . . . . .	15
3.6.1 Flexible Diaphragm Assumption . . . . .	17
3.6.2 Rigid Diaphragm Assumption . . . . .	18
3.7 Global Overturning Moment . . . . .	20
3.7.1 Global Overturning System vs Stacked Shear Wall Design . . . . .	21
3.7.2 Global Overturning Moment Calculation . . . . .	23
3.7.3 Global Overturning Moment Design Methodology . . . . .	24
3.7.4 Overturning Moment Tension Design . . . . .	27
3.7.5 Design For Coupling Action . . . . .	27
3.7.6 Shear Transfer Through CLT Panels . . . . .	29
3.7.7 Shear Transfer Through Custom Connection . . . . .	31
3.8 Lateral Wind Load Design . . . . .	32
CHAPTER 4 FULL DESIGN OF A TWELVE STORY CLT BUILDING .....	33
4.1 Properties and Assumptions . . . . .	33
4.2 Floor Sizing For Bending . . . . .	34

4.3	Floor Sizing for Vibration . . . . .	37
4.4	Wall Sizing for Vertical Loads . . . . .	38
4.5	Wall Sizing for Fire . . . . .	39
4.6	Wall Sizing for Perpendicular to Grain Compression . . . . .	39
4.7	Summary of Gravity Design Results . . . . .	40
4.8	Story Forces Determination . . . . .	40
4.9	Wall Bracket Selection for Shear Resistance . . . . .	41
4.10	Overturning Moment Compression Design . . . . .	48
4.11	Overturning Moment Tension Design . . . . .	50
4.12	Overturning Moment Shear Transfer . . . . .	51
	4.12.1 Panel and Wall Shear Transfer . . . . .	51
	4.12.2 Floor Panel Connection Design . . . . .	52
4.13	Lateral Wind Load Check . . . . .	53
CHAPTER 5 MODELING . . . . .		55
5.1	Full Model . . . . .	55
5.2	CLT Panels . . . . .	55
5.3	Connection Elements . . . . .	59
5.4	Mesh . . . . .	61
5.5	Load Cases . . . . .	61
5.6	ATS Modeling . . . . .	61
5.7	Supports . . . . .	62
CHAPTER 6 NONLINEAR STATIC ANALYSIS . . . . .		66
6.1	Global deformation . . . . .	67
6.2	ATS Rod Forces . . . . .	68
6.3	Lateral Shear Load on the Bracket Springs . . . . .	76
6.4	Floor Panel Connection Force . . . . .	77
6.5	Compression Load at Story One Bearing Walls . . . . .	78
CHAPTER 7 CONCLUSION AND NEXT STEPS . . . . .		91
7.1	Feasibility . . . . .	91
7.2	Drawbacks and Obstacles . . . . .	92
REFERENCES CITED . . . . .		93

## LIST OF FIGURES

Figure 1.1	A 5-layer CLT panel. ....	2
Figure 1.2	The Forte building. ....	4
Figure 1.3	The Stadthaus building. ....	5
Figure 1.4	The inside of the Wood Innovation and Design Center. ....	6
Figure 2.1	Wall and floor panel layouts. ....	11
Figure 3.1	Simpson Strong Tie bracket design information. ....	16
Figure 3.2	Allowable load directions. ....	16
Figure 3.3	Tributary areas for the flexible diaphragm for y-direction walls. ...	18
Figure 3.4	Free body diagram of the shear due to accidental torsion. ....	20
Figure 3.5	Global (left) and stacked shear wall (right) overturning moment. ..	22
Figure 3.6	Simple shear stack connected by coupling beams. ....	23
Figure 3.7	Location of ATS rods and compression due to lateral story forces. .	25
Figure 3.8	Simplified FBD of a CLT building. ....	26
Figure 3.9	A single 3-story ATS system. ....	28
Figure 3.10	Panel-to-panel connection. ....	30
Figure 3.11	Cross-section view of the shear connection. ....	31
Figure 4.1	Wall line labels for the x and y-direction walls. ....	42
Figure 4.2	Compression zones for x and y direction loading. ....	49
Figure 5.1	Model of a 12-story CLT building. ....	56
Figure 5.2	Model of a 12-story CLT building. ....	57
Figure 5.3	Model of a 12-story CLT building. ....	58
Figure 5.4	CLT properties used in AxisVM. ....	59
Figure 5.5	Examples of gaps and springs in the model. ....	61
Figure 5.6	y-direction lateral loading. ....	63
Figure 5.7	Steel properties used in AxisVM. ....	64
Figure 5.8	ATS rod placement. ....	65
Figure 6.1	ATS rod labels for x-direction loading. ....	66
Figure 6.2	ATS rod labels for y-direction loading. ....	67

Figure 6.3	Global deformation for load case 5 in the x-direction. ....	69
Figure 6.4	Global deformation for load case 7 in the x-direction. ....	70
Figure 6.5	Global deformation for load case 5 in the y-direction. ....	71
Figure 6.6	Global deformation for load case 7 in the y-direction. ....	72
Figure 6.7	Amplified deformation for load case 7 in the x-direction. ....	73
Figure 6.8	Story one ATS rod forces for load case 7 x-direction loading. ....	74
Figure 6.9	Story one ATS rod forces for load case 7 y-direction loading ....	75
Figure 6.10	Panel connection shears (in kips) at each interface for load case 5.	89
Figure 6.11	Panel connection shears (in kips) at each interface for load case 7.	90

## LIST OF TABLES

Table 4.1	Seismic Design Factors. ....	33
Table 4.2	CLT Properties. ....	33
Table 4.3	CLT Properties. ....	34
Table 4.4	Tabulated values used to calculate $EI_{eff}$ for 5 and 9 layers. ....	35
Table 4.5	Tabulated values used to calculate $EI_{eff}$ for 3 and 7 layers. ....	36
Table 4.6	$EI_{eff}$ for 3, 5, 7, and 9 layer floors. ....	36
Table 4.7	Tabulated values used to calculate $S_{eff}$ ....	36
Table 4.8	Factored bending strength, $M_b$ , and bending load, $M_d$ . ....	36
Table 4.9	Tabulated values used to calculate $GA_{eff}$ for 5 and 9 layers. ....	37
Table 4.10	Tabulated values used to calculate $GA_{eff}$ for 3 and 7 layers. ....	37
Table 4.11	$GA_{eff}$ for 3, 5, 7, and 9 layer floors. ....	38
Table 4.12	$l_{max}$ for 3, 5, 7, and 9 layers floors. ....	38
Table 4.13	Load in pounds on each story using 3, 5, 7, and 9 layer panels. ....	39
Table 4.14	Wall capacity and load at story 1. ....	39
Table 4.15	Tabulated values for the ELF procedure. ....	41
Table 4.16	$A_i$ and $L_i$ for X-direction wall lines. ....	42
Table 4.17	$A_i$ and $L_i$ for Y-direction wall lines. ....	42
Table 4.18	$V_{ti}$ values in kips for X-direction wall lines for each story. ....	43
Table 4.19	$V_{ti}$ values in kips for Y-direction wall lines for each story. ....	43
Table 4.20	Design shear (kips) for each x-direction wall line. ....	44
Table 4.21	Design shear (kips) for each y-direction wall line. ....	45
Table 4.22	Maximum allowed spacing (inches) for each x-direction wall line. ....	46
Table 4.23	Maximum allowed spacing (inches) for each y-direction wall line. ....	47
Table 4.24	Minimum required spacing of brackets in x and y directions. ....	47
Table 4.25	Location of end of compression zone and compression in each story. ....	50
Table 4.26	Tension in x and y direction on each story. ....	50
Table 4.27	Number of ATS rods required at each exterior wall, by story. ....	51
Table 4.28	Tabulated values used to calculate $(Ib/Q)_{eff}$ . ....	51

Table 6.1	Forces (kips) in each ATS rod for x-direction loading. ....	76
Table 6.2	Forces (kips) in each ATS rod for y-direction loading. ....	76
Table 6.3	Average shear load on the bottom and top of each story (kips). ...	80
Table 6.4	Shear (kips) on each wall line for load case 5 in the x-direction. ...	81
Table 6.5	Shear (kips) on each wall line for load case 7 in the x-direction. ...	82
Table 6.6	Shear (kips) on each wall line for load case 5 in the y-direction. ...	83
Table 6.7	Shear (kips) on each wall line for load case 7 in the y-direction. ...	84
Table 6.8	Spacing (inches) on each wall line for load case 5 in the x-direction.	85
Table 6.9	Spacing (inches) on each wall line for load case 7 in the x-direction.	86
Table 6.10	Spacing (inches) on each wall line for load case 5 in the y-direction.	87
Table 6.11	Spacing (inches) on each wall line for load case 7 in the y-direction.	88

## ACKNOWLEDGEMENTS

Dr. Shiling Pei, for providing the guidance, contacts, and expertise necessary to guide me and aid in completing this study.

Dr. Greg Kinglsey, P.E., P. Eng. of KL&A, Inc. for serving on the thesis defense committee, consistently reviewing my work, and providing necessary criticism and skepticism to ensure a complete design.

Dr. Scott Breneman, P.E., S.E. of WoodWorks, Steve Pryor of Simpson Strong Tie, and Phillip Line, P.E. of the American Wood Council for lending their collective CLT expertise to review and aid in developing the design procedure.

Dr. Jenó Balogh for his expertise and error troubleshooting for AxisVM modeling, in addition to adding features to AxisVM that were necessary for non-linear analysis of the 12-story CLT building.

Dr. Panos Kioulos and Dr. Paulo Tabares for serving on the thesis defense committee and remaining flexible with defense dates.

Scott Roman for providing continuous LaTeX support and troubleshooting.

Colonel (Retired) Paul Olsen, P.E., my uncle, for supporting, advising, and inspiring me, all while continuing to remind me of the important things in life.

## **CHAPTER 1**

### **HISTORY AND LITERATURE REVIEW**

The purpose of this study is to propose a simplified mechanistic design for a mid-rise, 12 story, CLT building for a location in North America with high seismicity, including a new solution to resist global overturning. This study will be the first full attempt at a CLT building design in the United States, with the potential to save detailing, construction, and material costs (compared to standard CLT and timber framing methods) using the newly proposed global overturning system. As the use and viability of CLT continues to grow and the cost continues to decrease, CLT projects will be beneficial in North America, as well as throughout the world, because of the highly sustainable nature of CLT as well as the potential for carbon negative projects.

Sustainable construction is one of many potential solutions to reducing global carbon emissions. As the population of the world continues to increase, new challenges are arising while at the same time old challenges are becoming more difficult to solve. One such challenge is urbanization: cities are growing rapidly, which leads to new buildings, which leads to increased CO<sub>2</sub> emissions.[1]

Tall buildings in the range of 8 to 20 stories are often used for residential and light commercial applications in modern cities, and are exclusively built with steel and concrete. Currently, steel construction accounts for 3% of global CO<sub>2</sub> emissions, while concrete accounts for 5%.[1]

A new highly-sustainable engineered wood material called cross-laminated timber (CLT) was developed in central Europe and has spread in the last two decades. CLT uses multiple layers of 1x or 2x dimension lumber, glue laminated together so that grain in each layer is perpendicular to the surrounding layers.[2] CLT panels can be manufactured to almost any size; only being limited by the size of the machines available. The CLT panels can then be pre-cut and pre-grooved into the necessary shapes and shipped to the CLT building construction site. The CLT panels are used as both floor and wall panels. An example of a CLT panel is shown in Figure 1.1.



**Figure 1.1:** A 5-layer CLT panel.[3]

The main advantage of CLT is sustainability without sacrifices - 1 m<sup>3</sup> of CLT can sequester (essentially store from the atmosphere) 1 tonne of CO<sub>2</sub>. [1] The sequestration is possible because of the long-term nature of buildings and the relatively large volume of CLT used compared to timber framing. Therefore, it is relatively easy for CLT to be carbon neutral, and in the cases of some manufacturers CLT projects can even have a negative carbon footprint, where the major carbon emissions in the entire process are during transport of the CLT panels. Normally, sustainability innovations require sacrifices in living standards, aesthetics, and schedule. CLT buildings minimize the potential for problems such as rot, pest, fungus and insect infestations by factory-drying panels to a moisture content below 12%. CLT is also a very good natural insulator and has good acoustic properties, requiring little additional treatment. [4]

Sustainable forestation is possible and being practiced in countries such as New Zealand, Japan, and Canada, among others. Additionally, CLT panels can be manufactured from smaller diameter trees, meaning there can be a faster turnover in tree cutting and growing. [1]

Construction is quick and efficient, as everything is pre-fabricated and the construction process is dry. Additionally, unlike prefabricated concrete, holes can be drilled anywhere in CLT panels and don't need to be drilled during the process of manufacturing of the CLT panels. The process works extremely well in urban environments as only conventional tools are needed, the project footprint is small, and there's very little dust and noise. The lower weight of the building also means there are

fewer demands on the foundation.[4]

Fire resistance of CLT is much better than traditional timber framing. Fire will char the exterior layers of CLT, leading to protection for the interior layers. Additionally, gypsum layers can be added to CLT panels to further strengthen the fire resistance.[5]

CLT panels are particularly strong at resisting gravity loads: the panels behave as solid wood pieces in load-bearing applications. In residential applications, there are usually enough wall lines that gravity load resistance is not the controlling factor.

The governing load case for CLT buildings in high-seismic or high-wind zones is likely to be the lateral load. Lateral loading behavior for CLT is the least understood aspect of its design, especially for multi-story CLT building systems. CLT panels are much stiffer than light-frame wood shear walls, meaning the walls themselves generally remain elastic and do not dissipate energy. Therefore, the connections require special considerations to develop ductility and dissipate energy. Failure to obtain ductility and energy dissipation leads to higher acceleration amplifications, which leads to high demands on global overturning - ie the building rocking back and forth as a whole. Global overturning is especially an issue in taller buildings.[4]

Multiple tall CLT buildings have been built overseas, including the 9-story Stadthaus apartment building in London, and the 10-story, 105' Forte Living building in Australia. The designers of Forte Living believe that 25-30 stories are possible with the same design. The Forte building was built in 38 weeks for \$11 million AUS.[6] The Forte building is shown in Figure 1.2.

The Stadthaus building was completed in 49 weeks (as opposed to 72 estimated for a similar building made of concrete) and stores 185,000 kg of carbon (opposed to emissions of 125,000 kg with the concrete design), while being comparable in cost. The timber structure itself was constructed in 27 days by four men (each working 3 days a week), while the entire project took 49 weeks total. As designers and contractors get more experience with CLT, the cost and build time will continue to be competitive for even larger scale projects.[4] The Stadthaus building is shown in Figure 1.3.

CLT buildings are also very aesthetically pleasing, as demonstrated by the 8 story, 96 ft tall Wood Innovation and Design Center in Canada. The building is not completely made out of CLT, but demonstrates the favorable aesthetics that CLT can

provide due to the decision to leave all of the structural elements (CLT panels and glulam beams and columns) visible to the end-users, shown in Figure 1.4.[1]



**Figure 1.2:** The Forte building.[7]



**Figure 1.3:** The Stadthaus building. [8]



**Figure 1.4:** The inside of the Wood Innovation and Design Center.[9]

On September 17th, 2015, the winners of the US Tall Wood Building Competition were announced. The competition awards \$1.5 million to the winning submissions to begin design work on tall CLT wood buildings. The west coast winner is the 12-story Framework Project, LLC, in Portland Oregon. The East Coast winner is 475 West 18th in New York City, with a target LEED Platinum certification, with other goals beyond what LEED requires.[10] Ideally these two buildings will be the first tall CLT buildings completed in the United States. The Framework Project is relevant to this study as seismic design will be necessary, and will be the first example of a real CLT project designed for major seismic forces.

Although most of the existing tall CLT buildings were constructed at locations with low seismicity, seismic engineering research on CLT lateral systems has been conducted by a number of researchers around the world. A number of attempts have been made to design CLT buildings with superior performance in moderate to large earthquakes, include a few full-scaled shake table tests on multi-story CLT buildings [11]. The University of Ljubljana conducted one of the first studies on lateral resistance of CLT. The study tested 15 solid CLT walls with different anchorage (connection) details and vertical load levels under monotonic and cyclic loading. The tests found

that the load-bearing capacity of CLT walls was limited by the strength of the anchorage and local failure of wood at the connections, and was increased by the presence of vertical loading.[12]

The next study by the same group tested the relationship between boundary conditions and wall resistance. It was found that the ultimate lateral strength of the wall is significantly increased if translation and rotation are restricted. Another study was then done with the intent of validating a numerical model for CLT walls with openings. It was found that openings in CLT walls that are up to 30% of the wall surface will not significantly reduce shear capacity, but will reduce the stiffness. This result confirms that panelized shear wall strength is largely controlled by the connections. Following tests included shake table tests on single-story CLT box assemblies and more single-panel tests with different arrangements and numbers of panels.[12]

Italy also conducted CLT research, beginning in the early 2000s, as part of the SOFIE project - one of the most comprehensive seismic performance studies of CLT systems to date. The SOFIE project included connection tests, CLT panel shear wall tests, and multiple full-scaled building system tests. Many of the tests attempted to improve on realism of the models, including shake table tests of three configurations of a one-story building with a realistic floorplan, doors, and windows. The one story assembly was found to retain the stiff but ductile characteristics expected of CLT buildings.[12]

A 3-story building was tested in order to determine the q-factor for Eurocode 8. The building was subjected to 15 ground motions, with only minor repairs between tests. The building remained standing, with the damage being concentrated to the hold-down connections for the CLT walls. The study determined that most earthquake damage will occur at the connections, with CLT panels remaining mostly elastic. Panelized CLT walls will develop ductility primarily through connections deformation. The major point of concern is the significant uplift resistance that is required on the anchor system and lower floors.[12]

A 7-story building was tested at the conclusion of the SOFIE project. During the tests, some damage occurred to the hold-down elements at the lower stories, which confirms the findings from the 3-story test that overturning resistance is a major

concern. After 10 tests, there was no displacement in the building, however high floor accelerations were measured at the top stories.[12]

Other studies have also been conducted to define CLT characteristics. It was found that panelized CLT walls (where the height is similar to the width) will rock about their corners and cause uplift and shear forces on the connections, while long wall panels (with a low height-to-length ratio) will be unable to rock and therefore subject the connections to pure shear. CLT panels can be modeled using shell or block elements with consideration for nonlinear effects such as contact, friction, and connection hysteresis. To this date, a full real collapse of a CLT building has not been observed. There is still research to be done, such as understanding panelized wall behavior in realistic 3D building configurations, developing a system to quantify CLT system damage and damage to nonstructural components, performance-based seismic design options, and lateral force resisting systems for large earthquakes.[12]

CLT is a promising material for achieving seismically resilient tall buildings, but currently there is no widely accepted approach for tall CLT building design for seismic regions in the U.S.

In this study, the discussion is limited to panelized tall CLT construction, in which long CLT panels serve as both the LFRS and gravity load bearing components. A good example for this construction style is the Stadthaus Building in London. Unlike a tall building with a concentrated core for LFRS surrounded by gravity frame on the exterior, panelized CLT buildings typically have smaller rooms and are more suitable for residential applications. In a traditional lateral design of multi-story building with shear wall systems, the lateral force demand is distributed to each designated shear wall line in the building floorplan. Next the individual shear wall stacks are designed for shear and overturning resistance.[4] This study presents an alternate view of the lateral force transferring mechanism in a panelized CLT building and develops a method to design and size overturning restraining system based on building global overturning demand.[12] The proposed approach seeks to simplify the construction of panelized tall CLT construction and provide good reliability for such buildings against overturning, which was identified by many experimental studies to be one of the greatest challenges of tall CLT construction.

## **CHAPTER 2**

### **THESIS APPROACH OVERVIEW**

The purpose of this study is to propose a simplified mechanistic design for mid-rise, 12 story, CLT building design for a location in North America with high seismicity, including a new solution to resist global overturning.

A CLT Building must be designed for all load cases present in ASCE 7-10.[13] Vertical loads are resisted by the bending strength of the CLT floor panels and the bearing strength of the CLT wall panels. Lateral loads are resisted by connector brackets with wood screws. The brackets are sized based on the worst-case scenario for a rigid and flexible diaphragm assumption. Overturning moments due to the lateral loads are resisted by the bearing strength of the CLT wall panels and the tensile strength of the Anchor Tie-Down System (ATS). The ATS is made up of steel rods surrounding the outside of the building in order to provide resistance to the tensile force due to the overturning moment. A specialized connection is designed to allow for transfer of shear forces across the building. In order to determine the seismic loads on each story, the equivalent lateral force procedure from ASCE 7-10 is used with an assumed R factor.

The 2015 NDS does recognize CLT as a structural material, but it does not contain enough information to conduct a full seismic design for CLT buildings. Nonetheless, applicable provisions from the NDS CLT chapter are used in this study to develop the design approach, while most of the additional information needed is obtained from The CLT Handbook.[14] Load resistance factor design (LRFD) is used. Although ASD is very widely used for wood design, the NDS is moving towards LRFD.[15] Note that the CLT handbook uses a general process that can then be multiplied by the applicable factors for LRFD or ASD. Therefore, some equations may appear to be ASD equations when they can also be used as LRFD equations, as long as the equations are multiplied by the appropriate LRFD factors.

A 12-story building is designed, as it is at the upper height-limit of the current CLT buildings and the definition of mid-rise residential structures. The floorplan is loosely modeled off of the Stadthaus CLT apartment building in the Murray Grove neighborhood of London. The floorplan used in this study is larger than the Stadthaus

floorplan due to the use of 12 stories in the study, compared to the 9-story Stadthaus. The wall line locations used in this study are shown in Figure 2.1a. The floor panel layout is shown in Figure 2.1b.

The floorplan features a 70' by 70' base, with two stairwells and four elevators located in the center of the building. There are four symmetrical apartment units. The four elevators can be split to access the bottom half or the top half of the building. Unused elevator shafts on the top half can be converted to storage space. The floor panels are divided to have a maximum side length of 35', and placed in a staggered pattern such that there is no continuous gap in the x-direction.

After the design is complete, the building is modeled and loaded using the design lateral forces through a nonlinear static analysis using a generalized finite element package, AxisVM.[16] The finite element model analysis results are compared with the simplified design calculation to quantify the accuracy of the design.



## CHAPTER 3

### CLT DESIGN APPROACH

The required steps for design are detailed in the following sections. The first step is the initial sizing of the CLT panels in the building, which will be used for both the wall and floor panels. The initial panel sizes are based on the strength and serviceability requirements. The vertical loads consist of the LRFD loads from Load Cases 1-7 from ASCE 7-10. The lateral loading is determined using the Equivalent Lateral Force (ELF) procedure from ASCE 7-10 Chapter 12. The load combinations considered in this study are LRFD Load Case 1 through Load Case 7.

#### 3.1 Floor Sizing for Bending

Floor size for CLT can be controlled by bending strength or vibration. The bending loads are obtained from ASCE 7-10 LRFD Load Combinations 1 and 2. Load Case 3 is not considered live roof load is taken to be the same as the live load, and the snow and rain loads will be less than the live load.

$$LC1 \quad 1.4D \tag{3.1}$$

$$LC2 \quad 1.2D + 1.6L \tag{3.2}$$

The combination of loads is used to determine the maximum moment in the floor panel using a one-way slab assumption assuming a propped cantilever. The propped cantilever accounts for the pin-like behavior at the exterior walls due to lack of support from continuation of the CLT floor panel. The maximum moment is given as:

$$M_d = \frac{w \times l^2}{8} \tag{3.3}$$

Where  $M_d$  is the maximum moment in  $\frac{lbft}{ft}$ ,  $w$  is the load per square foot from the LRFD load combinations, and  $l$  is the floor span of the short direction of the longest slab in the building, which is 15.5 ft in this case.

Chapter 10 of the NDS and Chapter 3 of the CLT Handbook are used to determine the bending strength of the CLT panels. The bending strength is given as:

$$M_b = F'_b S_{eff} \quad (3.4)$$

Where  $M_b$  is the unfactored bending strength,  $F'_b$  is the allowable bending stress of the CLT panel, and  $S_{eff}$  is given as:

$$S_{eff} = \frac{2EI_{eff}}{E_1 h} \quad (3.5)$$

Where  $EI_{eff}$  is the effective bending stiffness,  $E_1$  is the modulus of elasticity of the outermost layer, and  $h$  is the thickness of the whole CLT panel.  $EI_{eff}$  is given as:

$$EI_{eff} = \sum_{i=1}^n E_i b_i \frac{h_i^3}{12} + \sum_{i=1}^n E_i A_i z_i^2 \quad (3.6)$$

Where  $E_i$  is the modulus of elasticity of layer  $i$ ,  $b_i$  is 12 inches (assuming a 1 ft wide section is being designed),  $h_i$  is the thickness of layer  $i$ ,  $A_i$  is the cross-section area of layer  $i$ , and  $z_i$  is the distance from the centroid of the CLT panel cross-section to the centroid of layer  $i$ . Note that for layers 2 and 4, the bending orientation is in the minor axis. Because of the minor-axis bending, the modulus of elasticity of layers 2 and 4 is assumed to be the minor strength modulus of elasticity divided by 30, per APA PRG 320.

$M_b$  must be multiplied by a product-standard reduction factor of 0.85 (per the CLT Handbook Chapter 2.1.1 equation 2), a format conversion factor of 2.54, a bending factor of 0.85, and a lambda factor (per NDS Table 10.3.1):

$$M_b \times 0.85 \times 2.54 \times 0.85 \times \lambda \quad (3.7)$$

Where  $\lambda$  is 0.6 if Load Case 1 is used, and 0.8 if Load Case 2 is used.

### 3.2 Floor Sizing for Vibration

The vibration design is done in accordance with Chapter 7, Section 3 of the CLT Handbook. The maximum span is given as:

$$l_{max} = \frac{1}{12.5} \frac{(EI_{app})^{0.293}}{(\rho A)^{0.122}} \quad (3.8)$$

Where  $l_{max}$  is the maximum span,  $EI_{app}$  is the apparent stiffness in the span direction,  $\rho$  is the density of the CLT (multiplied by a factor of 1.0625), and  $A$  is the cross-section area of a 1 ft wide CLT section.  $EI_{app}$  is given as:

$$EI_{app} = \frac{1}{\frac{1}{EI_{eff}} + \frac{11.52}{GA_{eff}(12l)^2}} \quad (3.9)$$

Where  $l$  is the design span, which is the longest span in the short direction of an unsupported area of CLT floor panel.  $GA_{eff}$  is given as:

$$GA_{eff} = \frac{a^2}{\frac{h_i}{2G_1b} + \sum_{i=2}^{n-1} \frac{h_i}{G_1b} + \frac{h_n}{2G_1b}} \quad (3.10)$$

Where  $a$  is given as 5.5 and  $G_1$  is given as  $\frac{E_{major}}{16}$  for the major direction, and  $\frac{E_{minor}}{160}$  for the minor direction.

Therefore, if  $l_{max} > l$ , the design is adequate for vibration.

### 3.3 Wall Sizing for Vertical Loads

The wall size will depend on the ability of the wall to resist compression and buckling. Additionally, the size of the wall will control the perpendicular to grain compression stress on the floors. The wall capacity in psi is given as:

$$F'_c = F_c^* C_p \quad (3.11)$$

Where  $F_c^*$  is the major-axis allowable compression stress of the CLT multiplied by all NDS factors except the  $C_p$  factor.  $C_p$  is the stability factor.  $F_c^*$  is given as:

$$F_c^* = F_c * 2.4 * 0.9 * \lambda \quad (3.12)$$

Where 2.4 is the format factor, 0.9 is the resistance factor, and  $\lambda$  is 0.6 if Load Case 1 was used, 0.8 if Load Case 2 was used, and 1 with any other load case. The  $C_p$  factor is given as:

$$C_p = \frac{1 + (P_{cE}/P_c^*)}{2c} \sqrt{\left(\frac{1 + (P_{cE}/P_c^*)}{2c}\right)^2 - \frac{(P_{cE}/P_c^*)}{c}} \quad (3.13)$$

Where  $P_c^* = F_c^* A_{//}$ ,  $c$  is 0.9 for CLT, and  $P_{cE}$  is given as:

$$P_{cE} = \frac{\pi^2 EI'_{app-min}}{l^2} \quad (3.14)$$

Where  $l$  is the wall height, and  $EI'_{app-min} = 0.5184EI_{app}$

### 3.4 Wall Sizing for Perpendicular to Grain Compression

The bearing capacity of a CLT floor panel is given as:

$$F_{c\perp}A_{\perp} \tag{3.15}$$

Where  $F_{c\perp}$  is the perpendicular to grain allowable bearing stress, multiplied by a format factor of 1.67 and a resistance factor of 0.9, and  $A_{\perp}$  is the cross-sectional area of the wall that is bearing on the floor, assuming a 1-foot long section of wall. Bearing load is given as the load on the story (in pounds) divided by the total wall length of the story.

Because the vertical loads will not govern the wall sizes, the tributary areas are not considered. If a more accurate calculation of wall loading is required, tributary areas should be used.

### 3.5 Wall Sizing for Fire

One benefit of CLT over timber framing is fire resistance - in the event of a fire, there will be a charred layer of CLT. 3-layer panels can reach fire class F-30, meaning they will retain structural integrity for at least 30 minutes in a fire.[4] In the Stadthaus project, 5-layer panels are used to obtain a fire protection class of F 60.[4] Because in-depth design for fire resistance is outside the scope of this project, a minimum of 5-layer thick panels are used for walls and floors.

### 3.6 Wall Bracket Selection for Shear Resistance

Simpson Strong-Tie brackets with wood screws are used to connect floor panels to wall panels. The design strength of the connectors are determined based on the January 1, 2015 Simpson Strong-Tie memo titled “Connectors for Cross-Laminated Timber Construction”.[17] Using screws, the ABR9020 bracket has an allowable shear stress of 1480 lbs for ASD, and is 2 9/16” long. The ABR105 bracket has an allowable shear capacity of 1880 lbs for ASD, and is 3 9/16” long. The bracket information is given in Figure 3.1 and Figure 3.2 . Because story shears are very large for the 12-story building, ABR 105 brackets will be used. Because the Table values are given for ASD, they must be converted to LRFD. In ASCE 7-10 section 12.4.2.3, a multiplier of 0.7 is used to convert the seismic loading to ASD from LRFD. In order to keep the

demand/capacity ratio for seismic loading consistent between ASD and LRFD, the ASD connector strengths are increased by  $1/0.7 = 1.43$ . Therefore, the LRFD allowable shear capacity for ABR105 brackets is  $1880 * 1.43 = 2688$  lbs.

Model ID	Gauge	Dimensions (in.)			Fastener Schedule				Allowable Load (lbs.), $C_D = 1.60$			
		$W_1$	$W_2$	L	Horizontal Leg		Vertical Leg		$F_1$	$F_2$	$F_3$	$F_4$
					Quantity	Type	Quantity	Type				
ABR9020	14	$3\frac{7}{16}$	$3\frac{7}{16}$	$2\frac{9}{16}$	10	CNA4x60	10	CNA4x60	1085	780	1330	590
					10	SD10212	10	SD10212	1480	1200	1330	1010
ABR105	11	$4\frac{1}{8}$	$4\frac{1}{8}$	$3\frac{9}{16}$	14	CNA4x60	10	CNA4x60	1350	835	2300	1020
					14	SD10212	10	SD10212	1880	1235	2300	1475
AE116	11	$3\frac{9}{16}$	$1\frac{7}{8}$	$4\frac{9}{16}$	7	CNA4x60	18	CNA4x60	1720	1225	1550	650
					7	SD10212	18	SD10212	1850	1445	1850	1035

**Figure 3.1:** Simpson Strong Tie bracket design information.

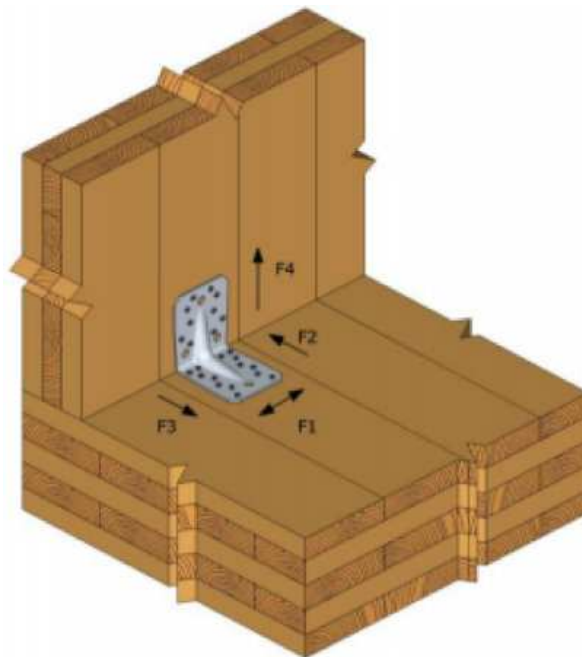


**Figure 3.2:** Allowable load directions.

Next, the available wall length must be determined in order to determine the unit shear demand in the wall. The calculated ELF shear was applied in both the x and y directions. The number of brackets in each wall line is determined by the total wall line shear demand and the length of the available wall length that can be used to install the connectors. Brackets can be attached to both sides of interior walls, and can be attached to the internal side of exterior walls.

Given the total story shear from the ELF method, the shear demand for each wall line can be determined using either a flexible or rigid diaphragm assumption. The flexible diaphragm assumption assumes that each wall line will take a portion of the story force proportional to the tributary area of the wall line. The rigid diaphragm assumption assumes that each wall line will take a portion of the story force proportional to the relative stiffness of the wall line. Because the exterior walls can only have brackets on the interior side, the exterior walls will have half of the stiffness of the interior walls. Because currently there is no well-recognized approach to determine whether a CLT diaphragm is rigid or flexible, the design in this study will consider both the rigid and flexible diaphragm assumptions to bound the final design. Therefore, regardless of how the diaphragm behaves, the design should be conservative.

### 3.6.1 Flexible Diaphragm Assumption

The tributary areas are obtained by equally dividing the floor area between each wall line. For example, if a wall had two walls running parallel to it, one 4' away and one 5' away, the tributary width would be 4' divided by 2 plus 5' divided by 2, which is 5.5'. The tributary area would then be the tributary width times the length of the building in each direction. The tributary areas for the y-direction walls are shown in Figure 3.3. The shear demand for each wall is therefore given as:

$$V_i = \frac{A_i}{\sum A} V_x \quad (3.16)$$

Where  $V_i$  is the shear on wall line  $i$ ,  $A_i$  is the tributary area of wall line  $i$ ,  $\sum A$  is the total area of the floorplan, and  $V_x$  is the story shear. The required spacing for each wall line is determined using equation 3.17.

$$s = V_n / \left( \frac{V_i}{L_i} \right) \quad (3.17)$$

Where  $s$  is the center-to-center spacing of the brackets, and  $V_n$  is the shear strength of the brackets.  $L_i$  is the length of wall line  $i$  that is available to brackets, and therefore counts interior walls as double their actual length.

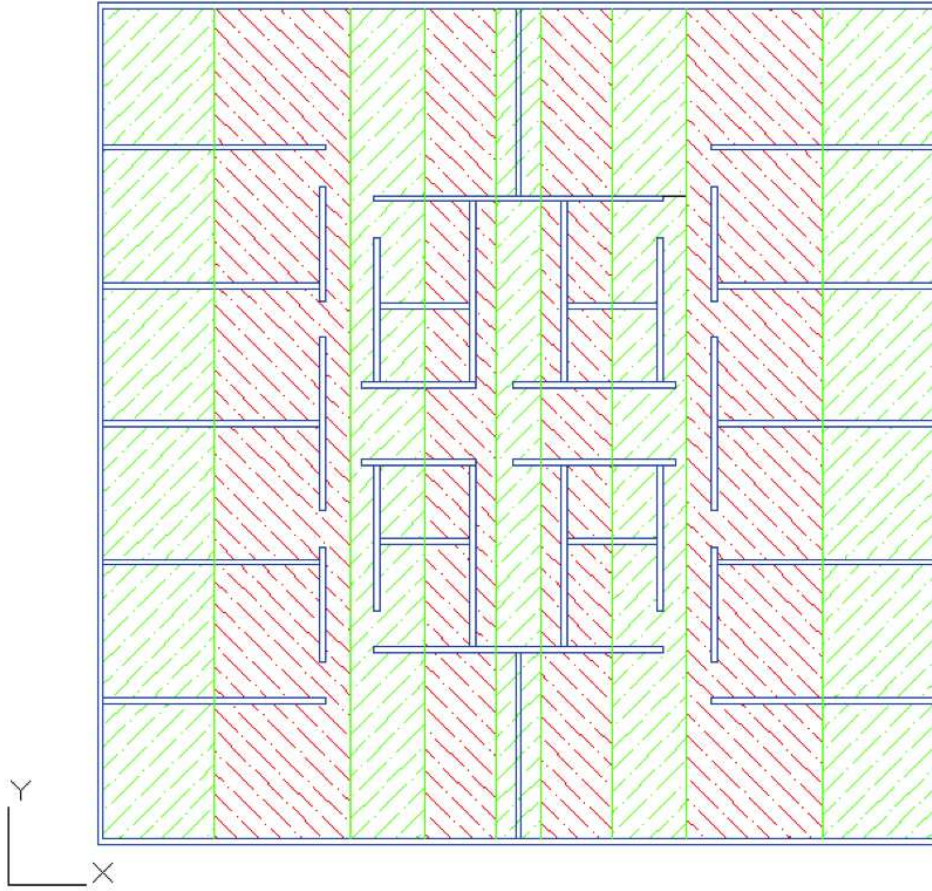


**Figure 3.3:** Tributary areas for the flexible diaphragm assumption for y-direction walls.

### 3.6.2 Rigid Diaphragm Assumption

Using the rigid diaphragm assumption, the stiffness of the wall lines need to be determined first. In this study, it is assumed that the wall line stiffness is proportional to the length of the wall lines. Furthermore, the floorplan is largely symmetric in both directions, thus the eccentricity is assumed to be zero and the story force on each wall line is given as:

$$V_i = \frac{L_i}{\sum L} V_x \quad (3.18)$$

Where  $V_i$  is the shear on wall line  $i$ , and  $L_i$  is the length of wall line  $i$ .  $\sum L$  is the total wall length available to brackets, and therefore counts the interior walls as double their actual length.  $V_x$  is the story shear. The required spacing for each wall line is determined using equation 3.17.

$$s = V_n / \left( \frac{V_i}{L_i} \right) \quad (3.19)$$

Where  $s$  is the center-to-center spacing of the brackets,  $V_n$  is the shear strength of the brackets,  $V_i$  is the shear on wall line  $i$ , and  $L_i$  is the available wall length for brackets of wall line  $i$ . By substituting equation 3.18 into equation 3.19, it is found that the bracket spacing will be uniform throughout the story:

$$s = V_n / \left( \frac{V_x}{\sum L} \right) \quad (3.20)$$

Note that the spacing applies to one side of a wall. Therefore, interior walls will have brackets spaced at  $s$  on each side of the wall, while the exterior walls will have brackets spaced at  $s$  on only the interior sides. It should also be noted that brackets will be required on both the top and bottom of the walls in order to ensure shear transfer.

The rigid diaphragm assumption also includes accidental torsion caused by locating the center of mass 5% of the length of the building away from the center of stiffness. In this study, the accidental torsion is considered approximately by increasing and decreasing the shear demands at the symmetric wall lines about the center of rigidity of the building. The decrease is proportional to the distance that the wall line is from the center of stiffness, and the stiffness is proportional to the length of the wall line. Therefore the share of shear that each wall line gets will be proportional to the moment arm from the center of rigidity (not where the story shear acts), as well as the  $L_i$  value of that shear wall.

The free body diagram of the accidental torsion is shown in Figure 3.4. Note that the accidental torsion forces,  $V_{ti}$ , only resist the accidental torsion moment caused by  $V_x$ . The accidental torsion forces do not resist the  $y$ -direction loading caused by  $V_x$ ; these forces are resisted by the shear forces on the wall determined in equation 3.18. Therefore, the free body diagram satisfies equilibrium for moment, but does not satisfy equilibrium for sum of forces in  $y$  unless the shear forces on the walls are added in to the diagram.

The total moment that must be resisted by the 5% accidental torsion is given as:

$$V_x L_{0.05} = \sum_{i=1}^n V_1 \frac{L_i l_i}{L_1 l_1} l_i \quad (3.21)$$

Where  $V_x L_{0.05}$  is the moment caused by accidental torsion,  $V_1$  is the shear at the first wall line (furthest from the center of rigidity),  $\frac{L_i l_i}{L_1 l_1}$  is the ratio of  $V_{ti}$  to  $V_1$  where  $i$  is the wall line, and  $l_i$  is the moment arm measured from the center of rigidity.  $V_1$  can be solved from equation 3.21, then  $V_i$  for the remaining wall lines can be solved using the ratio:

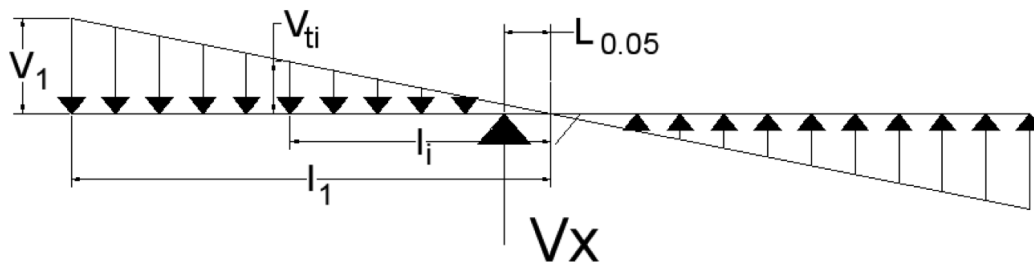


**Figure 3.4:** Free body diagram of the additional shear due to accidental torsion.

$$\frac{V_{ti}}{V_1} = \frac{L_i l_i}{L_1 l_1} \quad (3.22)$$

$V_{ti}$  is the shear caused by the moment due to accidental torsion. Using superposition, the  $V_i$  can be added back into the shear on each wall. The shear on each wall is related to the stiffness and deflection of each wall line.

Because bracket spacing is no longer uniform throughout the story due to accidental torsion, the new equation for spacing will be a modification of equation 3.19:

$$s = V_n / \left( \frac{V_x \pm V_{ti}}{L_i} \right) \quad (3.23)$$

Where  $V_{ti}$  is the shear due to accidental torsion. Note that depending on the direction of displacement of the center of mass, one side of the building will have a reduction in required spacing while the other side will increase. Because accidental torsion can happen in either direction, the reduction in required spacing should be used on all shear walls.

### 3.7 Global Overturning Moment

The purpose of the Anchor Tie-Down system (ATS) is to resist the tensile forces on the walls caused by the overturning moment that exists due to the lateral

seismic loads. The compressive forces are resisted by the compression strength of the CLT panels.

### 3.7.1 Global Overturning System vs Stacked Shear Wall Design

Traditionally, global overturning is dealt with by designing each shear wall stack to resist its own local overturning. Global overturning can be defined as the tendency of the entire building to overturn as one piece as a result of earthquake loading. As shown in Figure 3.5, a building has 3 shear wall segments and can be viewed in two ways with respect to overturning resistance.

The first method assumes that each shear wall segment will resist a portion of the overturning moment, where the lateral seismic load is evenly distributed between the shear wall segments. Each segment will experience compression and tension due to the moment, where the tension is resisted by the tie-down system in each segment. This method is called the stacked shear wall method, and is the traditional method used.

The second method assumes that the building will overturn globally - ie, the moment due to overturning will span the base of the entire building, instead of being distributed to the individual shear walls. This assumption relies on the building being rigid, as that is the only way the building can overturn as one unit. The tension due to the overturning moment will be resisted by a tie-down system at the edge of the building, while the shear walls at the other end will resist the compression.

The assumption of rigidity is contingent on the ability of the building to transfer shear in the vertical direction between different shear wall stacks. This concept is essentially identical to the couple shear wall / frame system used in steel and concrete construction. In traditional wood construction, it is very difficult to transfer vertical shear because the floor system in light-frame wood construction is mainly made of i-joists. As a result, the individual shear wall stacks have to be tied-down individually in order to resist overturning. The robustness of the CLT construction and floor itself provide an opportunity to utilize the global overturning model, however the detailed calculation and design approach must ensure that the correct demands be considered when designing the floor and wall details of such buildings.

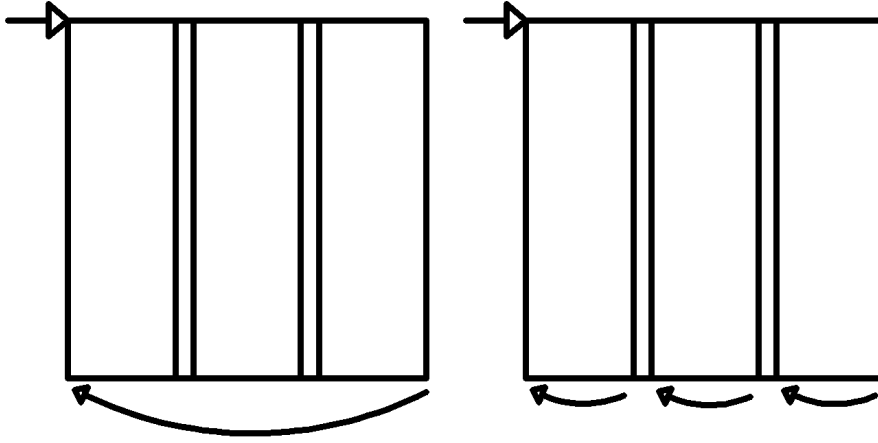


**Figure 3.5:** Global (left) and stacked shear wall (right) overturning moment.

Consider a simple example of 2 isolated shear wall stacks connected by coupling beams shown in Figure 3.6. A simple lateral earthquake load of magnitude  $P$  can be assumed to be acting on the top left corner of the building. In the case of local overturning, each of the two shear wall stacks will experience a lateral load of  $\frac{P}{2}$  acting at a height of  $H$ , giving a moment of  $\frac{PH}{2}$  at the base of each shear wall stack. The restoring moment due to the weight must also be subtracted, giving  $\frac{PH}{2} - \frac{WS}{2}$ , where  $S$  is the width of each shear wall stack. The tie-down system will have to resist the tension caused by the moment about the compression corner (which is the bottom right corner), where the tension is given by  $(\frac{PH-WS}{2})/s$ . The best-case scenario for moment resistance would be the shear wall stacks each accounting for half the length of the building, which would give a tie-down force of  $\frac{PH-W(L/2)}{2}/(L/2)$  at each stack, or simplified to  $\frac{PH}{L} - \frac{W}{2}$ .

If the building is assumed to be rigid, the total moment will be  $PH - 2\frac{WL}{2}$ , and the total tension force that must be resisted by the tie-down system will be  $\frac{PH-WL}{L}$ , or simplified to  $\frac{PH}{L} - W$ . Therefore, the isolated shear walls will actually have to resist more tension force in total than the global overturning tie-down system. Additionally, in the global overturning case there will only be one tie-down system at the end of the building, while in the isolated shear wall case a tie-down system is necessary at each shear wall. Note that this design is also only for one direction, when all four considered earthquake directions (+x, -x, +y, -y) must be accounted for. Therefore, as long as the global overturning method is validated, by using it there will be savings in terms of material, detailing, and construction time due to the reduction of necessary tie-down

elements.

In order for the global overturning assumption of rigidity to be valid, the floor panels between shear wall stacks must be able to act as coupling beams to transfer the out of plane shear between the shear wall stacks. The floor panel itself can transfer both shear and moment, but it is not continuous in one direction of the floorplan. Thus special connections must be implemented on the floor diaphragm panel interface to carry over the shear force. At mid-point between the two shear wall stacks, there is an inflection point for coupling. By placing the connections between the floor panels at the points of inflection, the connections only need to be designed for shear. The connections are placed at the points of inflection because they are weak points in the system; the floor panels and shear walls will be able to resist the moment and shear demands imposed elsewhere.

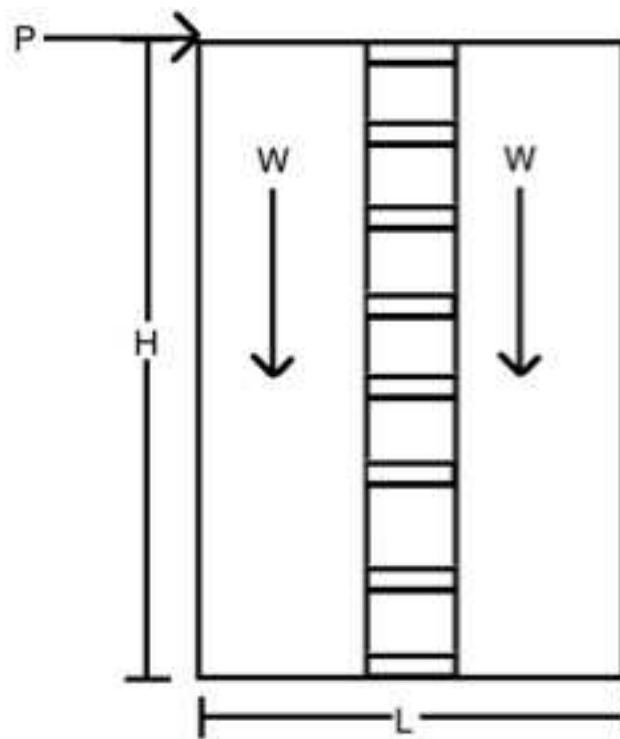


**Figure 3.6:** Simple shear stack connected by coupling beams.

### 3.7.2 Global Overturning Moment Calculation

The overturning moment due to the seismic load is calculated using the story forces calculated during the ELF procedure. The equation for the overturning moment

at story  $i$  is given by:

$$M_i = \sum_{j=1}^n Fx_j(H)(j - i + 1) \quad (3.24)$$

Where  $Fx_j$  is the story force at story  $j$ ,  $H$  is the story height, and  $(j - i + 1)$  is the number of stories between story  $i$  and story  $j$ . Equation 3.24 assumes that the moment is being summed from the lowest point of the wall, because that is where the maximum moment arm will be between story  $i$  and  $j$ . This means that for story 1, the moment will be summed for the ground floor of the building, and for story  $n$  (the stop story), the moment will be summed from the elevation of story  $n-1$ .

### 3.7.3 Global Overturning Moment Design Methodology

Traditionally, the overturning demand is calculated based on shear wall stacks assumed to be isolated from the building, and then resisted by hold-down or tie-down systems. Recent full-scale shaking table tests of multi-story building structures[11] observed that most of the tie-down demand and damage is caused by the global overturning (ie the entire story generating overturning moment as a cantilever beam). In this study, we will explore a new design approach for Anchor Tie-Down systems using global overturning.

The concept is shown in Figure 3.7. The overturning moment will be resisted by the tie-down system in tension and the CLT walls in compression on the other side of the floorplan. The design process will start by assuming that only the far side CLT wall line will resist compression (shown in Figure 3.7), then iteratively add more interior walls into the compression zone until the walls in compression are able to resist the compression demands imposed by the overturning moment.

The overturning moment will cause both compressive and tensile forces in the building, in addition to shear throughout the building. A free-body diagram is shown in Figure 3.8. It is assumed that the building will tip about point B, meaning compression forces will be concentrated at the exterior walls near point B, and tension will be concentrated at the ATS rods at point A. The weight is a combination of the dead load and live load, obtained from load combinations 5 and 7. The most exterior wall at point B is assumed to reach the capacity for perpendicular to grain compression,  $C_{crush}$ , before the next most exterior wall is engaged in compression. A wall in compression has

two components of compression from superposition:  $C_g$  and  $C_f$ .  $C_g$  is the evenly distributed wall load due to the weight,  $W$ . Therefore,  $\sum C_g = W$ .  $C_f$  is the remaining compression that must be applied to the wall in order for failure due to crushing to occur.  $C$  is the residual compression obtained when enough wall lines are used to fully resist the compression due to load cases 5 and 7. Note that this model assumes the entire building is rigid, and therefore shear forces must be able to be developed throughout the building.

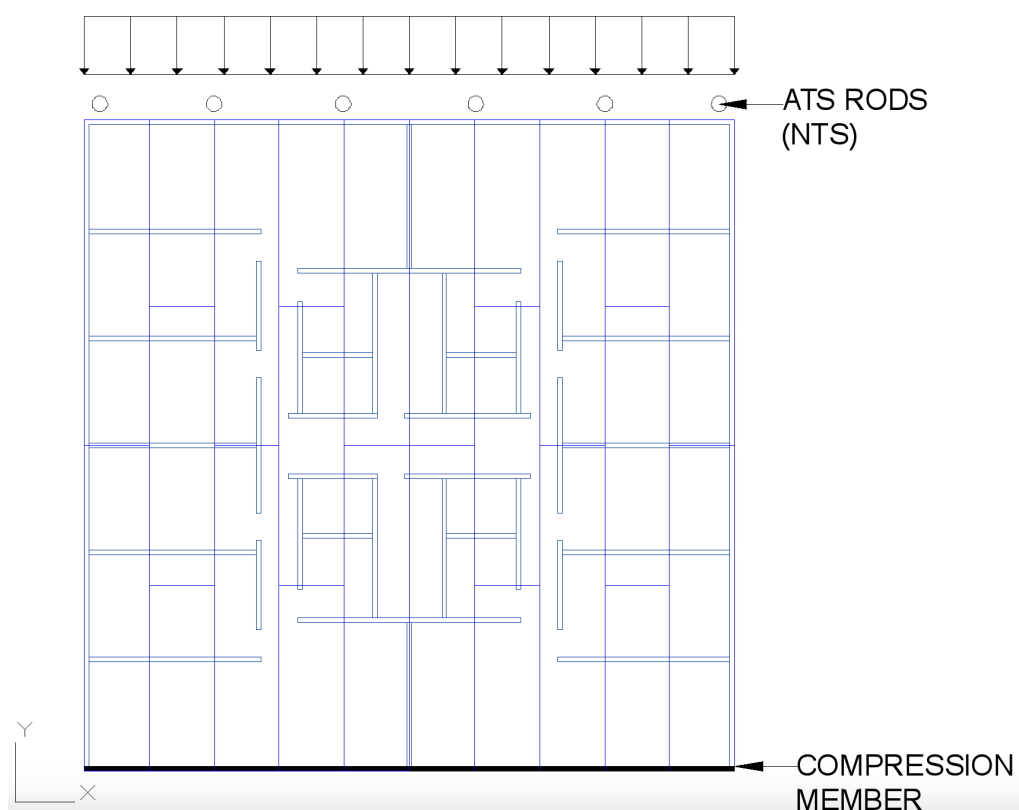


**Figure 3.7:** Location of ATS rods and compression due to the lateral story forces.

The process to determine the tension and compression to resist the overturning moment is iterative. Using only one wall line, it should be checked that the compression force,  $C$ , is less than the compression force for failure,  $C_f$ . If this is the case, then only one wall line is needed to resist the compression due to load cases 5 and 7. If this is not the case, then a second wall line should be added.  $C$  can be obtained by summing the moments about point A (in order to eliminate the unknown tension). Repeat this process of adding in wall lines until  $C$  is verified to be less than  $C_f$ . From here, the free body diagram is fully defined. The total tension that must be resisted can be determined by summing forces in  $z$  (the vertical direction in Figure 3.8). The total

compression that must be resisted will be the sum of  $C_f$ ,  $C_g$ , and  $C$ . However, because the calculation is based on iteratively adding wall lines until the compression demands are met, the compression resistance will be adequate when the moment diagram is fully defined.

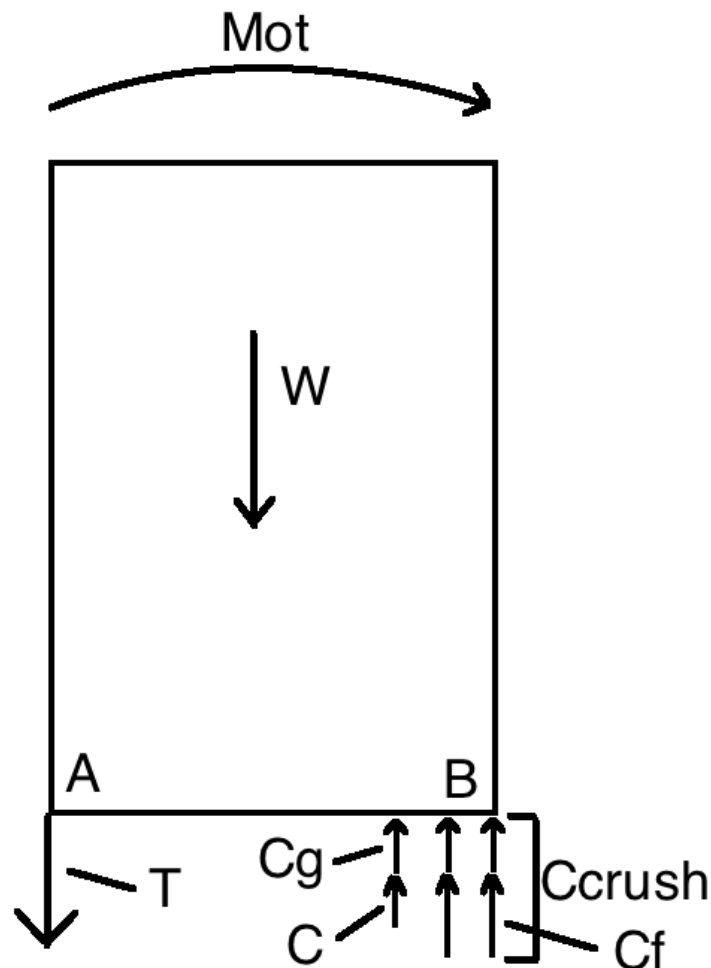


**Figure 3.8:** Simplified FBD of a CLT building.

Because both the walls in the x and y-directions will resist compression, the walls must be converted to their perpendicular direction. For example, if the overturning moment is acting about the x-axis (as shown in Figure 3.7, the walls that act in the y-direction must be converted to the corresponding location in y and length in x. The length will be the same, and the location in y will be the centroid of the portion of the wall. Before the conversion is done, the walls in y must be split up between the locations of the x-direction walls. By splitting up the y-direction walls, it is ensured that only the portion of the y-direction wall acting between each x-direction wall will be used. The result of converting the walls will be a list of wall locations and

corresponding lengths that can be used for the iterative process.

### 3.7.4 Overturning Moment Tension Design

The Anchor Tie-Down System (ATS) consists of steel rods spanning vertically between stories. There are existing ATS systems for application in light-frame wood construction.[18] An example 3-story ATS system from Simpson Strong Tie is shown in Figure 3.9. Note that the rod is tied to every floor, and therefore will transfer forces to each story. This is in contrast to other systems that only tie the rod to the top and bottom story. Some advantages of a system where all the floors are tied of are reduced drift, an efficient load patch, construction stability, and shrinkage accommodation at each story. Figure 3.7 illustrates the engaged ATS and exterior wall for the shown lateral story forces. The ATS will be in place at all four exterior walls, to account for all four directions of lateral loading.

ATS-SR10H150 rods will be used, as they are the strongest rods available from the Simpson Strong-Tie Anchor Tiedown Systems Catalog.[19] Each rod is 10/8” in diameter and has an allowable tensile capacity of 69,030 lbs for ASD. AISC Chapter D, “Design of Members in Tension”, specifies a tensile yielding ASD factor of 1.67 and an LRFD factor of 0.9. The ASD capacity is given as  $\frac{P_n}{\Omega}$ , and the LRFD capacity is given as  $\Phi P_n$ , meaning the ASD tensile capacity will be multiplied by 1.67\*0.9 to convert to LRFD. This gives an LRFD tensile capacity of 103.5 kips. Rods will be placed along the exterior walls of the building, which allows for the maximum possible moment arm.

Load Case 7 will be the governing load case for tension. The number of rods necessary on each exterior wall for each story will be the total tension divided by the allowable tensile strength of 103,545 lbs. More ATS rods will be required in lower stories.

### 3.7.5 Design For Coupling Action

The tension in the ATS rods and compression in the CLT needs to be transferred through the building in the form of a global shear force. In order for the tensile and compressive forces to develop, the shear forces must be resisted by the elements in building. The largest shear force demand will be the equal to compression force. The weight of the building will cause a smaller shear on the tension side of the

building. As this shear force is transferred throughout the floorplan, the cross-section of the floorplan that has the least shear resistance will control the shear strength.

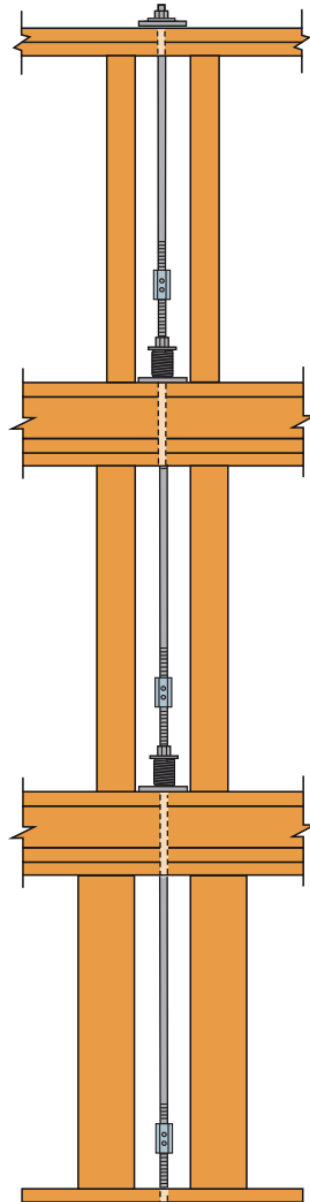


**Figure 3.9:** A single 3-story ATS system. [18]

The floor layout has a strong direction in shear, and a perpendicularly oriented weak direction. The strong direction will be along the longitudinal direction of the CLT panels: shear in this direction will be transferred through the CLT floor panel material itself, as well as the walls where applicable. The CLT floor panels likely will not span the entire strong direction, but as long as the discontinuities in the panels are staggered, there will be at least some CLT floor panels available in even the worst-case (least

available CLT for shear resistance) scenario.

The weak direction occurs because of continuous splicing in the longitudinal direction of the CLT panels. Any shear being transferred across the weak direction will have to be transferred across the panel connections, which are assumed to have little shear strength. In order to validate the underlying assumption for global overturning that the entire structure can transfer shear, these panel connections can be strategically placed underneath perpendicular wall lines. This placement ensures that the sections of the floor panels that have zero shear strength are supplemented by wall lines that are able to transfer the shear.

In many cases, however, this strategic placement is difficult or impossible due to the wall lines not allowing enough length for the walls to develop the full moment and shear that must be resisted. Therefore, a more general approach is to add specifically designed shear connections between the panels. These connections are made of steel dowels that fit between the panels. The dowels are held in place by steel end-caps that ensure load is being transferred purely in compression. A tensile load would cause uplift forces on the relatively weak glue, and is not desirable. A cross-section of an example of this connection is shown in Figure 3.10. The end caps will be effectively continuous (ie, the full length of the 70' interface between panels). However, the 70' length can be broken down into shorter pieces. Note that in reference to the connection, the top, middle, and bottom CLT layers are in the weak direction (the strong direction is perpendicular to the connection).

### 3.7.6 Shear Transfer Through CLT Panels

In the strong direction, it can be conservatively assumed that in the worst-case scenario there will be 50% of the floor diaphragm available for shear resistance. In the weak direction, the lesser strength of the CLT panels and the panel shear connections will control.

From the CLT Handbook, the shear strength for a 1' width of CLT panel is given as:

$$F'_v(Ib/Q)_{eff} \tag{3.25}$$

Where  $F'_v$  is the factored shear strength in psi, given as:

$$F_v * C_m * C_t * 2.88 * 0.75 * \lambda \quad (3.26)$$

Where  $C_m$  and  $C_t$  are 1, and lambda is 1.  $(Ib/Q)_{eff}$  is the effective area of a 1' width section of CLT that can be used, and is given as:

$$(Ib/Q)_{eff} = \frac{EI_{eff}}{\sum_{i=1}^{n/2+1} E_i h_i z_i} \quad (3.27)$$

Where  $EI_{eff}$  is the effective bending stiffness,  $E_i$  is the modulus of elasticity of layer  $i$ ,  $h_i$  is the thickness of layer  $i$ , except for the middle layer where it is half of the thickness.  $z_i$  is the distance from the centroid of layer  $i$  to the neutral axis, except for the middle layer, where it is the distance from the centroid to the top half of the middle layer.

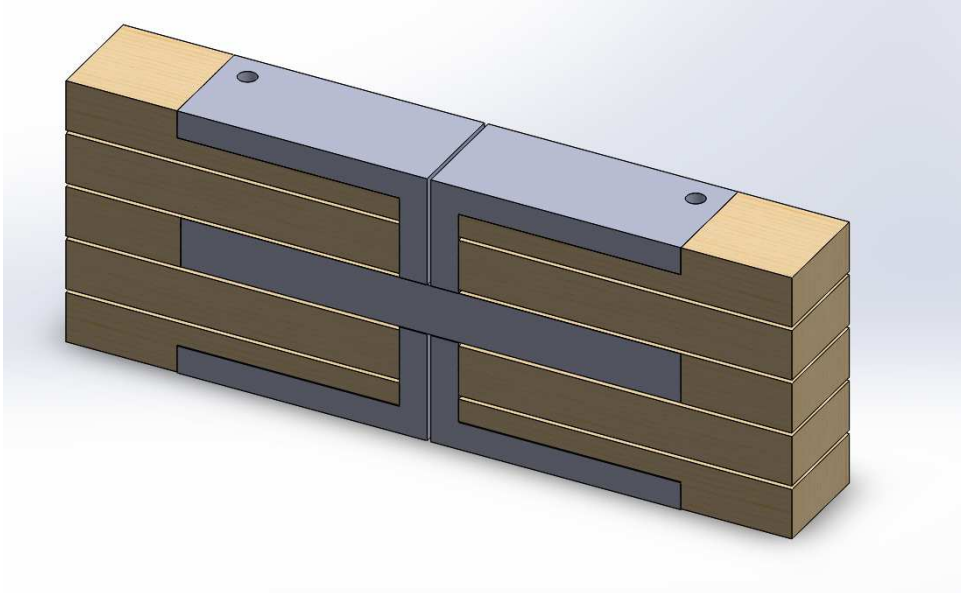


**Figure 3.10:** Panel-to-panel connection.

The shear resistance will therefore be the total length of the building times  $F'_v$  times the number of stories. The resistance can be divided by 2 for the conservative assumption that 50% of the cross-section will be panel-to-panel connections.

In the weak direction, the shear resistance of the panels will be the same as found in the strong direction, without the 50% reduction. At locations where there is a gap in the floor panels, the shear will be resisted by the walls. The shear strength for a 1' length of wall panel is obtained from equation 3.25. The exterior walls should be

conservatively ignored when calculating shear strength at the gaps between the floor panels.

### 3.7.7 Shear Transfer Through Custom Connection

A cross-section of the connection with the expected loading and resultant forces is shown in Figure 3.11. The gap between the two end caps should be as close to zero as possible, and is enlarged in the figure for clarity.

The eccentricity between the shear load and compression resistance (transferred from the steel caps to the wood) will cause a moment. In the case of the right-side end cap, the moment will cause clockwise rotation, therefore creating higher compression loads on one end of side of the cap, and low loads on the other end. The loading distribution on each side of the cap is assumed to be triangular. The distributed loading that the CLT panel exerts on the steel plates is shown in Figure 3.11.

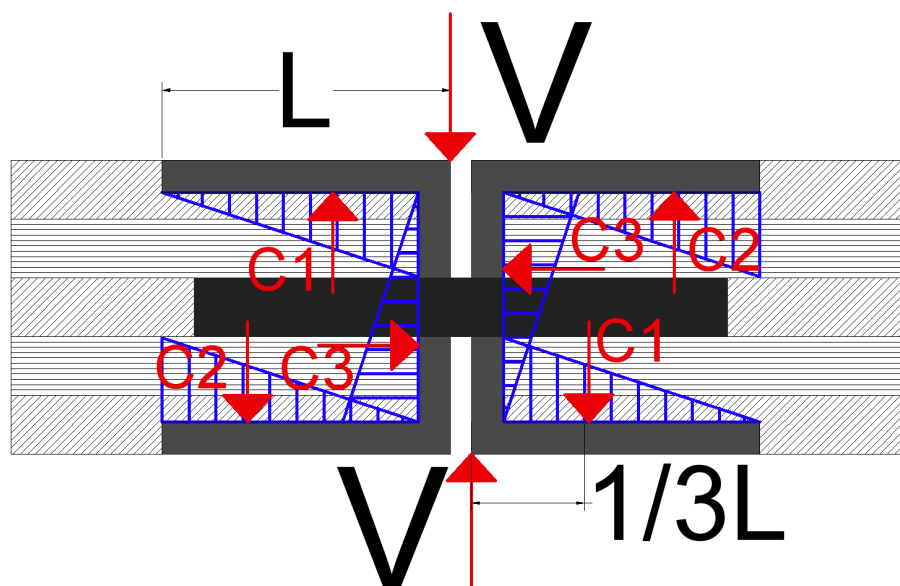


**Figure 3.11:** Cross-section view of the shear connection

The first failure mode of the connection is the shear failure of the steel dowels. The shear resistance is 0.6 times  $F_y$ , times a  $\phi$  factor of 1.0. The width of steel needed per story can be determined from the equation:

$$0.6F_y = \frac{V_{story}}{A} \quad (3.28)$$

The dowels can then be sized and spaced based on the required area of steel from equation 3.28.

The second failure mode of the connection is the perpendicular to grain compression transferred into the CLT from the end caps. From Figure 3.11,  $C_1$  is found to be equivalent to two times the shear load, or  $2V$ , and  $C_2$  is found to be equivalent to  $V$ .  $C_3$  is found to be zero. Therefore, the perpendicular compression is checked assuming a triangular distribution with a volume of  $2V$ . The peak value of the triangular distribution will be the load that must be designed for. The minimum required area of steel necessary for perpendicular to grain compression is given as:

$$A = \frac{4V}{F_{c\perp} \times 1.67 \times 0.9} \quad (3.29)$$

The third failure mode of the connection is the shear of the top and bottom of the steel caps due to the transfer of the compression load. The third failure mode will use equation 3.28.

The fourth failure mode of the connection is the bending failure of the top and bottom of the steel caps due to the transfer of the compression load. The following equation can be used to solve for the maximum length of the connection (which is dependent on the moment arm of the shear force), or the minimum thickness of the connection (where either the length or thickness is assumed):

$$F_b \geq \frac{Mc}{I} \quad (3.30)$$

The fifth failure mode is the shear of the CLT, which will use the same checks as section 3.7.6. Non-structural screws should be used on each end of the end caps to hold them in place.

### 3.8 Lateral Wind Load Design

The wind load should also be checked, although it is very unlikely that it will control due to the high-seismic location. The procedure found in ASCE 7-10 Chapter 27 is used as the building is not low-rise. The wind pressure obtained from the direction procedure can be used to determine the overturning moment and story shear at the base of the building. As long as the overturning moment due to wind is lower than the overturning moment due to seismic, wind load will not control.

## CHAPTER 4

### FULL DESIGN OF A TWELVE STORY CLT BUILDING

Using the design procedure described in Chapter 3, the following section is a step-by-step complete design of a 12-story CLT building located in Los Angeles, CA.

#### 4.1 Properties and Assumptions

The seismic factors are determined for the coordinates 34.044°N, 118.238°W. The seismic design factors are obtained from the USGS U.S. Seismic Design Maps.[20] The seismic factors are given in Table 4.1.

**Table 4.1:** Seismic Design Factors

<b>Occupancy</b>	3	<b>S<sub>s</sub></b>	2.377 g	<b>F<sub>a</sub></b>	<b>1</b>
<b>Site Class</b>	3	<b>S<sub>ds</sub></b>	0.832 g	<b>F<sub>v</sub></b>	1.5
<b>S<sub>ds</sub></b>	1.585	<b>I</b>	1	<b>R</b>	3
<b>S<sub>d1</sub></b>	0.832	<b>Site Class</b>	D		

The assumed properties of the CLT are shown in Table 4.2 and Table 4.3. The CLT panels are made CLT Grade E1, found in Table 1 of APA Standard PRG 320.[21] Grade E1 uses Spruce-Pine-Fir South (SPF). The properties of SPF can be found in Table 4A of the 2015 NDS Supplement.[22]. The R value is currently undefined for CLT, and is assumed in this study to be 3.[12]

**Table 4.2:** CLT Properties

		<b>Major</b>	<b>Minor</b>	
<b>Bending Strength</b>	<b>f<sub>b</sub></b>	1950	500	psi
<b>Modulus of Elasticity</b>	<b>E</b>	$1.7 \times 10^6$	$1.2 \times 10^6$	psi
<b>Tensile Strength</b>	<b>f<sub>t</sub></b>	1375	250	psi
<b>Compression Strength</b>	<b>f<sub>c</sub></b>	1800	650	psi
<b>Shear Strength</b>	<b>f<sub>v</sub></b>	135	135	psi
<b>Rolling Shear Strength</b>	<b>r<sub>v</sub></b>	45	45	psi

**Table 4.3: CLT Properties**

<b>Fc Perp</b>	<b>F<sub>c⊥</sub></b>	425	psi
<b>CLT Weight</b>	<b>W</b>	26.21	pcf
<b>Layer Thickness</b>	<b>h</b>	1.375	in
<b>Design Width</b>	<b>b</b>	12	in
<b>a factor</b>	<b>a</b>	5.5	
<b>Specific Gravity</b>	<b>SG</b>	0.42	

ASCE Load Combinations 1 and 2 (equation 3.1 and equation 3.2) are used to determine the loading. The dead load consists of the weight of the CLT panels, as well as a 30 psf supplementary dead load to account for the weight of the slab and carpet. Additionally, a dead load of 5 psf is added to each wall to account for a 1/2" thick layer of gypsum on each side for fire resistance.. The live load is 50 psf, which is obtained from ASCE 7-10 Table 4-1, assuming that the floor will be used for office use. Likely the building will be used for residential purposes, but the office assumption is more conservative and gives more usability flexibility. The design method assumes that the CLT panels will be 3, 5, 7, or 9 layers thick. It is expected that the required thickness of the CLT for a 12-story building will not exceed 9 layers.

## 4.2 Floor Sizing For Bending

The factored bending strength and bending load for 3, 5, 7, and 9 layer CLT panels are shown in Table 4.8.  $M_b$  is obtained from equation 3.3, where  $l$  is 15.5 feet (obtained from Figure 2.1a, and  $w$  is obtained from load cases 1 and 2 (equations 3.1 and 3.2). Load case 1 is given to be:

$$1.4 * SelfWt + 1.4 * 30 \quad (4.1)$$

Where 30 is the load in psf of the slab and carpet, and SelfWt is the weight of the floors in psf. SelfWt is given as  $(n)(W)(\frac{h}{12})$ , where  $n$  is the number of layers of CLT,  $h$  is the thickness of the CLT layers, and  $W$  is the weight of the CLT in pcf. The conversion factor of 12 is used to convert  $h$  from inches to feet. Load case 2 is given as:

$$1.2 * SelfWt + 1.6 * 50 + 1.2 * 30 \quad (4.2)$$

Where 50 is the live load of 50 psf.  $M_b$  is obtained from equations 3.4, 3.5, and 3.6, where the CLT properties from Table 4.2 and 4.3 are used. The  $M_b$  for load case for the corresponding  $M_d$  is used.

$EI_{eff}$  for 3, 5, 7, and 9 layer floors is calculated using equation 3.6, the values used for 5 and 9 layer floors are shown in Table 4.4. The values used for 3 and 7 layer floors are shown in Table 4.5. Separate tables are needed as the outside layer must be the strong direction, meaning the middle layer will be a different direction for 3 and 7 layers than for 5 and 9 layers.

The values of  $EI_{eff}$  are shown in Table 4.6.  $EI_{eff}$  is calculated using the tabulated values from Table 4.4 and Table 4.5, where the exterior layers are removed as the number of layers decreases. For example, to calculate the properties of the 3-layer floor, only the values from layers (ie, rows) 3, 4, and 5 are used.

**Table 4.4:** Tabulated values used to calculate  $EI_{eff}$  for 5 and 9 layers.

Layer	$E_i$ (psi)	$A_i$ (in <sup>2</sup> )	$z_i$ (in)	$E_i b_i \frac{h_i^3}{12} (\times 10^3 lbin^2)$	$E_i A_i z_i^2 (\times 10^6 lbin^2)$
1	$1.7 \times 10^6$	16.5	5.5	4419.3	848.5
2	$1.2 \times 10^6/30$	16.5	4.125	104	11.2
3	$1.7 \times 10^6$	16.5	2.75	4419.3	212.1
4	$1.2 \times 10^6/30$	16.5	1.375	104	1.2
5	$1.7 \times 10^6$	16.5	0	4419.3	0
6	$1.2 \times 10^6/30$	16.5	1.375	104	1.2
7	$1.7 \times 10^6$	16.5	2.75	4419.3	212.2
8	$1.2 \times 10^6/30$	16.5	4.125	104	11.2
9	$1.7 \times 10^6$	16.5	5.5	4419.3	848.5

$S_{eff}$  is determined using equation 3.5. The tabulated values used to calculate  $S_{eff}$ , shown in Table 4.7.

$M_b$  is obtained from equation 3.4, where  $F'_b$  is 4095 psi.  $M_d$  is obtained from equation 3.3, where  $w$  is 148 psf using Load Case 2.

It is apparent from Table 4.8 that 3 layer CLT floors will be adequate for

bending load. Because the floors do not transfer load to each other, 3 layer floors will be adequate for bending for all 12 stories.

**Table 4.5:** Tabulated values used to calculate  $EI_{eff}$  for 3 and 7 layers.

Layer	$E_i$ (psi)	$A_i$ ( $in^2$ )	$z_i$ (in)	$E_i b_i \frac{h_i^3}{12} (\times 10^3 lbin^2)$	$E_i A_i z_i^2 (\times 10^6 lbin^2)$
1	$1.7 \times 10^6$	16.5	4.1	4419.3	477.3
2	$1.2 \times 10^6/30$	16.5	2.8	104.0	5.0
3	$1.7 \times 10^6$	16.5	1.4	4419.3	53.0
4	$1.2 \times 10^6/30$	16.5	0.0	104.0	0.0
5	$1.7 \times 10^6$	16.5	1.4	4419.3	53.0
6	$1.2 \times 10^6/30$	16.5	2.8	104.0	5.0
7	$1.7 \times 10^6$	16.5	4.1	4419.3	477.3

**Table 4.6:**  $EI_{eff}$  for 3, 5, 7 and 9 layer floors

Layers	3	5	7	9
$EI_{eff} (\times 10^9 lbin^2)$	0.115	0.440	1.089	2.17

**Table 4.7:** Tabulated values used to calculate  $S_{eff}$

Layers	$EI_{eff}$	$E_1$	$h$
3	$0.115 \times 10^9$	$1.7 \times 10^6$	1.375
5	$0.440 \times 10^9$	$1.7 \times 10^6$	1.375
7	$1.089 \times 10^9$	$1.7 \times 10^6$	1.375
9	$2.16 \times 10^9$	$1.7 \times 10^6$	1.375

**Table 4.8:** Factored bending strength,  $M_b$ , and bending load,  $M_d$ .

Layers	3	5	7	9
$M_b$ (kft)	9.78	22.45	39.68	61.49
$M_d$ (kft)	3.81	4.02	4.24	4.46

### 4.3 Floor Sizing for Vibration

$l_{max}$ , the maximum short-direction span, is obtained from equations 3.8, 3.9, and 3.10. The tabulated values used to determine  $GA_{eff}$ , which needed for equation 3.8, are shown in Table 4.9.

**Table 4.9:** Tabulated values used to calculate  $GA_{eff}$  for 5 and 9 layers.

Layer	$G_i$ (psi)	$h/G/b$ (psi)
1	$1.7 \times 10^6/16$	$1.078 \times 10^6$
2	$1.2 \times 10^6/(16 * 10)$	$15.278 \times 10^6$
3	$1.7 \times 10^6/16$	$1.078 \times 10^6$
4	$1.2 \times 10^6/(16 * 10)$	$15.278 \times 10^6$
5	$1.7 \times 10^6/16$	$1.078 \times 10^6$
6	$1.2 \times 10^6/(16 * 10)$	$15.278 \times 10^6$
7	$1.7 \times 10^6/16$	$1.078 \times 10^6$
8	$1.2 \times 10^6/(16 * 10)$	$15.278 \times 10^6$
9	$1.7 \times 10^6/16$	$1.078 \times 10^6$

**Table 4.10:** Tabulated values used to calculate  $GA_{eff}$  for 3 and 7 layers.

Layer	$G_i$ (psi)	$h/G/b$ (psi)
1	$1.7 \times 10^6/16$	$1.078 \times 10^6$
2	$1.2 \times 10^6/(16 * 10)$	$15.278 \times 10^6$
3	$1.7 \times 10^6/16$	$1.078 \times 10^6$
4	$1.2 \times 10^6/(16 * 10)$	$15.278 \times 10^6$
5	$1.7 \times 10^6/16$	$1.078 \times 10^6$
6	$1.2 \times 10^6/(16 * 10)$	$15.278 \times 10^6$
7	$1.7 \times 10^6/16$	$1.078 \times 10^6$

From Table 4.12, it is determined that 5 layer floors are necessary for vibration. This is a thicker requirement than the bending load requirement. Therefore, 5 layer floors will be used throughout the building.

Using equation 3.10,  $GA_{eff}$  for 3, 5, 7 and 9 layer panels is shown in Table 4.11

**Table 4.11:**  $GA_{eff}$  for 3, 5, 7 and 9 layer floors

Layers	3	5	7	9
$GA_{eff} (\times 10^6 lb)$	1.8495	0.9247	0.6165	0.4624

$S_{eff}$  is determined using equation 3.5. The tabulated values used to calculate  $S_{eff}$ , shown in Table 4.7.

For a 15.5' span, the values for  $l_{max}$  are given for 3, 5, 7, and 9 layer floors in Table 4.12.

**Table 4.12:**  $l_{max}$  for 3, 5, 7, and 9 layer floors.

Layers	3	5	7	9
$l_{max}$ (kft)	13.01	17.45	19.91	20.54

#### 4.4 Wall Sizing for Vertical Loads

The wall load uses Load Combinations 1 and 2, where the dead load due to the self-weight will be the weight of the walls and floors of the stories above. Using the worst-case of load combinations 1 and 2, Table 4.13 is generated and gives the total load in pounds on each story, assuming either uniform 3, 5, 7, or 9 layer walls throughout the structure. In all cases load case 2 governs.

The load on each story can be divided by the total parallel to grain wall area,  $A_{//}$ , of the story to determine the load in psi on each story. Note that  $A_{//}$  does not include perpendicular to grain layers, so for example a 5 layer panel would have an  $A_{//}$  equal to the thickness of 3 layers. The load on each story can then be compared to  $F'_c C_p$  to determine if the wall sizes are adequate. The capacities and loads on story 1 for a building using 3, 5, 7, and 9 layer wall panels (and 5 layer floor panels) are shown in Table 4.14. Story 1 is used because it's the worst-case story.

By comparing the load to the capacity, it can be seen that 3 layer walls (using a story height of 9 ft) will be adequate throughout the structure for compression and buckling.

**Table 4.13:** Load in pounds on each story using 3, 5, 7, and 9 layer panels

<b>Story</b>	<b>3</b>	<b>5</b>	<b>7</b>	<b>9</b>
<b>1</b>	$9.07 \times 10^6$	$9.64 \times 10^6$	$1.02 \times 10^7$	$1.08 \times 10^7$
<b>2</b>	$8.31 \times 10^6$	$8.82 \times 10^6$	$9.33 \times 10^6$	$9.84 \times 10^6$
<b>3</b>	$7.54 \times 10^6$	$8.00 \times 10^6$	$8.46 \times 10^6$	$8.92 \times 10^6$
<b>4</b>	$6.78 \times 10^6$	$7.18 \times 10^6$	$7.59 \times 10^6$	$8.00 \times 10^6$
<b>5</b>	$6.01 \times 10^6$	$6.37 \times 10^6$	$6.72 \times 10^6$	$7.08 \times 10^6$
<b>6</b>	$5.24 \times 10^6$	$5.55 \times 10^6$	$5.86 \times 10^6$	$6.16 \times 10^6$
<b>7</b>	$4.48 \times 10^6$	$4.73 \times 10^6$	$4.99 \times 10^6$	$5.24 \times 10^6$
<b>8</b>	$3.71 \times 10^6$	$3.92 \times 10^6$	$4.12 \times 10^6$	$4.32 \times 10^6$
<b>9</b>	$2.95 \times 10^6$	$3.10 \times 10^6$	$3.25 \times 10^6$	$3.40 \times 10^6$
<b>10</b>	$2.18 \times 10^6$	$2.28 \times 10^6$	$2.38 \times 10^6$	$2.49 \times 10^6$
<b>11</b>	$1.41 \times 10^6$	$1.46 \times 10^6$	$1.52 \times 10^6$	$1.57 \times 10^6$
<b>12</b>	$6.47 \times 10^5$	$6.47 \times 10^5$	$6.47 \times 10^5$	$6.47 \times 10^5$

**Table 4.14:** Wall capacity and load at story 1.

<b>Layers</b>	<b>3</b>	<b>5</b>	<b>7</b>	<b>9</b>
<b><math>F'_c C_p</math> (psi)</b>	1409.1	2569.2	2965.0	2915.6
<b>Load (psi)</b>	349.40	247.35	196.32	165.71

#### 4.5 Wall Sizing for Fire

Because 3-layer panels are adequate for the gravity loads, 5-layer panels are used for fire to provide a sacrificial layer in case of a fire and meet the minimum fire requirements defined previously. Gypsum could also be added to the exterior of the 5-layer walls, but fire resistance calculations are outside the scope of this project.

#### 4.6 Wall Sizing for Perpendicular to Grain Compression

Next, the perpendicular to grain compression must be checked. From equation 3.15, it is determined that for 5 layer walls, the perpendicular to grain bearing capacity is 52,699 lbs over 1 ft of wall length. From Table 4.13, it is determined that the bearing

load at story 1 for 5-layer panels is 12,244 lbs over 1 ft of wall length. Therefore the 5 layer wall capacity is greater than the load. Because the walls are equal sizes, the initial assumption is valid. If the walls varied in size throughout the different stories, then the design would have to be iterated.

#### 4.7 Summary of Gravity Design Results

The 12-story building will use 5 layer CLT floors and 5 layer CLT walls for each 9' tall story. This thickness will be adequate for gravity loading under dead and live loads. The strength of the wall and diaphragm does not control the design. The floor design is controlled by vibration, and the wall design is controlled by fire resistance restrictions.

#### 4.8 Story Forces Determination

Based on the equivalent lateral force procedure from ASCE 7-10, the total base shear,  $V$ , is equal to  $C_s W$ . Currently there is no seismic force modification factor for CLT shear wall systems. Based on earlier work by Pei et al. 2014 [12] an estimated R factor of 3.0 was adopted in this study. Note that rigorous analysis and justification must be in place to propose a suitable R factor for CLT construction, which is out of the scope of this study. Given an R factor of 3,  $C_s$  is determined in ASCE 7-10 section 12.8.1.1 using the  $S_{ds}$ ,  $S_{D1}$ ,  $S_1$ , T, R, and I from Table 4.1.  $C_s$  is found to be 0.4139.  $W$  is the seismic weight, which is the entirety of the dead load of the building (except the bottom half of the first story, which is part of the foundation). The CLT material dead weight was calculated using a density of 26.21 pcf. An additional secondary dead load of 30 psf on the floors is added to account for nonstructural components such as the slab, carpet, and other fixtures installed.

Each floor has an area of 4828 sq ft with 5-layer (6.875" thick) panels. Each floor has 787 ft of 5-layer walls (6.875" thick) that are 9' tall each, leading to a total wall volume of 4057.97 ft<sup>3</sup> per story. The weight of the CLT plus the 30 psf dead load on the floors and 5 psf load on the walls gives a weight of 366,230 lbs per story, except the roof which is 280,650 lbs. Note that in this case one story is defined as the floor and half of the walls above and below the floor. Therefore, the roof is the floor panels and half of the walls below the floor panels. The total seismic weight is 4309 kips. The base

shear is found to be 1784 kips.

The building period is determined using ASCE 7-10 equation 12.8-7, where  $C_t$  is 0.02 and  $x$  is 0.75 from ASCE 7-10 Table 12.8-2. The period,  $T$ , is determined to be 0.67 seconds. The lateral story forces are found using ASCE 7-10 equations 12.8-11 and 12.8-12 where  $w_i$  is 366.23 kips for each story, except the roof which is 280.65 kips.

The story shear for each story is found using ASCE 7-10 equation 12.8-13. The tabulated values used in the ELF procedure including the values of  $F_i$ , the story shear  $V_i$ , and the story overturning moment,  $M_i$ , are given in Table 4.15. A value of  $k=2$  is used.

**Table 4.15:** Tabulated values for the ELF procedure.

Story	$h_x$ (ft)	$w_x$ (k)	$wh_x^k$ (kft <sup>2</sup> )	$C_{vx}$	$F_i$ (k)	$V_i$ (k)	$M_i$ (kft)
1	9	366.23	29665	0.0016	3	1784	133352
2	18	366.23	118659	0.0065	12	1781	117300
3	27	366.23	266982	0.0146	26	1770	101427
4	36	366.23	474634	0.0260	46	1743	85936
5	45	366.23	741616	0.0406	72	1697	71037
6	54	366.23	1067927	0.0584	104	1625	56946
7	63	366.23	1453567	0.0795	142	1521	43887
8	72	366.23	1898536	0.1038	185	1379	32083
9	81	366.23	2402835	0.1314	234	1194	21764
10	90	366.23	2966463	0.1622	289	959	13161
11	99	366.23	3589420	0.1963	350	670	6508
12	108	280.65	3273502	0.1790	319	319	2042
<b>Total</b>		4309.18	18283804				

The story shear occurs directly below the story. For instance, the shear on the walls below the floor of story 1 will be 1784 kips (associated with story 1), while the shear on the walls directly above the floor of story 1 will be 1781 kips (associated with story 2).

#### 4.9 Wall Bracket Selection for Shear Resistance

Figure 4.1 shows the wall lines in the  $x$  and  $y$  directions. Note that the length of the wall does not affect the tributary area. The spacing is calculated using equation 3.17 for the flexible diaphragm assumption and 3.20 for the rigid diaphragm assumption. The length of each wall line available to brackets,  $L_i$  and the tributary area for each wall line,  $A_i$  are obtained from Table 4.16 for  $x$ -direction walls and Table 4.17

for y-direction walls. Note that  $L_i$  for interior walls is doubled to account for the placement of brackets on each side of the walls.

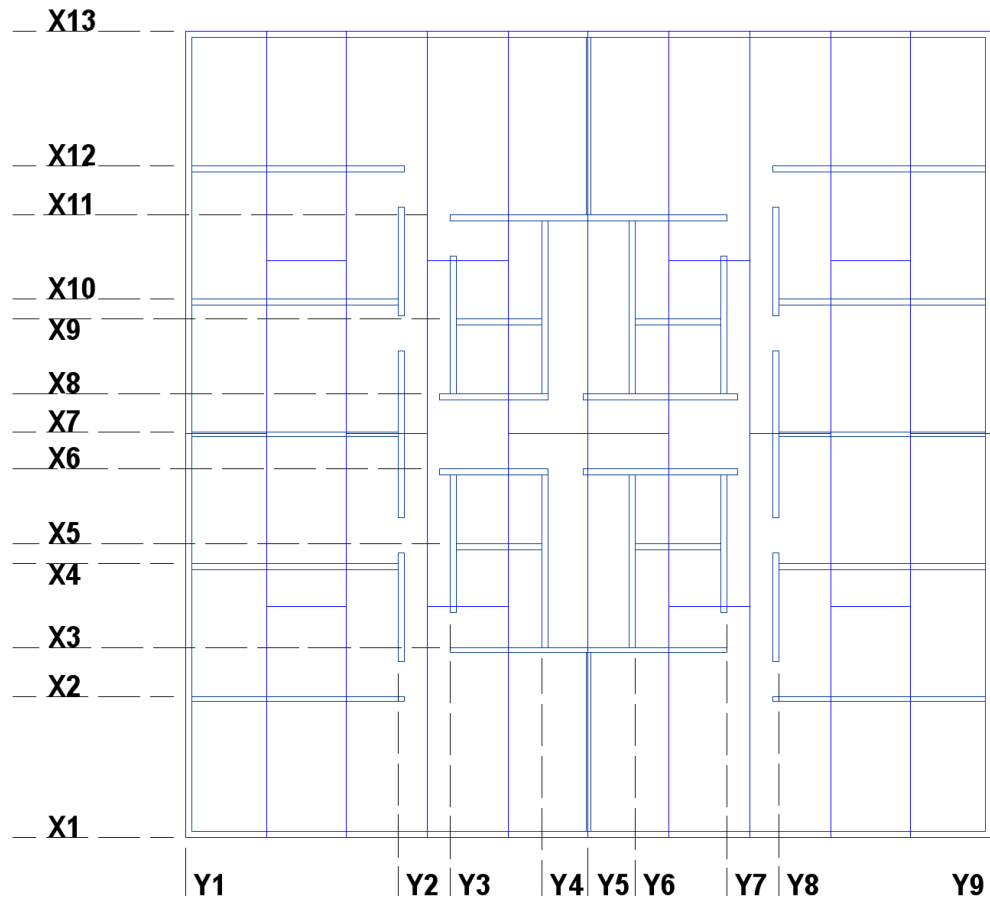


Figure 4.1: Wall line labels for the x and y-direction walls.

Table 4.16:  $A_i$  and  $L_i$  for X-direction wall lines.

Wall Line	X1	X2	X3	X4	X5	X6	X7	X8	X9	X10	X11	X12	X13
$A_i$ ( $ft^2$ )	403	551	403	315	289	341	228	341	289	315	403	551	403
$L_i$ ( $ft$ )	70	74	48	74	28	46	74	46	28	74	48	74	70

Table 4.17:  $A_i$  and  $L_i$  for Y-direction wall lines.

Wall Line	Y1	Y2	Y3	Y4	Y5	Y6	Y7	Y8	Y9
$A_i$ ( $ft^2$ )	639	796	420	411	298	411	420	796	639
$L_i$ ( $ft$ )	70	67	42	60	62	60	42	67	70

The shear values added or subtracted from each wall line,  $V_{ti}$ , are obtained from equation 3.22 and 3.23. The values of  $V_{ti}$  are shown in Table 4.18 for the x-direction walls and 4.19 for the y-direction in order to represent accidental torsion.

**Table 4.18:**  $V_{ti}$  values in kips for X-direction wall lines for each story.

Wall Line	X1	X2	X3	X4	X5	X6	X7	X8	X9	X10	X11	X12	X13
1	50	35	18	17	6	3	0	-3	-6	-17	-18	-35	-50
2	49	35	18	17	6	3	0	-3	-6	-17	-18	-35	-49
3	49	35	18	17	6	3	0	-3	-6	-17	-18	-35	-49
4	48	34	18	17	5	3	0	-3	-5	-17	-18	-34	-48
5	47	33	18	17	5	3	0	-3	-5	-17	-18	-33	-47
6	45	32	17	16	5	3	0	-3	-5	-16	-17	-32	-45
7	42	30	16	15	5	3	0	-3	-5	-15	-16	-30	-42
8	38	27	14	13	4	2	0	-2	-4	-13	-14	-27	-38
9	33	23	12	12	4	2	0	-2	-4	-12	-12	-23	-33
10	27	19	10	9	3	2	0	-2	-3	-9	-10	-19	-27
11	19	13	7	7	2	1	0	-1	-2	-7	-7	-13	-19
12	9	6	3	3	1	1	0	-1	-1	-3	-3	-6	-9

**Table 4.19:**  $V_{ti}$  values in kips for Y-direction wall lines for each story.

Story	Y1	Y2	Y3	Y4	Y5	Y6	Y7	Y8	Y9
1	70	31	17	7	0	-7	-14	-31	-70
2	70	31	17	7	0	-7	-14	-31	-70
3	69	31	17	7	0	-7	-14	-31	-69
4	68	31	17	7	0	-7	-14	-31	-68
5	66	30	17	7	0	-7	-14	-30	-66
6	64	29	16	7	0	-7	-13	-29	-64
7	60	27	15	6	0	-6	-12	-27	-60
8	54	24	13	6	0	-6	-11	-24	-54
9	47	21	12	5	0	-5	-10	-21	-47
10	38	17	9	4	0	-4	-8	-17	-38
11	26	12	7	3	0	-3	-5	-12	-26
12	13	6	3	1	0	-1	-3	-6	-13

Table 4.20 and Table 4.21 show the design shear values for each wall line for both the rigid and flexible diaphragm assumption for each story, for the x-direction and y-direction wall lines, respectively. Table 4.22 and Table 4.23 show maximum spacing allowed for each wall line for both the rigid and flexible diaphragm assumption for each story, for the x-direction and y-direction wall lines, respectively. In the tables, “f” represents a flexible assumption while “r” represents a rigid assumption.

**Table 4.20:** Design shear (kips) for each x-direction wall line for rigid and flexible diaphragm assumptions.

Story		X1	X2	X3	X4	X5	X6	X7	X8	X9	X10	X11	X12	X13
1	f	149	102	74	58	53	63	42	63	53	58	74	102	149
1	r	215	105	66	96	36	56	88	53	30	79	48	70	116
2	f	148	102	74	58	53	63	42	63	53	58	74	102	148
2	r	215	105	66	96	36	56	87	53	30	79	47	70	116
3	f	147	101	74	58	53	62	42	62	53	58	74	101	147
3	r	213	104	65	95	36	55	87	52	30	78	47	70	115
4	f	145	99	73	57	52	62	41	62	52	57	73	99	145
4	r	210	103	64	94	35	55	86	52	30	77	46	68	112
5	f	141	97	71	55	51	60	40	60	51	55	71	97	141
5	r	205	100	63	92	34	53	83	50	29	75	45	67	108
6	f	135	93	68	53	49	57	38	57	49	53	68	93	135
6	r	196	96	60	88	33	51	80	48	28	72	43	64	101
7	f	127	87	63	50	45	54	36	54	45	50	63	87	127
7	r	183	89	56	82	31	48	75	45	26	67	41	60	92
8	f	115	79	57	45	41	49	32	49	41	45	57	79	115
8	r	166	81	51	74	28	43	68	41	23	61	37	54	78
9	f	99	68	50	39	36	42	28	42	36	39	50	68	99
9	r	144	70	44	64	24	37	59	35	20	53	32	47	61
10	f	80	55	40	31	29	34	23	34	29	31	40	55	80
10	r	116	56	35	52	19	30	47	28	16	42	26	38	40
11	f	56	38	28	22	20	24	16	24	20	22	28	38	56
11	r	81	39	25	36	13	21	33	20	11	30	18	26	13
12	f	27	18	13	10	10	11	7.5	11	10	10	13	18	27
12	r	39	19	12	17	6.4	10	16	9.5	5.4	14	8.5	13	20

**Table 4.21:** Design shear (kips) for each y-direction wall line for rigid and flexible diaphragm assumptions

Story		Y1	Y2	Y3	Y4	Y5	Y6	Y7	Y8	Y9
<b>1</b>	<b>f</b>	236	147	78	76	55	76	78	147	236
<b>1</b>	<b>r</b>	301	126	76	103	102	95	62	95	161
<b>2</b>	<b>f</b>	235	147	77	76	55	76	77	147	235
<b>2</b>	<b>r</b>	301	126	76	103	102	95	62	95	161
<b>3</b>	<b>f</b>	234	146	77	75	54	75	77	146	234
<b>3</b>	<b>r</b>	299	125	76	102	102	95	62	94	160
<b>4</b>	<b>f</b>	230	144	76	74	54	74	76	144	230
<b>4</b>	<b>r</b>	294	124	75	100	100	93	61	93	158
<b>5</b>	<b>f</b>	224	140	74	72	52	72	74	140	224
<b>5</b>	<b>r</b>	286	120	73	98	97	91	59	90	153
<b>6</b>	<b>f</b>	215	134	71	69	50	69	71	134	215
<b>6</b>	<b>r</b>	274	115	70	94	93	87	57	86	147
<b>7</b>	<b>f</b>	201	125	66	65	47	65	66	125	201
<b>7</b>	<b>r</b>	257	108	65	88	87	81	53	81	138
<b>8</b>	<b>f</b>	182	114	60	59	42	59	60	114	182
<b>8</b>	<b>r</b>	233	98	59	79	79	74	48	73	125
<b>9</b>	<b>f</b>	158	98	52	51	37	51	52	98	158
<b>9</b>	<b>r</b>	201	85	51	69	68	64	42	63	108
<b>10</b>	<b>f</b>	127	79	42	41	30	41	42	79	127
<b>10</b>	<b>r</b>	162	68	41	55	55	51	33	51	87
<b>11</b>	<b>f</b>	89	55	29	28	21	28	29	55	89
<b>11</b>	<b>r</b>	113	47	29	39	38	36	23	36	61
<b>12</b>	<b>f</b>	42	26	14	14	10	14	14	26	42
<b>12</b>	<b>r</b>	54	23	14	18	18	17	11	17	29

**Table 4.22:** Maximum allowed spacing (inches) for each x-direction wall line for rigid and flexible diaphragm assumptions.

Story		X1	X2	X3	X4	X5	X6	X7	X8	X9	X10	X11	X12	X13
1	f	15	12	10	21	8.5	12	28	12	8.5	21	10	12	15
1	r	10	11	12	12	13	13	14	14	15	15	16	17	19
2	f	15	12	10	21	8.5	12	28	12	8.5	21	10	12	15
2	r	11	11	12	12	13	13	14	14	15	15	16	17	19
3	f	15	12	11	21	8.5	12	29	12	8.5	21	11	12	15
3	r	11	11	12	13	13	13	14	14	15	15	16	17	20
4	f	16	12	11	21	8.7	12	29	12	8.7	21	11	12	16
4	r	11	12	12	13	13	14	14	14	15	15	17	17	20
5	f	16	12	11	22	8.9	12	30	12	8.9	22	11	12	16
5	r	11	12	12	13	13	14	14	15	16	16	17	18	21
6	f	17	13	11	23	9.3	13	31	13	9.3	23	11	13	17
6	r	12	12	13	14	14	15	15	15	16	17	18	19	22
7	f	18	14	12	24	10	14	33	14	10	24	12	14	18
7	r	12	13	14	15	15	16	16	16	17	18	19	20	25
8	f	20	15	13	27	11	15	37	15	11	27	13	15	20
8	r	14	15	15	16	16	17	18	18	19	20	21	22	29
9	f	23	18	16	31	13	18	42	18	13	31	16	18	23
9	r	16	17	18	19	19	20	20	21	22	23	24	25	37
10	f	28	22	19	38	16	22	53	22	16	38	19	22	28
10	r	20	21	22	23	23	25	25	26	28	28	30	32	57
11	f	40	31	28	55	23	31	76	31	23	55	28	31	40
11	r	28	30	31	33	34	35	36	37	40	40	43	45	179
12	f	85	66	58	115	47	66	159	66	47	115	58	66	85
12	r	59	64	66	69	70	74	76	78	83	85	91	95	114

**Table 4.23:** Maximum allowed spacing (inches) for each y-direction wall line for rigid and flexible diaphragm assumptions

Story		Y1	Y2	Y3	Y4	Y5	Y6	Y7	Y8	Y9
<b>1</b>	<b>f</b>	10	7.4	8.7	13	18	13	8.7	7.4	10
<b>1</b>	<b>r</b>	7.5	8.6	8.9	9.4	10	10	11	11	14
<b>2</b>	<b>f</b>	10	7.4	8.8	13	18	13	8.8	7.4	10
<b>2</b>	<b>r</b>	7.5	8.6	8.9	9.4	10	10	11	11	14
<b>3</b>	<b>f</b>	10	7.4	8.8	13	18	13	8.8	7.4	10
<b>3</b>	<b>r</b>	7.6	8.6	8.9	9.5	10	10	11	11	14
<b>4</b>	<b>f</b>	10	7.5	8.9	13	19	13	8.9	7.5	10
<b>4</b>	<b>r</b>	7.7	8.7	9.1	10	10	10	11	12	14
<b>5</b>	<b>f</b>	10	7.7	9.2	13	19	13	9.2	7.7	10
<b>5</b>	<b>r</b>	7.9	9.0	9.3	10	10	11	11	12	15
<b>6</b>	<b>f</b>	11	8.1	10	14	20	14	10	8.1	11
<b>6</b>	<b>r</b>	8.2	9.4	10	10	11	11	12	13	15
<b>7</b>	<b>f</b>	11	8.6	10	15	21	15	10	8.6	11
<b>7</b>	<b>r</b>	8.8	10	10	11	11	12	13	13	16
<b>8</b>	<b>f</b>	12	10	11	16	24	16	11	10	12
<b>8</b>	<b>r</b>	10	11	11	12	13	13	14	15	18
<b>9</b>	<b>f</b>	14	11	13	19	27	19	13	11	14
<b>9</b>	<b>r</b>	11	13	13	14	15	15	16	17	21
<b>10</b>	<b>f</b>	18	14	16	24	34	24	16	14	18
<b>10</b>	<b>r</b>	14	16	16	18	18	19	20	21	26
<b>11</b>	<b>f</b>	26	20	23	34	49	34	23	20	26
<b>11</b>	<b>r</b>	20	23	24	25	26	27	29	30	37
<b>12</b>	<b>f</b>	53	41	49	71	102	71	49	41	53
<b>12</b>	<b>r</b>	42	48	49	53	55	57	61	64	78

The minimum values for the maximum required spacing for each story is shown in Table 4.24. The spacing used in design cannot exceed these minimum values.

**Table 4.24:** Minimum required spacing of brackets in x and y directions for each story for the flexible and rigid assumptions.

Story	1	2	3	4	5	6	7	8	9	10	11	12
<b>s<sub>x</sub> (in) flexible</b>	8.5	8.5	8.5	8.7	8.9	9.3	10	11	13	16	23	47
<b>s<sub>y</sub> (in) flexible</b>	7.4	7.4	7.4	7.5	7.7	8.1	8.6	10	11	14	20	41
<b>s<sub>x</sub> (in) rigid</b>	10	11	11	11	11	12	12	14	16	20	28	59
<b>s<sub>y</sub> (in) rigid</b>	7.5	7.5	7.6	7.7	7.9	8.2	8.8	10	11	14	20	42

The smallest spacing in Table 4.24 is 7.4 inches, which is larger than the length of the bracket and is therefore feasible. On the first floor, the minimum spacing required when accounting for both rigid and flexible ranges from 7.4 to 10.1 inches, so it is not very advantageous to have different spacings on each wall line. Therefore, the minimum required spacing should be used for all wall lines. The spacing for the flexible assumption governs the minimum required spacing for all wall lines.

#### 4.10 Overturning Moment Compression Design

Given the calculated overturning demand for each story in Table 4.26, the simplified force couple model in Figure 3.8 can be used to check the compression force on the bearing walls under combined dead load and overturning. First,  $C_{crush}$  is given as 52,699 lbs per foot of wall length. The weight,  $W$ , is obtained from load cases 5 and 7, and is determined in pounds. Per ASCE 7-10 section 12.4.2.3, a  $0.2S_{ds}$  factor is added or subtracted from the dead load factor. For load case 5, on story 1,  $W$  is equal to  $9.22 \times 10^6$  lbs. For load case 7 on story 1,  $W$  is equal to  $2.43 \times 10^6$  lbs.

Initially, the total area of the wall lines engaged in compression at the first story is not known. An iterative process is needed to identify the total wall area under compression through trial-and-error. Using the exterior wall for the first iteration it is determined that  $C_g = W$ . Because  $C_g$  is resisting  $W$ ,  $C_g$  can then be converted to  $\frac{lb}{ft}$  by dividing  $W$  by the length of the wall being used, which is 70 feet for the first wall line. From here it is apparent that  $C_g > C_f$ , and therefore more walls will be needed. When adding in more walls,  $C_g$  should be determined by dividing  $W$  by the total wall length currently being used.

After more iteration, it is determined that for load case 5 (which controls compression), the compression zone in story 1 will extend 16 feet into the building for a moment about the y-axis, and 9.625 feet for a moment about the x-axis. The total compression being resisted at story one is 7190 kips for a moment about the y-axis, and 7230 kips for a moment about the x-axis. Therefore, every wall until 16 feet in y or 9.625 feet in x will reach the crushing load, at which point the last walls in the compression zone will resist the remainder of the load.

The location of the compression zones are shown in Figure 4.2 from the edge and the total compression being resisted by each story is shown in Table 4.25.  $d_x$  is the

distance from the edge of the building that the x-direction walls are, and therefore  $d_x$  is a distance in the y-direction. It follows that  $d_y$  is the x-direction distance from the edge of the building of the y-direction walls. Only the results for load case 5 are shown in Table 4.25, as load case 5 is the compression-controlling load case. Note that for the wall lines in stories 7 through 12 in both the x and y directions, only the edge walls are needed to resist compression.

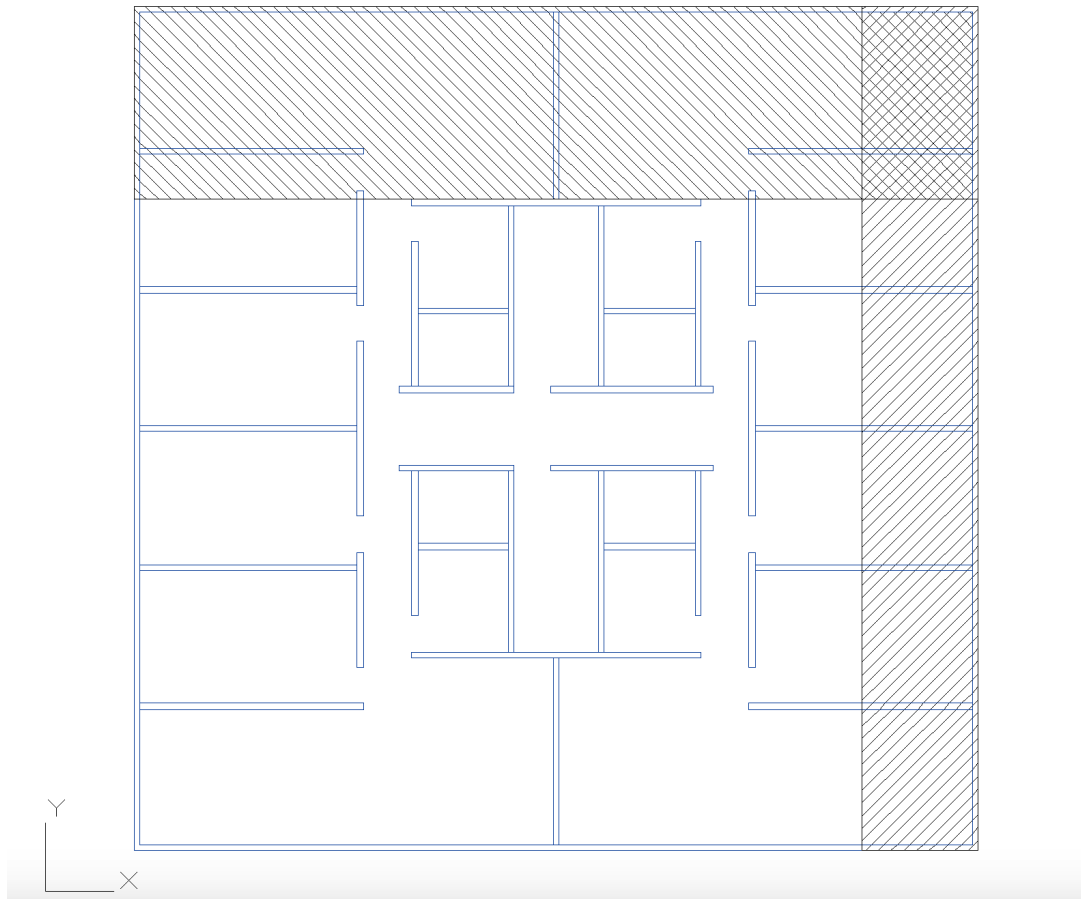


**Figure 4.2:** Compression zones for x and y direction loading.

Because none of the compression zones in Table 4.25 exceed the length of the building, the building is adequately designed to resist the compression demands imposed by the overturning moment.

**Table 4.25:** Location of end of compression zone and total compression in each story for x and y-direction wall lines.

Story	$d_x$ (ft)	$d_y$ (ft)	$C_x$ (kips $\times 10^3$ )	$C_y$ (kips $\times 10^3$ )
1	16	9.625	7.19	7.23
2	12	9.625	6.44	6.51
3	12	9.625	5.69	5.79
4	6.25	9.625	5.00	5.07
5	6.25	9.625	4.32	4.35
6	6.25	9.625	3.66	3.66
7	0.5	0.5	3.05	3.05
8	0.5	0.5	2.46	2.46
9	0.5	0.5	1.88	1.88
10	0.5	0.5	1.33	1.33
11	0.5	0.5	0.81	0.81
12	0.5	0.5	0.33	0.33

#### 4.11 Overturning Moment Tension Design

The tension design consists of selecting ATS rods that are able to resist the tension demands imposed by the overturning moment. The tension is governed by the shape of the compression zone - ie, if the compression zone is large, there will be a less moment arm available for the tension to resist the moment, thus requiring a larger tension force. The tension, however, is counteracted by the weight of the building. Therefore, load case 7 governs as there lower factors on the dead load (compared to load case 5) and there is no live load. The total tension that must be resisted at story 1 is found to be 922 kips for a moment about the x-axis and 922 kips for a moment about the y-axis. The total tension to be resisted is obtained by summing the forces in the z-direction in Figure 3.8. Load Case 7 should be used as the governing load case for tension design. The tension on each story for x and y-direction walls is given Table 4.26.

**Table 4.26:** Tension in x and y direction on each story.

Story	1	2	3	4	5	6	7	8	9	10	11	12
Tension x	922	795	669	543	422	306	199	106	32	-19	-39	-22
Tension y	922	795	669	543	422	306	199	106	32	-19	-39	-22

It is found that on story 1, each exterior wall will require 10 ATS rods. The rods are 10/8" in diameter with a strength of 103.5 kips. In stories 10, 11, and 12, the restoring moment due to the weight is larger than the moment due to the story forces,

and therefore no ATS rods are necessary. The number of rods required per story for each exterior wall is shown in Table 4.27.

**Table 4.27:** Number of ATS rods required at each exterior wall, by story.

Story	1	2	3	4	5	6	7	8	9	10	11	12
No. Of (Rods)	9	8	7	6	5	3	2	1	1	0	0	0

It should be noted that the size or number of the ATS rods can be decreased at upper stories. For example, of the 9 ATS rods used in story 1, only 8 would have to continue through story 2, 7 through story 3, and so on. Alternatively, 9 rods could be used throughout the entire structure on each wall with SST coupling devices used to decrease the rod size in upper stories.

## 4.12 Overturning Moment Shear Transfer

The largest shear that the building experiences will be the total compression on the building, which is 7230 kips, or 603 kips of shear on each story. This shear will need to be transferred through every cross-section of the building.

### 4.12.1 Panel and Wall Shear Transfer

The tabulated values used to calculate  $(Ib/Q)_{eff}$  are shown in Table 4.28. Note that only the top half of the CLT panel is used, as it is a Q calculation.

**Table 4.28:** Tabulated values used to calculate  $(Ib/Q)_{eff}$ .

Layer	E (x10 <sup>6</sup> psi)	z (in)	Ehz
1	1.7	2.75	6.428
2	1.2/30	1.375	0.076
3	1.7	0.688	0.8041

$(Ib/Q)_{eff}$  is found to be 60.23  $in^2$ .  $F'_v$  is determined to be 918 psi from equation 3.26. From equation 3.25, the shear strength for a 1' width of CLT panel is equal to 55,291  $\frac{lb}{ft}$ . Multiplying the shear strength by 35' (assuming only half of the building length is able to take shear due to gaps in the floor) gives a strength of 3870 kips per story, which is able to resist the 603 kips of shear imposed on the story.

It is conservatively assumed that the exterior walls will not take any of the shear load. The height of interior walls on each story needed to take the shear can be

calculated by dividing the demand, 603 kips, by the strength, 55.3 kips/ft, giving a required height of 11 feet. Therefore, as long as two interior wall are present across a panel-to-panel interface with no other way of resisting shear, the shear will be adequately transferred. However, this shear transfer mechanism is not available at the long splices of floor where there are no interior walls. A connection detail must be installed at the splice to transfer this shear demand.

#### 4.12.2 Floor Panel Connection Design

There are two locations in the weak direction where a 70' long gap in the floor with no CLT panel to take the shear. The two locations are shown in Figure 4.3. In these cases, the floor panel connections will take all of the shear (albeit realistically with some contribution from the exterior walls).

If the 70' long gaps were moved to overlap the adjacent wall lines, there would not be enough wall length available for the walls to properly develop the shear that must be transferred. Therefore, instead of placing the gaps near wall lines, the gaps are placed directly between two wall lines, and a connection is designed to resist the forces that must be transferred across the gap.

Because the shear connections are placed directly between two wall lines, an inflection point will occur at the shear connections. Therefore, there will be no moment being transferred between the floor panel connections; only shear.

The first failure mode is checked using equation 3.28 a V of 603 kips, assuming 1.375" diameter dowels. It is found that over the 70' length of the interface, 19 steel dowels are required.

The second failure mode is checked using equation 3.29. The minimum length of the connection for perpendicular to grain compression is found to be 4.5 inches.

The third failure mode is checked using equation 3.28. The minimum thickness required for shear of the steel is found to be 0.066" thick.

The fourth failure mode is checked using equation 3.30, where the length of the connection is assumed to be 6" (greater than the minimum of 4.5 inches),  $I = \frac{1}{12}bt^3$ , and b is 70'. The minimum required thickness of steel is found to be 0.729 inches.

From the design constraints of each failure mode, each 70' interface will have 19 equally spaced 1.375" diameter dowels, held in place by steel end caps that are 6"

long at the top and bottom and 3/4" thick.

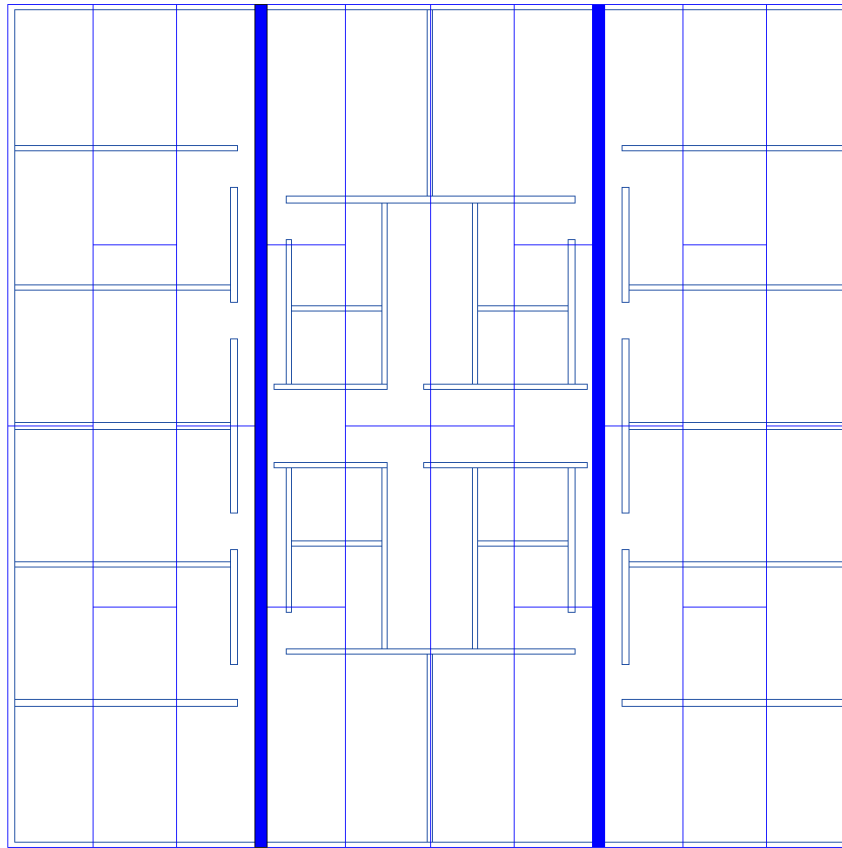


**Figure 4.3:** The locations of the panel-to-panel interfaces with no interior walls to resist shear.

#### 4.13 Lateral Wind Load Check

The basic wind speed,  $V$ , is determined from ASCE 7-10 Fig 26.5 1A, for Risk Category III buildings (to be conservative). From the table,  $V$  is found to be 115 mph.

ASCE Load Combination 6 will be used,  $0.9D+1.0W$ . From ASCE 7-10 Table 26.6-1, the wind directionality factor,  $k_d$ , is found to be 0.85. Because the building is in an urban area and over 30 ft tall, the surface roughness category is B and the exposure category is C.

Because the building is not low-rise, the direction procedure found in ASCE 7-10 Chapter 27 will be used. The building is designated as an enclosed simple diaphragm building in accordance with section 26.2, which allows Part 2 to be used. The building is classified as a Class 2 building. From section 26.8,  $k_{zt}$  is permitted to be

1.0. From section 26.10.1, the building is considered to be enclosed.

The net wall pressure,  $p_h$  and  $p_0$ , are found from Table 27.6-1 for exposure C, where  $h=108$  ft,  $\frac{L}{B}=1$ , and  $V=115$ . From the Table and interpolation,  $p_h=46.28$  and  $p_0=35.96$  psf. From Table 27.6-2, it's determined that the roof force required to investigate overturning is 0.

The total overturning force due to the wind at story 1 will therefore be the volume of the trapezoidal prism caused by  $p_h$  and  $p_0$ , which is equal to:

$$\frac{p_h + p_0}{2} * h * L \quad (4.3)$$

Where  $h$  is the total building height and  $L$  is the length of the wall. The force is equal to 310,867.2 lbs, with the centroid located at 56.3 ft from the base. This leads to an overturning moment due to the wind of 17,489 kft, which is less than the seismic overturning moment of 133,352 kft. While the load factors in load case 4 are larger for Snow, Rain, and Live Roof than in load case 5, it is apparent that the overturning moment due to the seismic load will govern due to the full magnitude of difference between the seismic and wind overturning moment.

## CHAPTER 5

### MODELING

AxisVM structural modeling software is used to conduct a non linear analysis of the building design. The model consists of shell elements, gap elements, springs, loads, and nodal supports.

#### 5.1 Full Model

A full isometric view of the model is shown in Figures 5.1, 5.2, and 5.3. Figure 5.1 shows the building with hidden lines and labeled supports and ATS rods. Figure 5.2 shows the rendered building. Figure 5.3 shows the wire-frame model. The exterior walls are split into 35' sections for the model, as 70' sections are difficult for transportation and installation.

#### 5.2 CLT Panels

Most of the CLT modeling parameters can be obtained from Table 4.2 and Table 4.3, and plugged directly into AxisVM material properties. The AxisVM inputs are shown in Figure 5.4. The CLT panels are modeled as shell elements.

Poisson's ratio should have 6 inputs: one for each combination of stretching (x, y, z) and shrinking (x, y, z). However, AxisVM only allows for one Poisson's ratio input,  $\nu$ , which is taken as 0.29. 0.29 is the maximum Poisson's ratio value for wood.[23]

The thermal expansion of wood ranges from  $17 \times 10^{-6}$  to  $25 \times 10^{-6}$  in/in/°F. The maximum value of  $25 \times 10^{-6}$  in/in/°F is used.[23]

The 5% modulus of elasticity value,  $E_{0.05}$ , is 5% of the strong-direction modulus of elasticity, which is equal to 85 ksi.

PRG 320 assumes the shear modulus,  $G$ , is equal to  $E/16$ . The mean shear modulus is reported as the mean of 3 layers of strong direction and 2 layers of weak direction wood, which gives a  $G_{mean}$  of 93.75 ksi.

The  $k_{cr}$  value is a coefficient for cracking, and is taken as 1.[24]

The partial factor,  $\nu_m$ , is taken as 1.

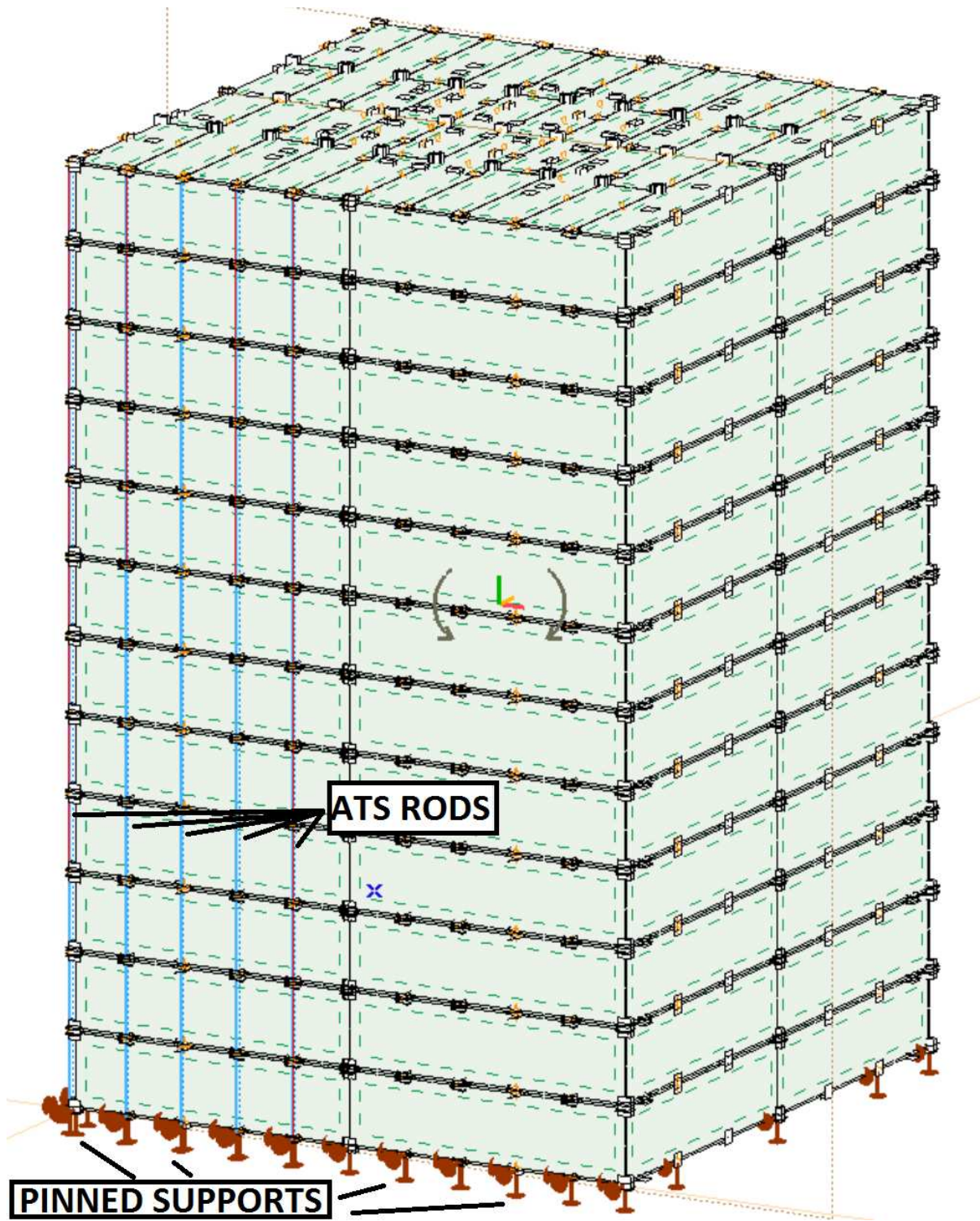
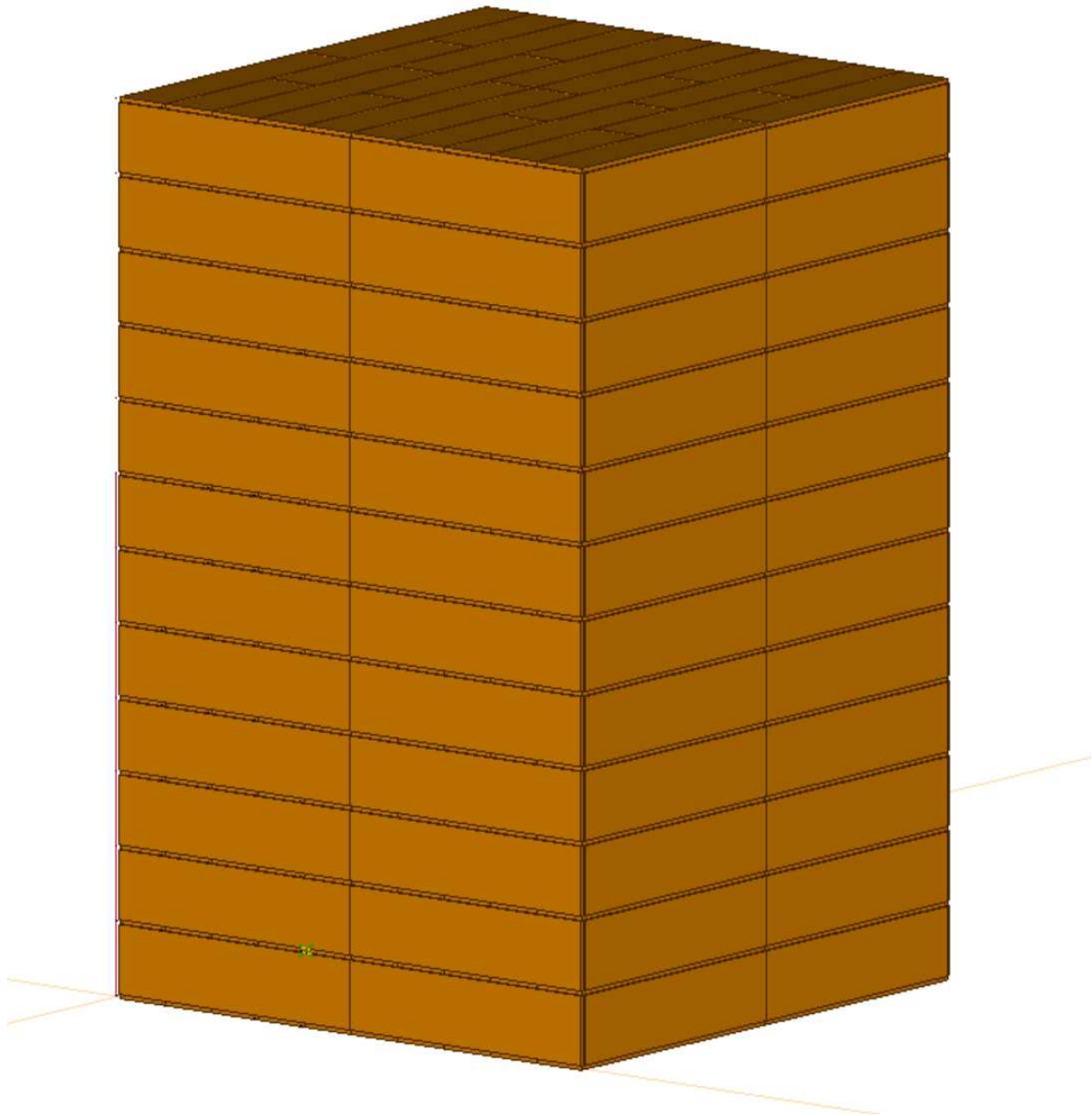
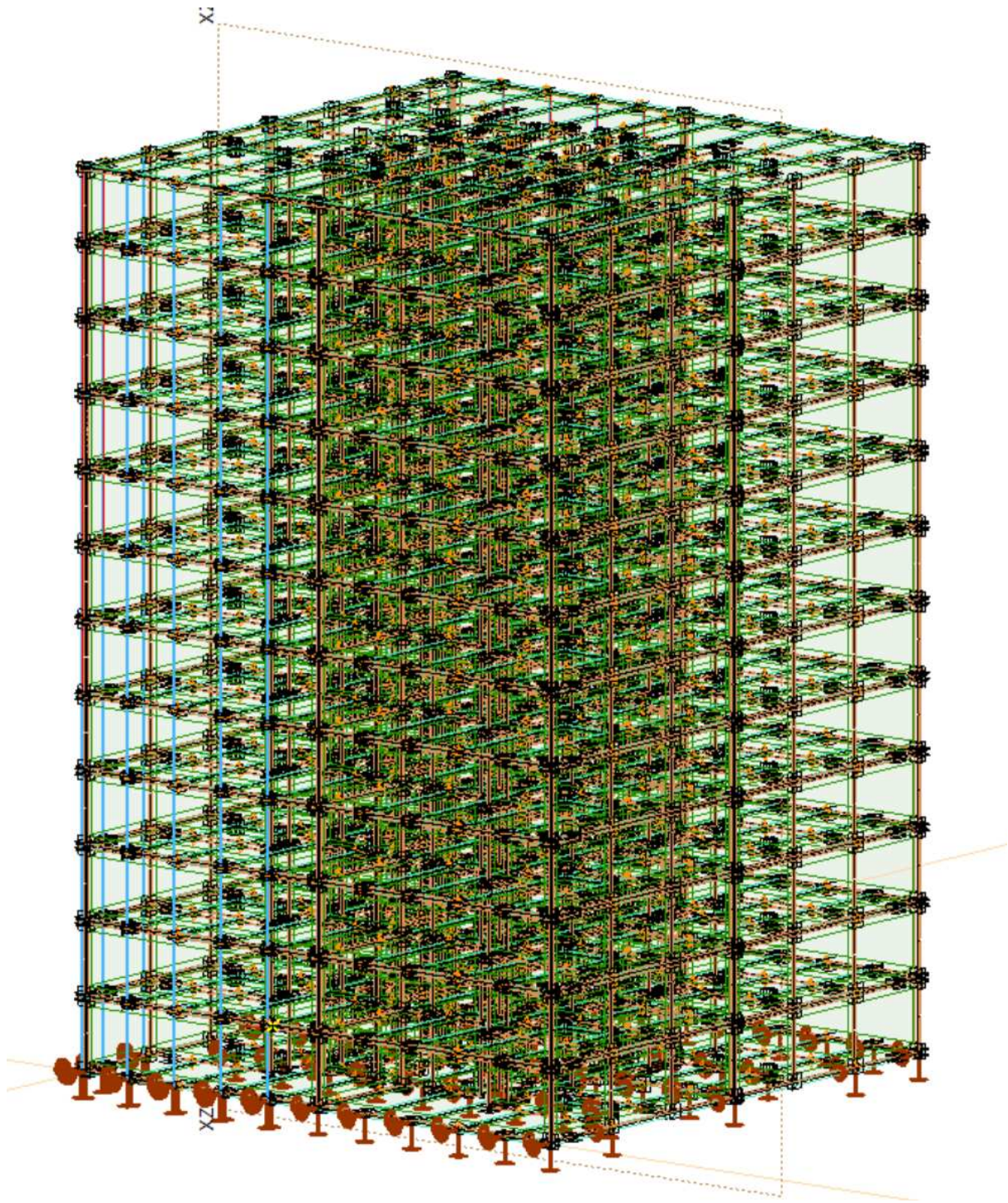


Figure 5.1: Model of a 12-story CLT building.



**Figure 5.2:** Model of a 12-story CLT building.



**Figure 5.3:** Model of a 12-story CLT building.

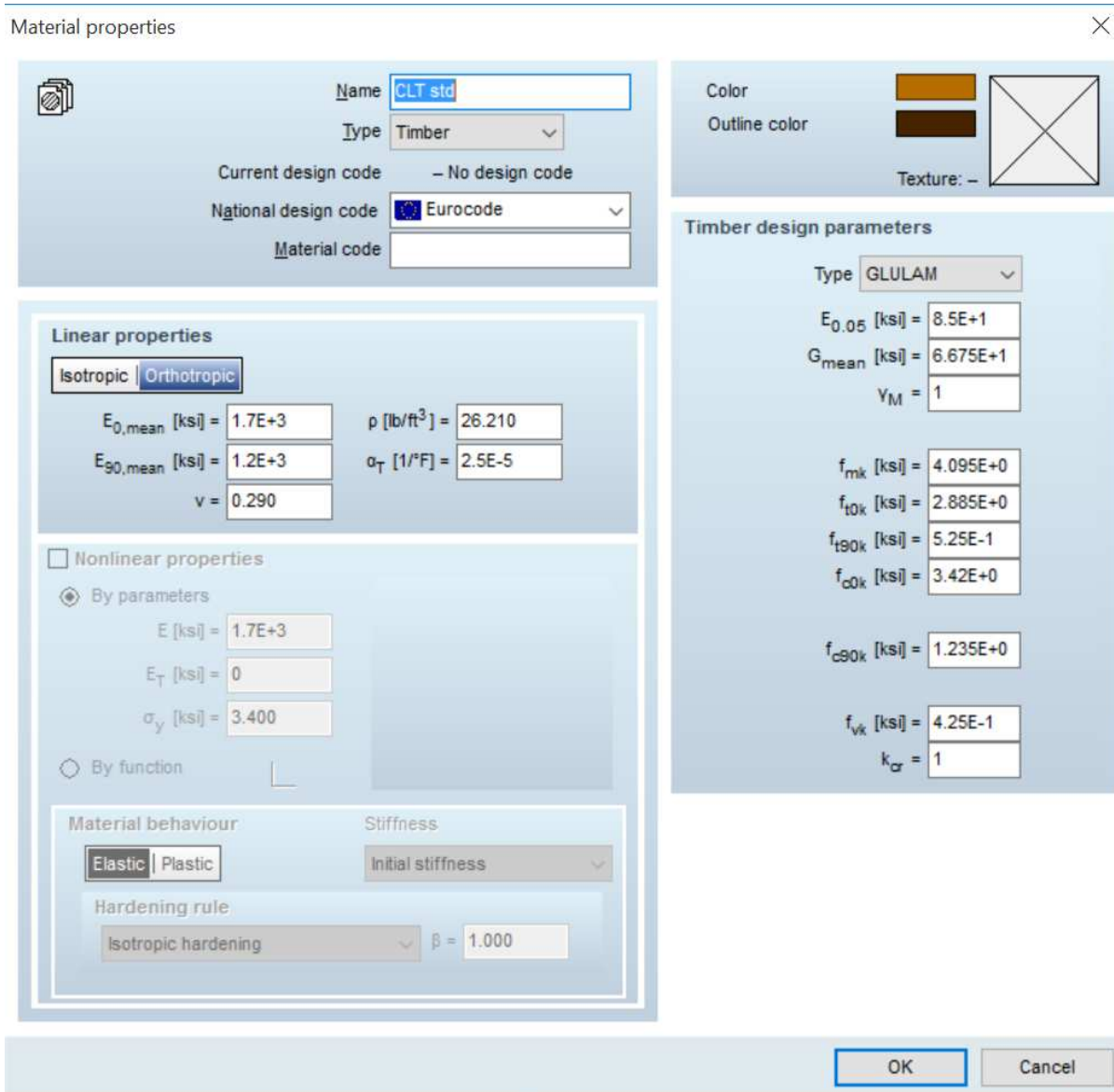


Figure 5.4: CLT properties used in AxisVM.

### 5.3 Connection Elements

Because the analysis is linear, the connections are modeled using stiffness parameters. The parameters are estimated from proprietary connection data from Simpson Strong Tie. The stiffness is 15238 lb/in in direction F1, 34233 lb/in in direction F2 and F3, and 29809 lb/in in direction F4 in reference to the directions in Figure 3.2. The factored maximum allowable strength in F1, F2, F3, F4 is 2688 lbs, 1766 lbs, 3289 lbs, and 2109 lbs respectively. The stiffness parameter in the z (vertical direction) and y (horizontal shear) for the floor panel connections are calculated using the equation for the shear modulus:

$$G = \frac{F/A}{\Delta x/l} \quad (5.1)$$

Where  $G$  is the shear modulus,  $\frac{F}{\Delta x}$  is the stiffness parameter,  $l$  is the length of the connection, and  $A$  is the cross-sectional area of the connection.  $G$  for steel is given as 10800 ksi,  $l$  is taken as the full 12 inches length of the connection to be conservative, and  $A$  is the cross-sectional area of a 1.375" diameter steel rod. Using these values, the stiffness parameter is determined to be 2673 kip/in for each connection for shear.

The stiffness parameter in the  $x$  (axial) direction can be determined using the equation for deformation strain:

$$\frac{P}{\delta} = \frac{AE}{L} \quad (5.2)$$

Where  $\frac{P}{\delta}$  is the stiffness parameter,  $A$  is the cross-sectional area,  $E$  is the modulus of elasticity of steel (given as 29000 ksi), and  $L$  is the length of the connection (12 inches). The axial stiffness parameter is determined to be 3588 kip/in for each connection.

Two gap elements are used for every CLT panel-to-panel interface to prevent overlapping panels during deflection. To simplify the mesh and decrease model run-time a maximum of two springs are used for each CLT panel interface with stiffness parameters defined based on the connection stiffness and the number of connections the spring is representing. The number of connections represented by the spring is determined by the length of the panel and the required spacing of the connections.

The number and location of gap elements and springs will remain constant from story to story, however the stiffness of the springs will decrease as the story number increases. The stiffness is inversely proportional to the spacing. The stiffness of the springs in the interior walls is double that of the exterior walls.

The gap elements are placed as close as possible to the end of each wall without disturbing the mesh. The gap elements are compression elements, meaning the gap can expand with almost no resistance (very low stiffness), but when contact is created (due to compression), the gap develops a very large compression stiffness.

An example of gaps and springs placed in the model is shown in Figure 5.5. Gaps are circled, while springs are boxed. The portion of the building shown is a corner, with two CLT floor panels and walls above and below them. Note that the gaps and springs are placed such that the connection to the floor panels occurs on the edge

of the floor panels.

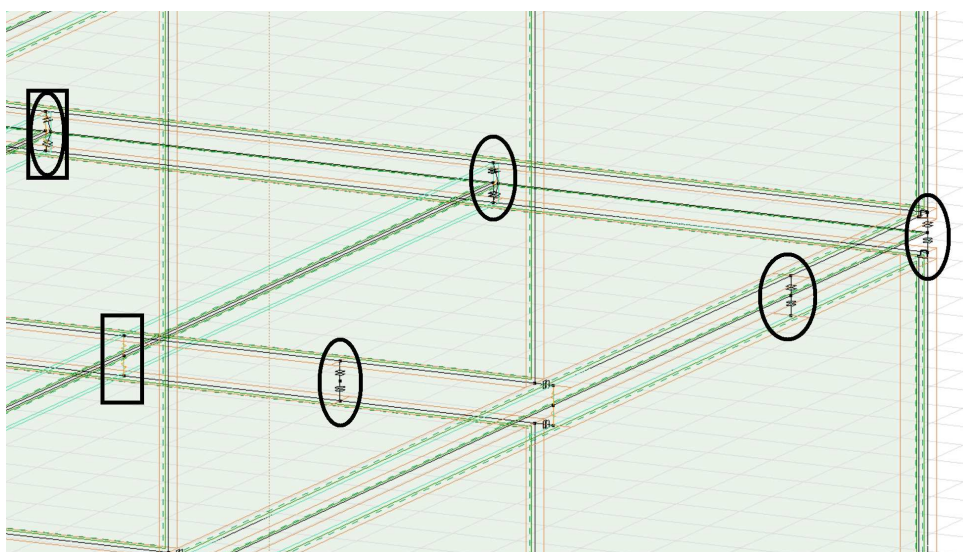


**Figure 5.5:** Example of gaps and springs in the model

#### 5.4 Mesh

The springs and gap elements are placed strategically in order to make the mesh as simple as possible. The mesh is generated with a target of using 48” quadrilateral elements. When nodes are closer than 48” to each other, the mesh is finer. All elements in the mesh are quadrilaterals, which satisfies the desired mesh properties.

#### 5.5 Load Cases

For both load case 5 and 7, an analysis was run for lateral loading applied (at each story) in the x and y directions. Each load case also contains live load and dead load, including gravity load. Figure 5.6 shows example lateral loading the y-direction.

#### 5.6 ATS Modeling

The ATS rods are modeled as truss elements, attached at each end to the side of the building with rigid springs (ie, the strongest springs possible). The rods are also placed not to disturb the mesh. This restriction leads to 7 rods being placed on the y-direction wall and 8 rods placed on the x-direction wall. The rods are sized equally and add up to the total area of steel on each story. For instance, on story 1, 9 rods at 10/8” diameter each are required per the design analysis. Therefore, 11.04 in<sup>2</sup> of steel is

required on each wall. Split between 7 rods for the y-direction walls, this amounts to 1.58 in<sup>2</sup> per rod, or a diameter of 1.42" per rod. In upper stories, where zero ATS rods are required, an equivalent of 1 ATS rod is still used.

For the x-direction load cases, only rods on the west (left) half of the building are included, as the east ATS rods are expected to be in compression and the ATS rods have an assumed compression design strength of zero ksi. For the y-direction load cases, only rods on the south half of the building are used. The ATS rod layout for the x-direction load cases is shown in Figure 5.8. The locations of the ATS rods are circled. Additionally, the gaps used on the walls are represented by squares. The springs are also visible as faded orange zig-zags.

The inputs used to model the steel are shown in Figure 5.7. Note the mass of the ATS rods is taken to be zero so as not to interfere with the stiffness of the CLT. This would be more important in a dynamic analysis.

## 5.7 Supports

Pin supports were placed at the corners of every ground-level floor panel as well as the ground-level ATS rod bases to ensure accurate load transfer into the ground and ensure stability. This enables compression load to be transferred into all wall lines, instead of being concentrated to exterior wall lines (if there were only supports on the exterior).

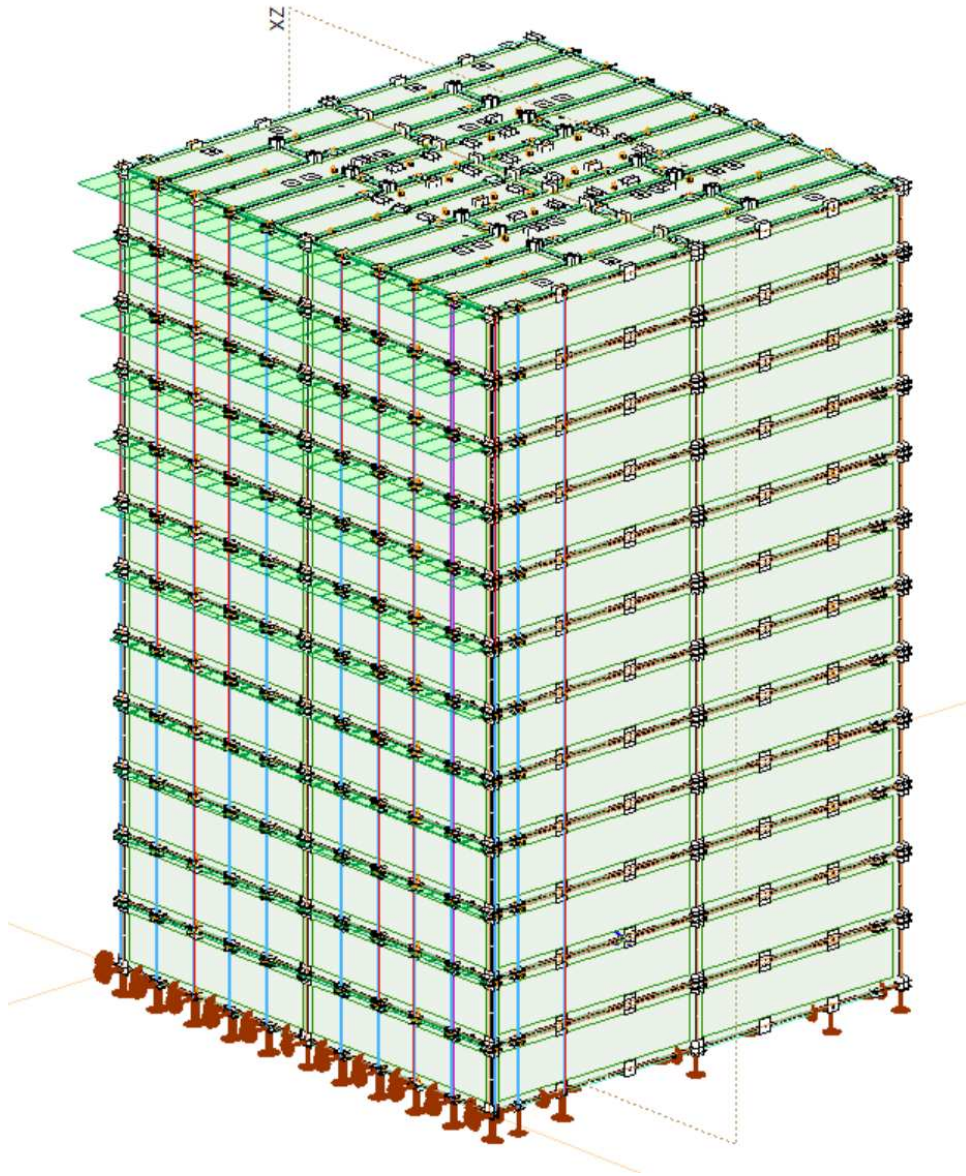


Figure 5.6: y-direction lateral loading

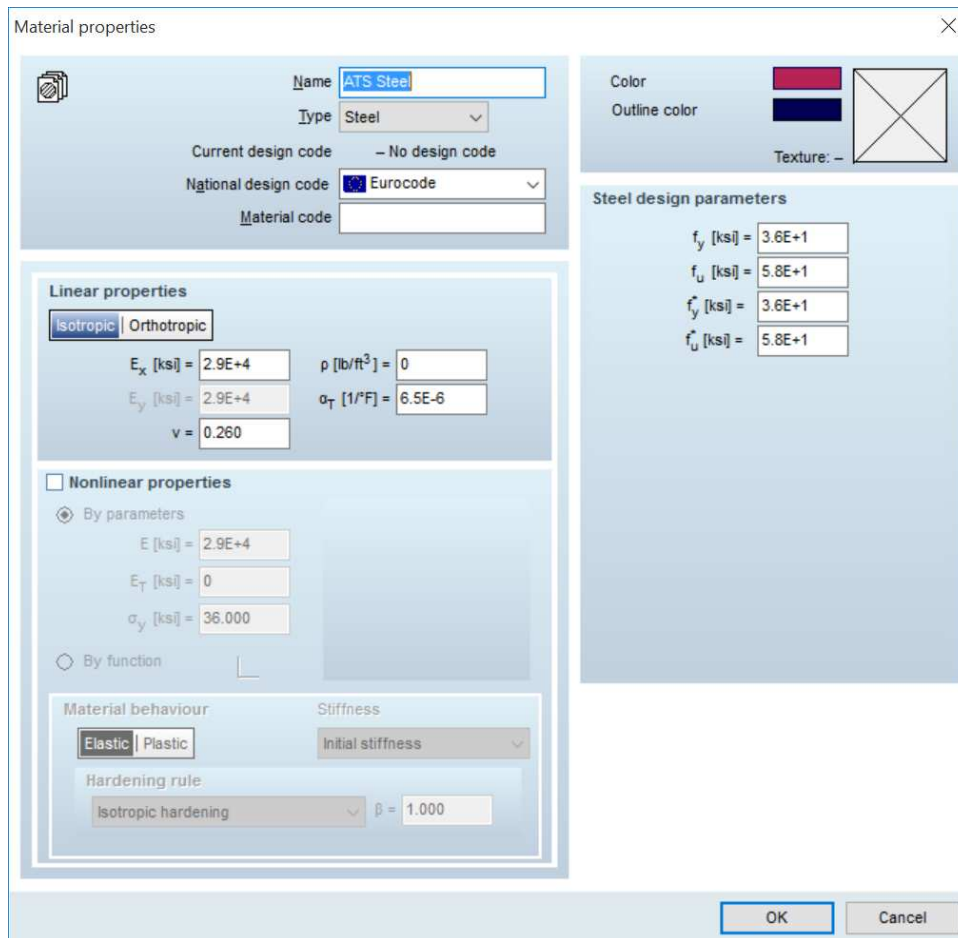


Figure 5.7: Steel properties used in AxisVM.

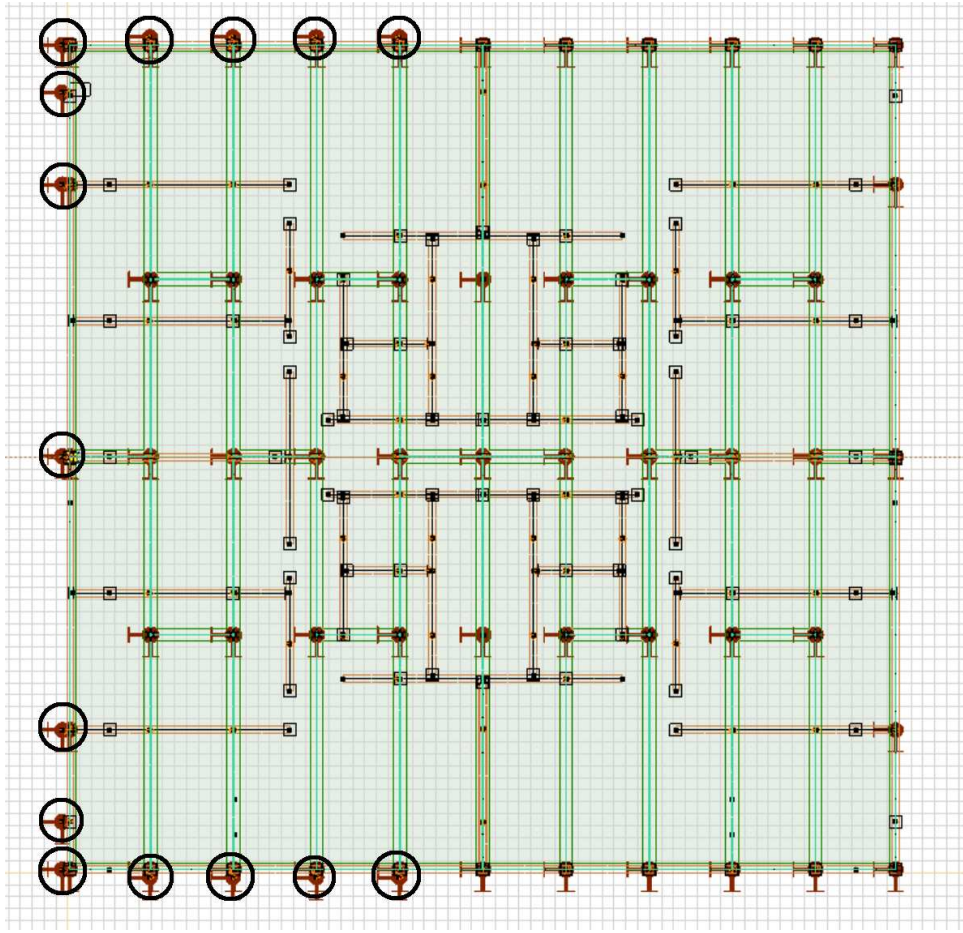


Figure 5.8: ATS rod placement for x-direction loading.

## CHAPTER 6

### NONLINEAR STATIC ANALYSIS

A nonlinear analysis is run for load cases 5 and 7 with lateral loading in the x and y directions. The results of interest are the global deformation shape of the model, the tension forces in the ATS rods, the shear forces in the springs, the shear forces in the panel-to-panel connection springs, and the compression experienced at the base story due to overturning. The wall lines referenced in the following sections are labeled in Figure 4.1. The ATS rod labels are shown in Figure 6.1 for x-direction loads and Figure 6.2 for y-direction loads.

The initial results are promising in terms of the feasibility of the design. The discrepancies between the expected design values and the model values were identified and explained based on decisions made in the modeling process.

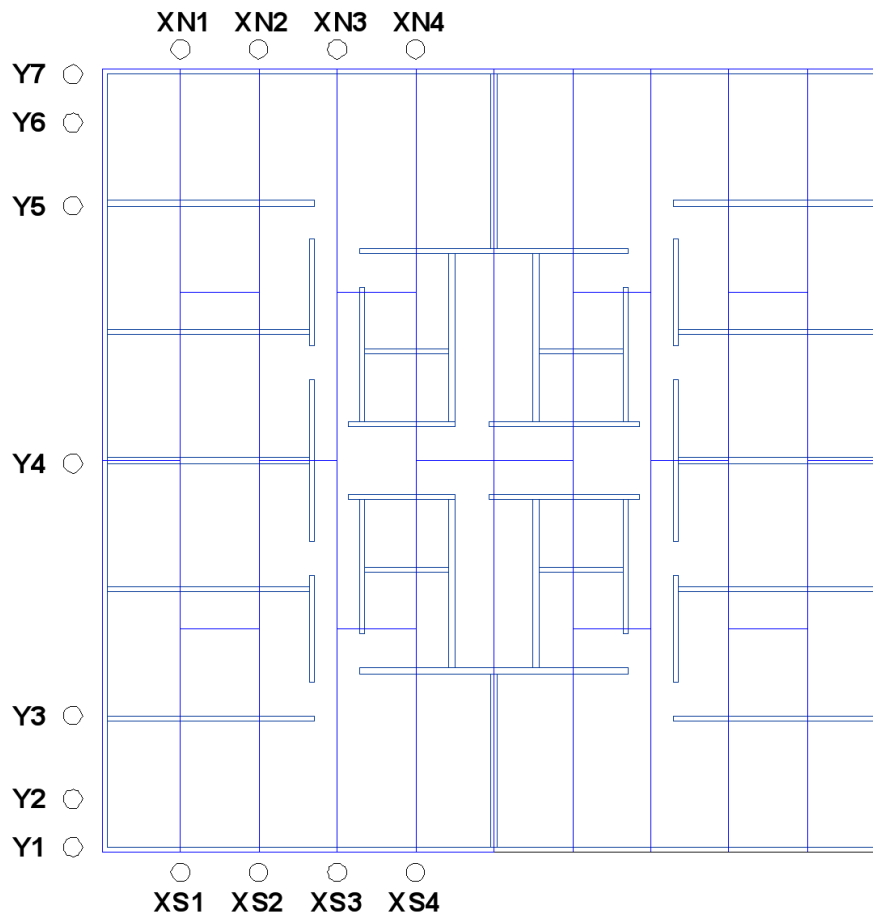


**Figure 6.1:** ATS rod labels for x-direction loading.

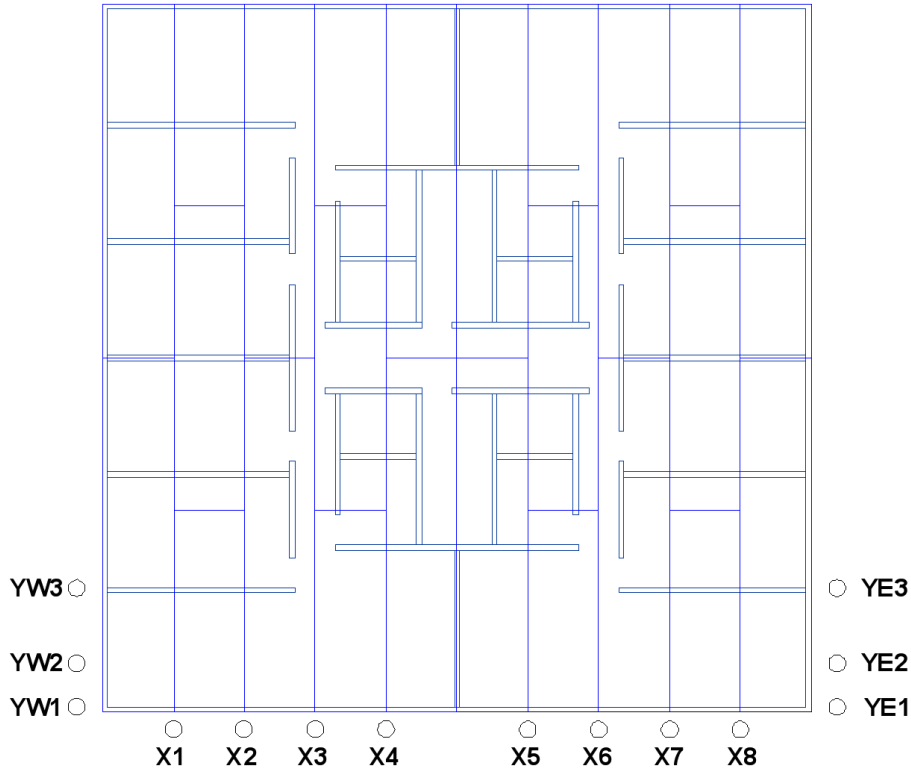


**Figure 6.2:** ATS rod labels for y-direction loading.

## 6.1 Global deformation

Figure 6.3 shows the global deformation for load case 5 in the x-direction. The displacement at the center node in the circled line of nodes is 3.321" in the x-direction, with a total displacement of 3.631". Figure 6.4 shows the global deformation for load case 7 in the x-direction. The displacement of the center node in the circled line of nodes is 3.537" in the x-direction, with a total displacement of 3.3.625". Figure 6.5 shows the global deformation for load case 5 in the y-direction. The displacement of the center node in the circled line of nodes is 4.376" in the y-direction, with a total displacement of 4.391". Figure 6.6 shows the global deformation for load case 7 in the y-direction. The displacement of the center node in the circled line of nodes is 4.509" in the y-direction, with a total displacement of 4.514". In order to more clearly show the deflected shape of the shear connections that are expected to behave as coupling beams, Figure 6.7 shows the amplified deformation for load case 7 in the x-direction.

Figure 6.7 shows that the building is not behaving in a truly rigid manner, but is still able to transfer shear throughout the building. Because of the use of pin

connections at the bottom of the building (which represent the foundation), the building is restrained from truly overturning as one structure. The circled areas on the deformed shape show examples of the panel-to-panel interface acting as a coupling beam, where the rest of the building is acting like shear wall stacks. Despite the not truly rigid behavior, as long as the coupling beams (and all other cross sections) are able to transfer the shear forces, tie-down rods will not be necessary in the interior walls. Additionally, the displacement between point A and point B in the Figure 6.7 in the z-direction is 0.351 inches for load case 7, compared to x-direction deformations of 3.603 and 3.563 inches for point A and B respectively, meaning the building is deflecting more globally than it is locally. The deformation is primarily bending-controlled with some shear deflection present.

## 6.2 ATS Rod Forces

The expected worst-case (load case 7) ATS rod forces in the first story compared to the ATS rod forces determined by the analysis are shown in Figure 6.8 for the x-direction load and Figure 6.9 for the y-direction.

The ATS rod forces on each story are shown in Table 6.1 for the x-direction load and Table 6.2 for the y-direction load.

In Figure 6.8, it is apparent that the tension due to overturning moment is greatest at the corners of the building. The initial design assumed even distribution of ATS rods based on the assumption that the out-of-plane floorplan was rigid. However, it is apparent that the middle of the floorplan is less stiff, and therefore the rods in the middle are not as effective. In Figure 6.9, the ATS rods at the edge take the largest amount of tension.

By comparing Table 4.26 with the total values in Table 6.1 and Table 6.2, it can be seen that the total tension in each story is less than expected. In story 1, for example, the expected total tension is 922 kips. For the x direction, the model gives a tension of 705 kips, and in the y direction gives a tension of 635 kips. This is an indication that the ATS rods have enough strength to resist the tension demands, as long as they are properly placed or allowed to reach inelastic failure and distribute the forces to other rods.

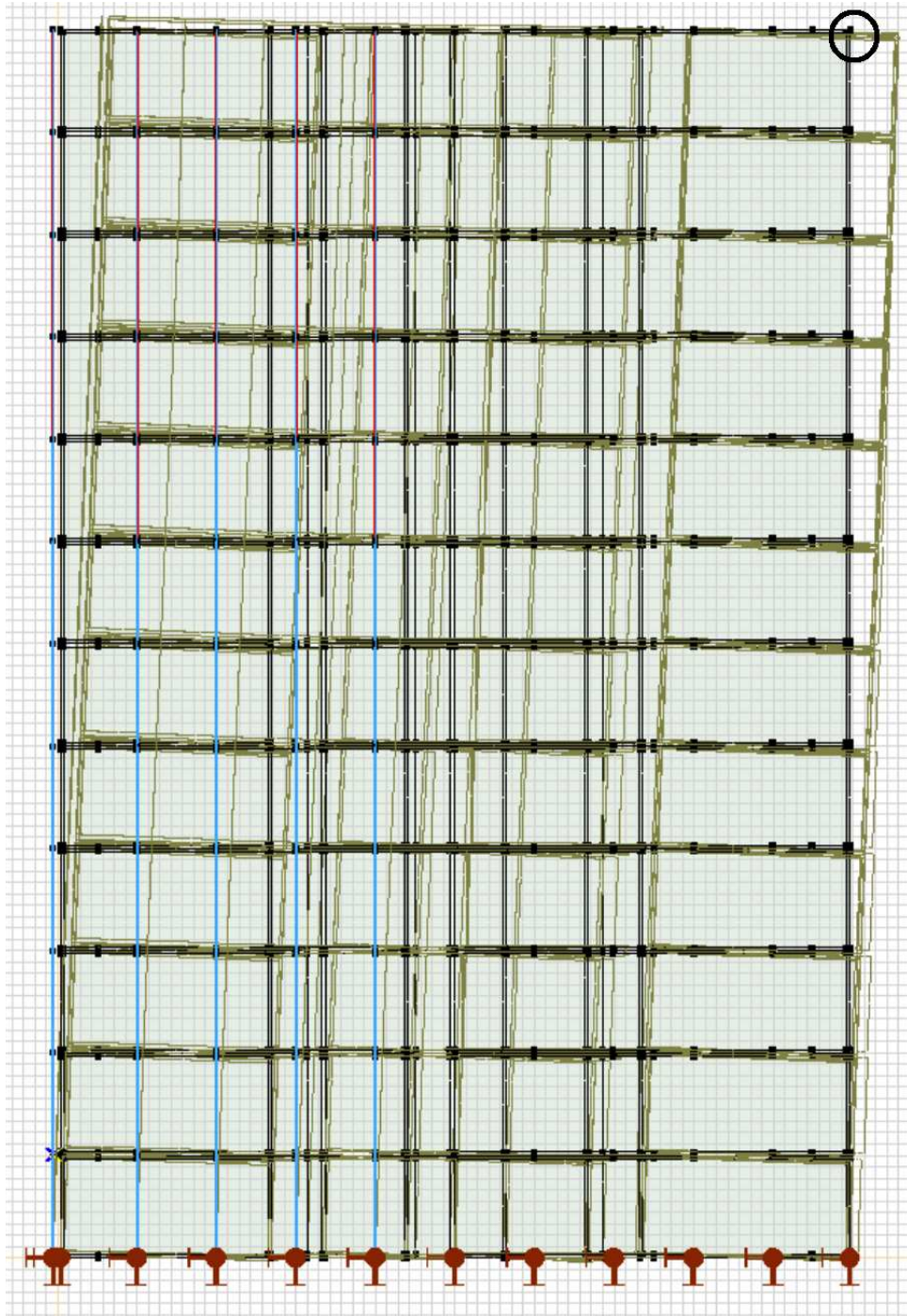


**Figure 6.3:** Global deformation for load case 5 in the x-direction

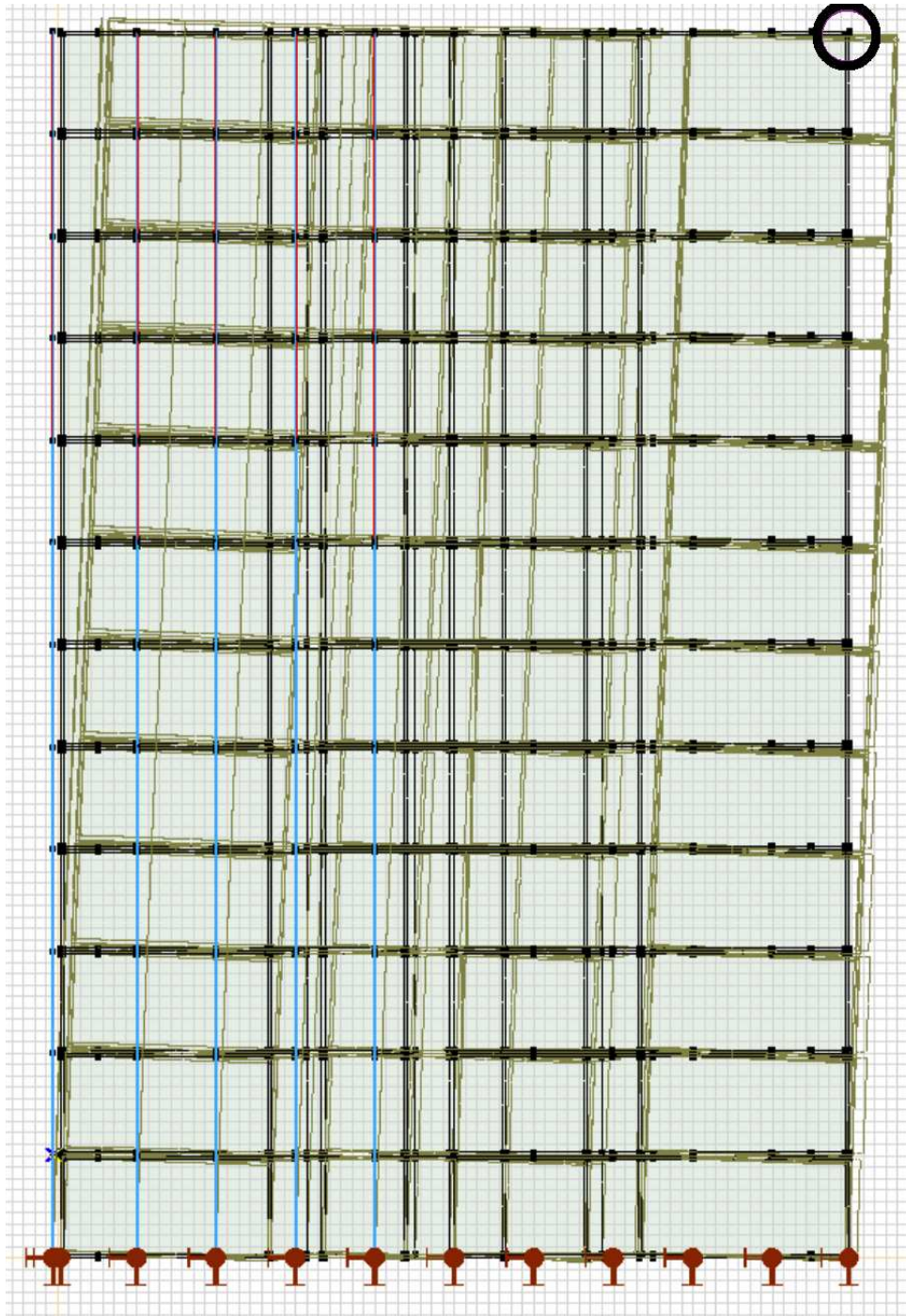


Figure 6.4: Global deformation for load case 7 in the x-direction

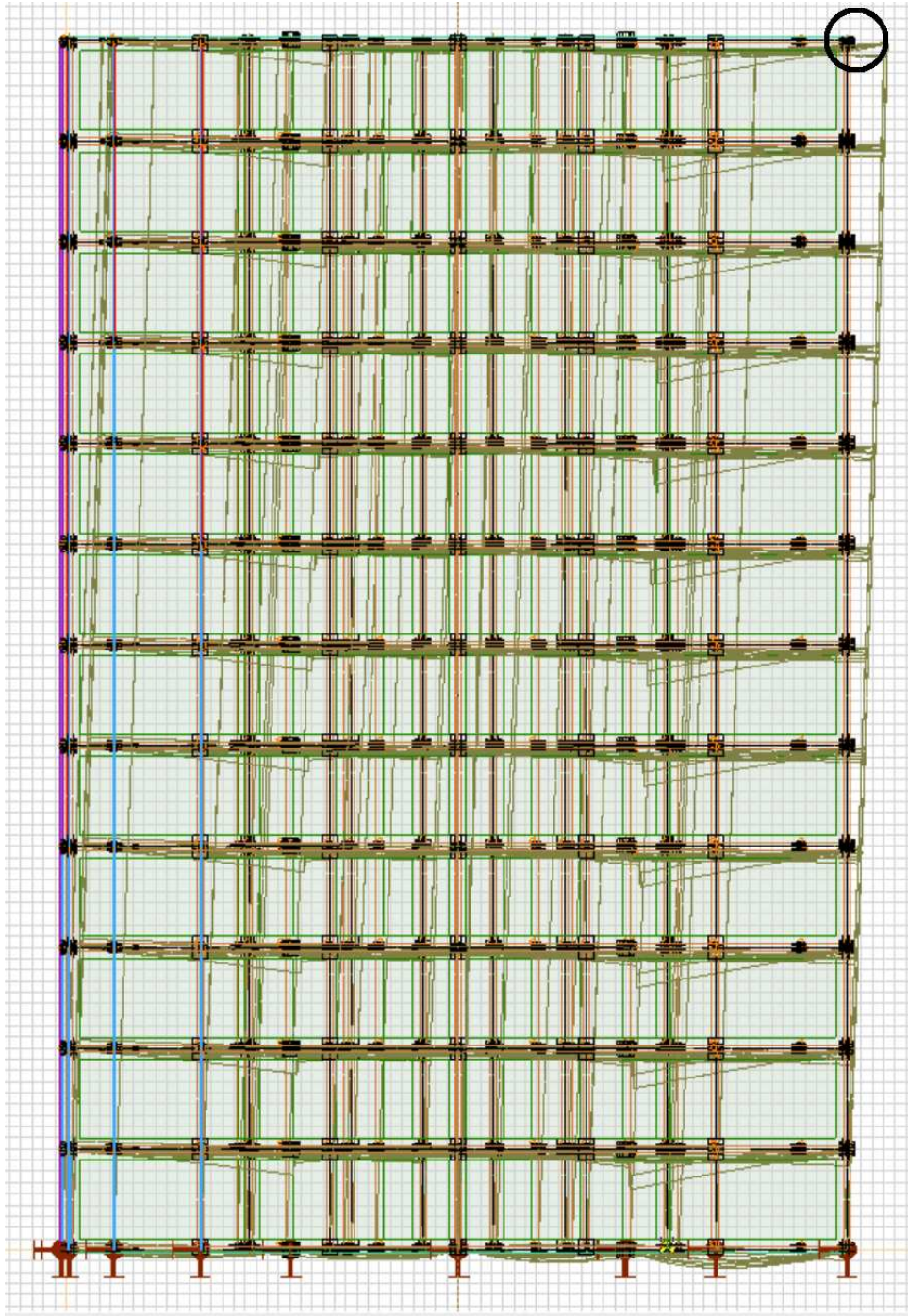


Figure 6.5: Global deformation for load case 5 in the y-direction

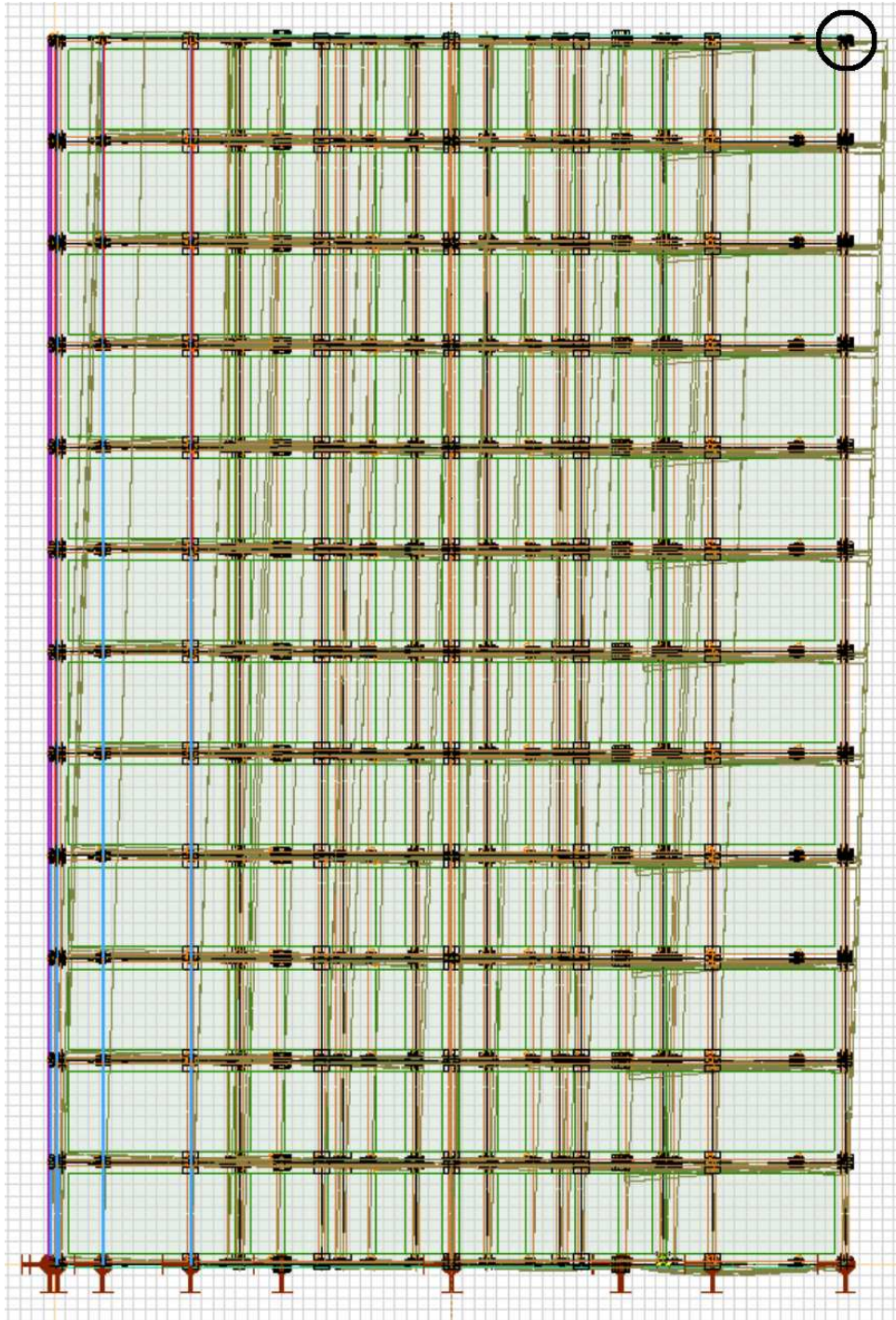


Figure 6.6: Global deformation for load case 7 in the y-direction

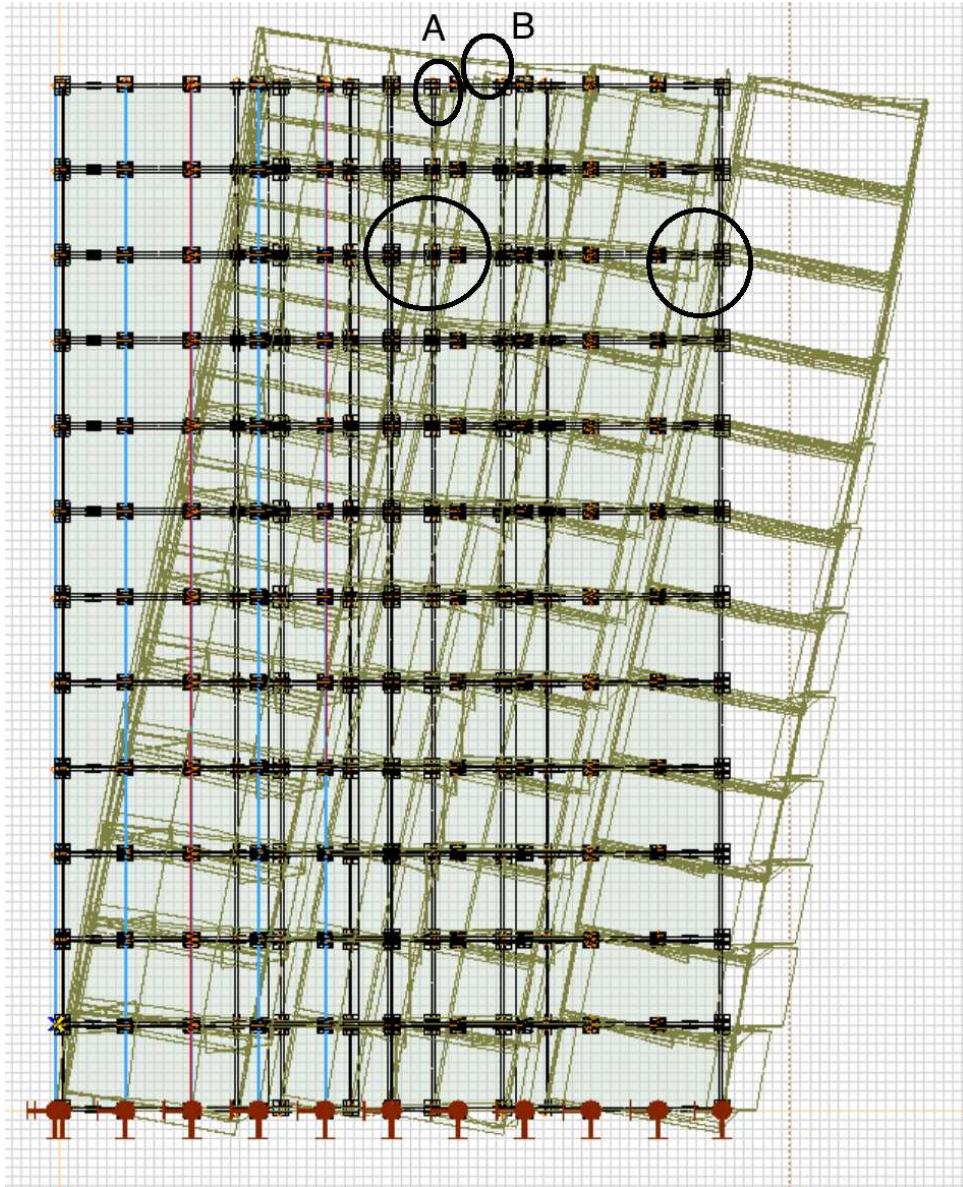
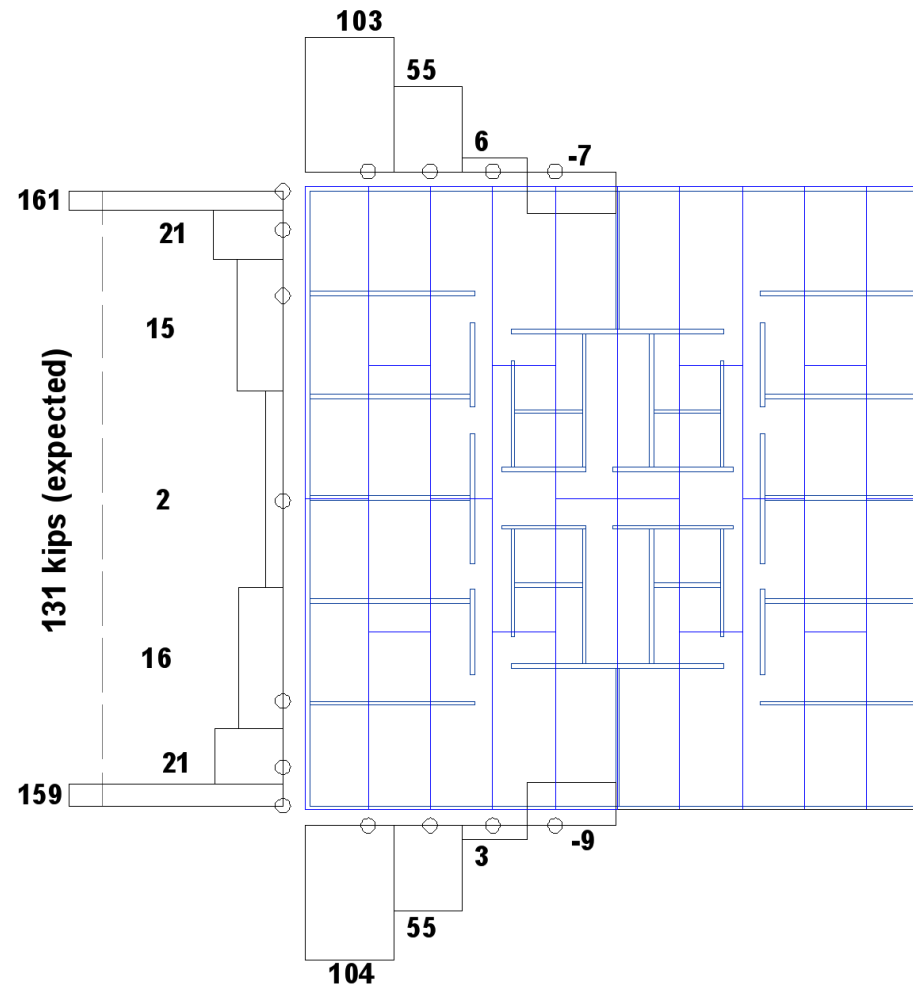
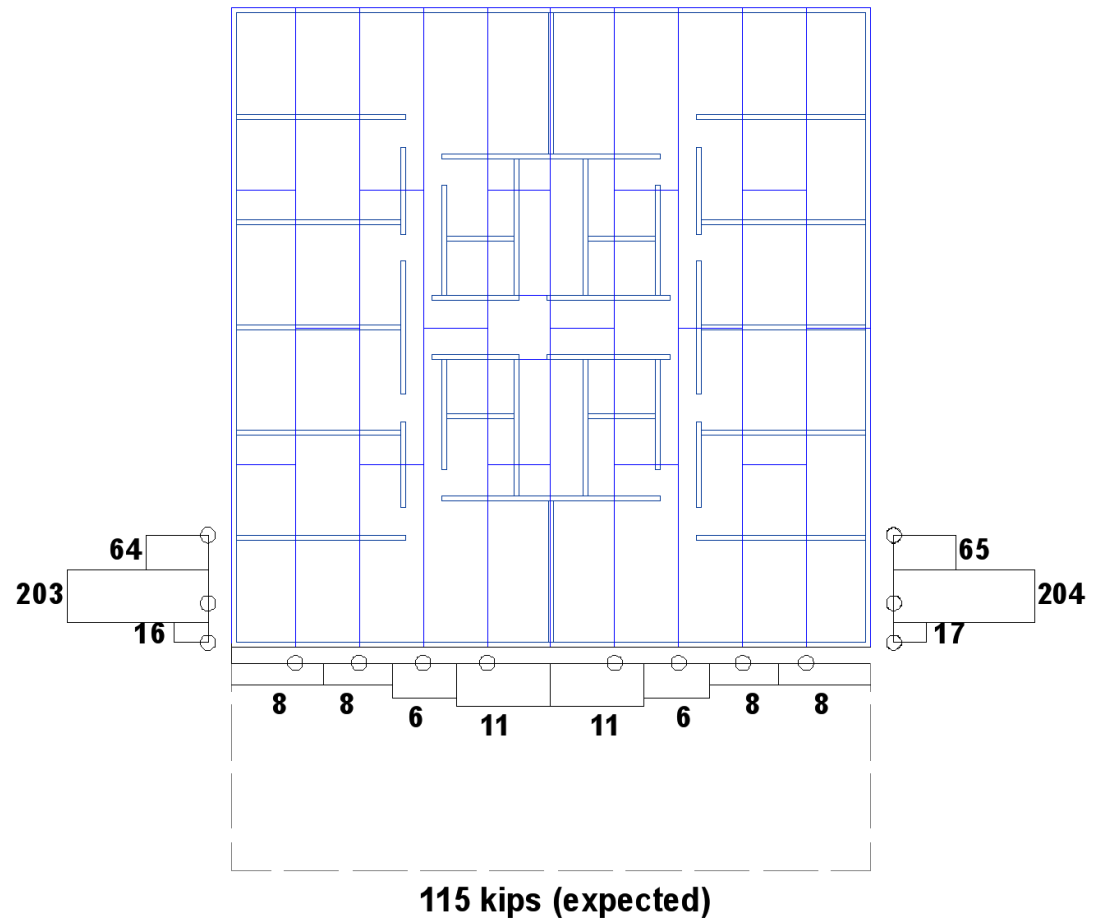


Figure 6.7: Amplified deformation for load case 7 in the x-direction



**Figure 6.8:** Story one ATS rod forces compared to the expected value for load case 7 x-direction loading



**Figure 6.9:** Story one ATS rod forces compared to the expected value for load case 7 y-direction loading

**Table 6.1:** Forces (kips) in each ATS rod for x-direction loading.

ATS Rod	1	2	3	4	5	6	7	8	9	10	11	12
<b>Y1</b>	159	117	83	56	37	23	13	5.2	1.0	-0.2	-0.3	0.1
<b>Y2</b>	21	18	15	12	8.7	6.2	4.4	2.3	1.2	0.5	1.0	8.7
<b>Y3</b>	16	15	14	12	8.3	5.8	4.2	1.8	0.9	0.4	0.2	0.1
<b>Y4</b>	1.5	1.5	1.3	1.1	0.8	0.5	0.3	0.1	0.0	0.0	0.0	0.0
<b>Y5</b>	15	13	12	10	6.6	4.4	3.0	1.2	0.6	0.2	0.1	0.1
<b>Y6</b>	21	17	15	12	8.5	6.1	4.3	2.2	1.1	0.5	0.9	8.5
<b>Y7</b>	161	120	86	59	40	25	14	6.3	1.4	-0.2	-0.2	0.2
<b>XS1</b>	104	72	52	38	25	16	10	4.2	1.1	0.2	0.1	0.4
<b>XS2</b>	55	39	34	27	18	12	8.6	3.4	1.7	0.7	0.6	0.2
<b>XS3</b>	3.4	14	17	17	14	10	7.7	3.5	2.0	0.9	1.0	0.8
<b>XS4</b>	-9.2	1.8	8.9	11	9.0	6.9	5.4	2.5	1.4	0.7	0.8	0.8
<b>XN1</b>	103	74	55	40	27	18	11	4.9	1.7	0.2	0.2	0.4
<b>XN2</b>	55	41	36	29	20	13	10	4.0	2.0	0.7	0.6	0.2
<b>XN3</b>	6.3	15	19	19	15	11	8.5	3.9	2.3	1.1	1.0	0.7
<b>XN4</b>	-7.4	3.9	11	13	10	7.8	6.0	2.8	1.7	0.9	0.9	0.5
<b>Total</b>	705	563	460	354	247	166	111	48	20	6.3	6.9	22

**Table 6.2:** Forces (kips) in each ATS rod for y-direction loading.

ATS Rod	1	2	3	4	5	6	7	8	9	10	11	12
<b>YW1</b>	16	14	12	10	7.4	5.5	4.1	2.6	1.5	0.9	1.5	7.6
<b>YW2</b>	203	99	62	39	24	13	7.2	2.3	-0.4	-0.3	-0.4	-0.2
<b>YW3</b>	65	53	44	30	19	12	7.5	2.7	1.3	0.5	0.4	0.2
<b>X1</b>	8.0	4.8	7.8	7.0	5.4	4.3	3.4	1.6	1.2	0.6	0.6	0.7
<b>X2</b>	8.4	7.8	7.7	6.7	5.0	3.8	3.0	1.4	0.8	0.3	0.3	0.1
<b>X3</b>	5.7	8.3	7.6	6.5	5.0	3.8	2.8	1.4	0.6	0.2	0.1	0.0
<b>X4</b>	11	10	7.7	6.2	4.9	3.6	2.4	1.3	0.3	0.0	0.0	1.1
<b>X5</b>	11	10	7.7	6.3	4.9	3.6	2.4	1.3	0.3	0.0	0.0	1.1
<b>X6</b>	5.7	8.3	7.7	6.6	5.1	3.8	2.8	1.4	0.6	0.2	0.1	0.0
<b>X7</b>	8.5	7.9	7.8	6.8	5.1	3.8	3.0	1.4	0.8	0.3	0.3	0.1
<b>X8</b>	8.3	5.0	8.0	7.1	5.5	4.3	3.4	1.6	1.2	0.6	0.6	0.7
<b>YE1</b>	17	14	12	10	7.5	5.5	4.1	2.6	1.5	0.9	1.5	7.6
<b>YE2</b>	203	98	62	40	24	13	7.2	2.4	-0.4	-0.3	-0.4	-0.2
<b>YE3</b>	65	53	44	30	19	12	7.5	2.7	1.3	0.5	0.4	0.2
<b>Total</b>	635	394	298	212	142	92	61	27	11	4.3	5.2	19

### 6.3 Lateral Shear Load on the Bracket Springs

The average shear load on the springs that represent brackets across all the wall lines on each story is given in Table 6.3 for both load cases. All shear loads are taken as positive regardless of their in-plane direction. The shear load in Table 6.3 is

determined at both the bottom and top of the walls in the story. In the table, “b” stands for “bottom” and “t” stands for “top”.

The shear load on each wall line on each story is shown in Table 6.4 and Table 6.5 for the x-direction, and Table 6.6 and Table 6.7 in the y-direction. The required spacing based on the total shear load on each wall line on each story is shown in Table 6.8 and Table 6.9 for load cases 5 and 7 in the x-direction, respectively. Table 6.10 and Table 6.11 give the average required spacing for load cases 5 and 7 in the y-direction. “t” represents the top portion of the story, and “b” represents the bottom.

From Table 6.4 through Table 6.11, it is apparent that the exterior walls take a larger share of the shear than expected and require smaller spacings than expected. The middle of the floor plan is less stiff, and the out-of-plane floor plan is not rigid, which both contributed to the larger shear demands on the exterior walls. The exterior walls are able to use half as many brackets per foot as the interior walls, which means it is more difficult to meet the shear demands. Therefore, one option for design could be to design all of the shear resistance for the interior shear walls, while using as few brackets as possible for the exterior shear walls. The exterior brackets will reach plasticity quickly, but there will be far fewer brackets to repair or replace.

#### **6.4 Floor Panel Connection Force**

The panel connection out-of-plane shear is determined from left (west) to right (east) for each story. The reported values in Figure 6.10 and 6.11 show the total shear force at each 70' long panel-to-panel interface for each story (1 through 12) for load cases 5 and 7, respectively. The bottom interfaces are not included because the supports lead to 0 shear at those locations. The total shear is also shown, as well as a total using the absolute values of the shear at each location.

The floor panel connection shear varies largely from the expected values. The main reason for the variance is that during the design process it, the connections were designed under the assumption that the walls and floor panels do not resist the shear while the floor panel connections are engaged. This is a conservative assumption, as demonstrated in Figure 6.10 and Figure 6.11 by the shear values that are significantly smaller than the expected value of 602 kips at each panel. The small shear values taken by the shear connections demonstrate that the building is theoretically able to transfer

the shear forces across every cross-section, including the coupling beams where the 70' continuous gaps are present.

The shear forces are generally the largest on the east and north sides of the building, and decrease in magnitude towards the west and south ends. This matches the shape of the expected shear diagram, where the largest shear is at the compression end of the building, and decreases in a roughly linear trend in relation to the weight of the building until the tension end of the building. Were total shear shown, including the shear taken by the walls, it is expected that the shear would decrease in a more clearly defined linear trend.

Negative shear values are present, indicating deflection on the compression side that are higher than (relative to z) the deflection on the tension side. The negative shear values at the panel-to-panel interface (between wall lines Y2 and Y3, and between wall lines Y7 and Y8) can be explained by the positive deflection at points A and B (and their corresponding points on the other interface) in Figure 6.7. The positive deflection does not occur at the exterior walls, because there is no discontinuity at the exterior walls between wall lines Y2 and Y3, or between Y7 and Y8. The springs located at the exterior walls will retain positive shear values, however the deflections that occur in the interior of the building will cause larger negative shear values, resulting in an overall negative shear value on the story.

The negative deflection at the middle interface, located at wall line Y5, will occur only at the exterior walls. The interior walls are continuous, while the exterior walls are separated at wall line Y5. The separation causes the exterior walls to rotate separately, leading to a positive deflection (and therefore negative shear) between the west end of the east wall and the east end of the west wall.

## **6.5 Compression Load at Story One Bearing Walls**

The compression load at story 1 is determined using the vertical gap and spring elements at the base of story 1 for the load case 5 model. Because the total compression experienced by the model is desired, any springs that are in tension are not included in the calculation. The compression check only uses the gap and spring elements in the compression zone - ie the zone outside of the influence of the ATS rods.

For the x-direction loading, the compression experienced in the compression

zone is 8346 kips. For the y-direction loading, the compression experienced in the compression zone is 10966 kips.

The compression loads at story one for each direction of loading are larger than the expected values of 7190 kips for x-direction loading and 7230 kips for y-direction loading. Most of the error is due to the initial assumption that the exterior walls would fail before any of the interior walls took any of the compression load. Realistically, the compression will be spread more evenly to the interior walls lines, which have a smaller moment arm, resulting in a larger total compression value.

Note that the compression load does not include springs in tension, meaning there are actually less springs and gaps available than expected to take the compression loading. However, the simplification decisions used in modeling mean that gaps are under-utilized. In a more complex model, there would be more gap elements available to take the compression, which would mean less imbalanced tension members that should be in compression.

**Table 6.3:** Average shear load on the bottom and top each story (kips)

Story		LC5 X	LC5 Y	LC7 X	LC7 Y
<b>1</b>	b	1803	1845	1722	1745
	t	2097	1820	1998	1746
<b>2</b>	b	1923	1762	1835	1744
	t	1839	1744	1799	1744
<b>3</b>	b	1686	1731	1597	1732
	t	1733	1732	1701	1732
<b>4</b>	b	1690	1706	1621	1707
	t	1594	1709	1560	1707
<b>5</b>	b	1491	1660	1425	1661
	t	1586	1664	1575	1662
<b>6</b>	b	1522	1590	1478	1590
	t	1434	1594	1427	1591
<b>7</b>	b	1368	1488	1297	1488
	t	1455	1492	1439	1488
<b>8</b>	b	1369	1349	1331	1349
	t	1309	1353	1260	1349
<b>9</b>	b	1238	1168	1156	1169
	t	1284	1175	1260	1167
<b>10</b>	b	1209	944	1160	948
	t	1120	951	1060	939
<b>11</b>	b	1079	701	994	678
	t	997	682	980	667
<b>12</b>	b	1060	444	975	386
	t	942	438	849	372

**Table 6.4:** Shear (kips) on each wall line on each story, top and bottom, for load case 5 in the x-direction

Story		X1	X2	X3	X4	X5	X6	X7	X8	X9	X10	X11	X12	X13	Total
<b>1</b>	b	536	98	19	43	11	74	277	74	12	39	19	99	502	1803
	t	619	85	18	36	26	80	336	83	24	36	18	87	647	2097
<b>2</b>	b	577	135	6.6	46	13	87	196	89	11	53	6.3	136	565	1923
	t	578	79	4.3	34	12	73	243	75	10	34	4.5	82	610	1839
<b>3</b>	b	532	107	8.1	40	8.0	85	146	88	8.3	38	6.7	109	509	1686
	t	535	84	9.4	31	17	74	199	77	16	32	7.6	84	568	1733
<b>4</b>	b	493	121	16	42	15	91	147	93	14	52	15	121	472	1690
	t	498	68	17	31	10	76	160	78	10	30	16	70	530	1594
<b>5</b>	b	459	100	20	30	5.5	87	106	89	5.9	28	19	101	440	1491
	t	466	92	21	32	17	79	143	81	16	33	20	91	496	1586
<b>6</b>	b	428	111	21	39	16	94	110	97	14	50	21	110	411	1522
	t	436	73	22	27	6.0	78	125	80	6.2	26	21	72	462	1434
<b>7</b>	b	399	99	20	37	7.2	85	95	88	7.9	26	20	99	385	1368
	t	406	99	20	34	18	79	121	81	16	35	20	98	427	1455
<b>8</b>	b	369	100	19	40	16	95	92	97	14	51	19	99	357	1369
	t	372	86	20	34	5.6	77	103	79	5.3	32	21	85	390	1309
<b>9</b>	b	332	98	23	42	8.9	80	89	82	9.2	31	22	98	324	1238
	t	326	96	25	40	18	75	105	77	17	41	25	95	345	1284
<b>10</b>	b	287	94	27	44	17	92	81	93	15	55	29	92	283	1209
	t	271	89	31	40	7.4	72	86	74	6.6	36	32	88	288	1120
<b>11</b>	b	229	94	32	46	13	86	81	87	13	37	34	94	232	1079
	t	194	88	34	50	14	68	95	70	13	51	36	87	197	997
<b>12</b>	b	145	97	44	75	19	109	82	109	17	81	45	95	142	1060
	t	109	105	70	69	17	65	70	67	16	63	74	104	114	942

**Table 6.5:** Shear (kips) on each wall line on each story, top and bottom, for load case 7 in the x-direction

Story		X1	X2	X3	X4	X5	X6	X7	X8	X9	X10	X11	X12	X13	Total
<b>1</b>	t	572	60	22	32	7.5	73	221	76	8.0	29	22	60	541	1722
	b	653	69	21	32	8.3	74	255	77	7.4	32	37	70	664	1998
<b>2</b>	t	599	81	3.3	38	5.5	83	192	86	6.2	41	38	81	582	1835
	b	601	59	2.0	30	4.4	71	208	74	3.9	29	37	60	621	1799
<b>3</b>	t	545	63	10	27	5.6	86	133	89	5.9	26	20	60	527	1597
	b	553	79	11	22	8.0	74	164	77	6.7	22	33	76	576	1701
<b>4</b>	t	504	84	17	30	8.1	91	142	94	6.8	35	42	82	485	1621
	b	514	58	18	23	5.0	77	148	79	5.3	23	17	55	537	1560
<b>5</b>	t	470	68	21	26	5.6	89	88	92	6.0	20	20	66	452	1425
	b	481	95	22	25	11	81	124	83	10	26	21	93	504	1575
<b>6</b>	t	440	95	22	30	10	97	105	99	9.0	36	22	92	423	1478
	b	450	67	22	27	5.5	80	104	82	5.5	26	22	65	472	1427
<b>7</b>	t	409	67	21	35	6.6	88	66	90	7.0	29	21	65	393	1297
	b	416	100	21	29	12	82	105	84	11	28	21	97	434	1439
<b>8</b>	t	373	95	18	33	11	97	88	99	10	37	18	93	360	1331
	b	379	68	20	33	6.2	78	79	80	6.0	31	21	66	393	1260
<b>9</b>	t	333	72	22	40	7.4	82	59	84	7.7	34	22	69	323	1156
	b	332	95	24	34	13	78	95	80	12	34	24	94	345	1260
<b>10</b>	t	288	87	26	37	12	93	78	95	11	40	27	86	280	1160
	b	275	70	29	38	6.7	73	67	75	6.4	35	30	68	288	1060
<b>11</b>	t	233	74	30	46	10	81	58	82	10	41	31	71	226	994
	b	200	85	30	43	11	70	90	72	10	42	32	85	210	980
<b>12</b>	t	145	89	37	62	13	101	83	101	12	63	38	88	142	975
	b	116	86	56	63	14	65	52	66	13	58	59	84	118	849

**Table 6.6:** Shear (kips) on each wall line on each story, top and bottom, for load case 5 in the y-direction

Story		Y1	Y2	Y3	Y4	Y5	Y6	Y7	Y8	Y9	Total
<b>1</b>	b	520	99	157	92	108	92	158	99	520	1845
	t	520	99	129	106	111	106	129	99	521	1820
<b>2</b>	b	516	140	93	73	117	73	93	140	516	1762
	t	516	140	83	74	117	74	83	140	517	1744
<b>3</b>	b	514	151	66	73	119	74	66	152	515	1731
	t	515	151	67	74	119	74	67	152	515	1732
<b>4</b>	b	504	154	61	73	120	73	61	154	505	1706
	t	504	154	62	73	121	73	62	154	505	1709
<b>5</b>	b	486	152	59	73	121	73	59	152	486	1660
	t	486	152	61	72	122	73	61	152	486	1664
<b>6</b>	b	461	146	57	70	121	70	57	146	461	1590
	t	461	146	59	70	122	70	59	146	461	1594
<b>7</b>	b	429	136	54	65	118	65	54	136	430	1488
	t	429	136	56	65	119	65	56	136	430	1492
<b>8</b>	b	391	122	49	58	109	58	49	122	391	1349
	t	391	122	51	58	109	58	51	122	391	1353
<b>9</b>	b	343	105	41	47	94	47	41	106	344	1168
	t	343	105	45	46	94	46	45	106	344	1175
<b>10</b>	b	284	86	34	31	71	31	34	86	285	944
	t	284	86	38	30	72	30	38	87	285	951
<b>11</b>	b	208	66	31	18	55	18	31	66	209	701
	t	208	66	30	14	46	14	30	66	208	682
<b>12</b>	b	107	41	39	12	46	12	39	41	107	444
	t	107	42	30	18	44	18	30	42	107	438

**Table 6.7:** Shear (kips) on each wall line on each story, top and bottom, for load case 7 in the y-direction

Story		Y1	Y2	Y3	Y4	Y5	Y6	Y7	Y8	Y9	Total
<b>1</b>	b	542	92	114	74	99	74	115	93	542	1745
	t	542	92	114	73	102	73	115	92	542	1746
<b>2</b>	b	533	141	75	68	108	68	75	141	534	1744
	t	534	141	75	68	109	68	75	141	534	1744
<b>3</b>	b	528	151	62	68	113	68	62	151	529	1732
	t	528	151	62	68	113	68	62	151	529	1732
<b>4</b>	b	515	150	59	70	119	70	59	150	515	1707
	t	515	150	59	70	119	70	59	150	515	1707
<b>5</b>	b	491	146	59	72	124	72	59	146	492	1661
	t	491	146	59	72	124	72	59	146	492	1662
<b>6</b>	b	462	140	58	72	126	72	58	140	463	1590
	t	463	140	58	72	126	72	58	140	463	1591
<b>7</b>	b	428	131	54	69	124	69	54	131	429	1488
	t	428	131	54	69	124	69	54	131	429	1488
<b>8</b>	b	387	119	50	61	115	61	50	119	388	1349
	t	387	119	50	61	115	61	50	119	388	1349
<b>9</b>	b	339	104	43	50	97	50	43	104	340	1169
	t	339	104	42	49	97	49	43	104	340	1167
<b>10</b>	b	280	88	37	33	71	33	37	88	280	948
	t	280	88	34	33	71	33	34	88	280	939
<b>11</b>	b	205	67	30	15	43	15	30	67	206	678
	t	205	67	25	14	42	14	25	67	205	667
<b>12</b>	b	105	40	29	6.6	25	6.6	29	40	105	386
	t	104	47	16	11	16	11	16	47	105	372

**Table 6.8:** Spacing (inches) on each wall line on each story, top and bottom, for load case 5 in the x-direction

Story		X1	X2	X3	X4	X5	X6	X7	X8	X9	X10	X11	X12	X13
<b>1</b>	b	4.2	24	80	55	80	20	8.6	20	73	62	82	24	4.5
	t	3.6	28	84	66	35	18	7.1	18	37	65	84	27	3.5
<b>2</b>	b	3.9	18	234	52	68	17	12	17	79	45	246	18	4.0
	t	3.9	30	359	69	78	20	10	20	87	71	344	29	3.7
<b>3</b>	b	4.2	22	191	59	114	17	16	17	109	62	231	22	4.4
	t	4.2	29	164	77	54	20	12	19	58	75	204	28	4.0
<b>4</b>	b	4.6	20	96	57	60	16	16	16	66	46	103	20	4.8
	t	4.5	35	90	78	87	20	15	19	88	79	98	34	4.3
<b>5</b>	b	4.9	24	78	80	165	17	23	17	152	85	81	24	5.1
	t	4.8	26	74	75	53	19	17	18	57	72	79	26	4.6
<b>6</b>	b	5.3	21	74	62	58	16	22	15	64	48	75	22	5.5
	t	5.2	33	72	87	151	19	19	19	145	94	73	33	4.9
<b>7</b>	b	5.7	24	78	64	126	17	25	17	115	91	79	24	5.9
	t	5.6	24	77	69	51	19	20	18	55	67	77	24	5.3
<b>8</b>	b	6.1	24	82	60	57	16	26	15	64	47	82	24	6.3
	t	6.1	28	77	70	161	19	23	19	169	75	74	28	5.8
<b>9</b>	b	6.8	24	68	57	101	19	27	18	99	76	70	24	7.0
	t	6.9	25	63	60	50	20	23	19	54	59	62	25	6.6
<b>10</b>	b	7.9	26	56	54	54	16	29	16	60	44	54	26	8.0
	t	8.3	27	51	60	122	21	28	20	137	66	48	27	7.8
<b>11</b>	b	10	25	48	51	71	17	29	17	69	65	45	25	10
	t	12	27	46	48	62	22	25	21	68	47	43	27	11
<b>12</b>	b	16	25	35	32	48	14	29	14	53	30	34	25	16
	t	21	23	22	35	54	23	34	22	56	38	21	23	20

**Table 6.9:** Spacing (inches) on each wall line on each story, top and bottom, for load case 7 in the x-direction

Story		X1	X2	X3	X4	X5	X6	X7	X8	X9	X10	X11	X12	X13
<b>1</b>	b	3.9	40	70	75	121	20	11	20	112	84	70	40	4.2
	t	3.5	35	73	76	109	20	9.4	19	121	74	42	34	3.4
<b>2</b>	b	3.8	30	473	63	163	18	12	17	147	58	41	29	3.9
	t	3.8	41	778	78	206	21	11	20	230	83	42	40	3.6
<b>3</b>	b	4.1	38	160	87	163	17	18	17	154	93	78	40	4.3
	t	4.1	30	141	110	113	20	15	19	135	109	48	31	3.9
<b>4</b>	b	4.5	28	90	80	112	16	17	16	133	68	37	29	4.7
	t	4.4	41	85	102	180	19	16	19	172	105	91	43	4.2
<b>5</b>	b	4.8	35	75	91	163	17	27	16	151	119	77	36	5.0
	t	4.7	25	72	94	83	18	19	18	94	92	75	26	4.5
<b>6</b>	b	5.1	25	71	79	90	15	23	15	100	67	72	26	5.3
	t	5.0	36	70	88	165	19	23	18	163	93	70	37	4.8
<b>7</b>	b	5.5	35	74	69	137	17	36	16	128	83	75	37	5.7
	t	5.4	24	73	83	74	18	23	18	82	84	74	25	5.2
<b>8</b>	b	6.1	25	84	73	83	15	27	15	93	64	85	26	6.3
	t	6.0	35	76	73	146	19	30	19	151	77	75	36	5.7
<b>9</b>	b	6.8	33	69	60	122	18	40	18	117	69	72	34	7.0
	t	6.8	25	64	70	69	19	25	19	76	71	64	25	6.5
<b>10</b>	b	7.8	27	59	64	76	16	31	16	86	60	57	28	8.1
	t	8.2	34	53	62	135	20	36	20	142	68	52	35	7.8
<b>11</b>	b	10	32	52	52	88	18	41	18	87	59	50	33	10
	t	11	28	51	56	84	21	27	21	88	57	48	28	11
<b>12</b>	b	16	27	41	38	68	15	29	15	75	38	40	27	16
	b	20	28	28	38	66	23	46	22	69	41	26	28	19

**Table 6.10:** Spacing (inches) on each wall line on each story, top and bottom, for load case 5 in the y-direction

Story		Y1	Y2	Y3	Y4	Y5	Y6	Y7	Y8	Y9
<b>1</b>	b	4.3	22	8.6	21	19	21	8.6	22	4.3
	t	4.3	22	11	18	18	18	10	22	4.3
<b>2</b>	b	4.4	15	15	26	17	26	15	15	4.4
	t	4.4	15	16	26	17	26	16	15	4.4
<b>3</b>	b	4.4	14	20	26	17	26	20	14	4.4
	t	4.4	14	20	26	17	26	20	14	4.4
<b>4</b>	b	4.5	14	22	26	17	26	22	14	4.5
	t	4.5	14	22	26	17	26	22	14	4.5
<b>5</b>	b	4.6	14	23	27	16	27	23	14	4.6
	t	4.6	14	22	27	16	27	22	14	4.6
<b>6</b>	b	4.9	15	24	28	16	27	24	15	4.9
	t	4.9	15	23	28	16	28	23	15	4.9
<b>7</b>	b	5.3	16	25	30	17	30	25	16	5.3
	t	5.3	16	24	30	17	30	24	16	5.3
<b>8</b>	b	5.8	18	28	33	18	33	28	18	5.8
	t	5.8	18	27	34	18	34	26	18	5.8
<b>9</b>	b	6.6	21	33	41	21	41	33	20	6.6
	t	6.6	20	30	42	21	42	30	20	6.6
<b>10</b>	b	7.9	25	40	62	28	62	40	25	7.9
	t	7.9	25	35	64	28	63	35	25	7.9
<b>11</b>	b	11	33	44	110	36	109	44	33	11
	t	11	33	45	138	44	138	45	33	11
<b>12</b>	b	21	53	35	156	43	156	35	53	21
	b	21	51	45	109	46	108	45	51	21

**Table 6.11:** Spacing (inches) on each wall line on each story, top and bottom, for load case 7 in the y-direction

Story		Y1	Y2	Y3	Y4	Y5	Y6	Y7	Y8	Y9
<b>1</b>	b	4.2	23	12	26	20	26	12	23	4.2
	t	4.2	23	12	26	20	26	12	23	4.2
<b>2</b>	b	4.2	15	18	28	18	28	18	15	4.2
	t	4.2	15	18	29	18	29	18	15	4.2
<b>3</b>	b	4.3	14	22	28	18	28	22	14	4.3
	t	4.3	14	22	28	18	28	22	14	4.3
<b>4</b>	b	4.4	14	23	28	17	28	23	14	4.4
	t	4.4	14	23	28	17	28	23	14	4.4
<b>5</b>	b	4.6	15	23	27	16	27	23	15	4.6
	t	4.6	15	23	27	16	27	23	15	4.6
<b>6</b>	b	4.9	15	23	27	16	27	23	15	4.9
	t	4.9	15	23	27	16	27	23	15	4.9
<b>7</b>	b	5.3	17	25	28	16	28	25	17	5.3
	t	5.3	17	25	28	16	28	25	17	5.3
<b>8</b>	b	5.8	18	27	32	17	32	27	18	5.8
	t	5.8	18	27	32	17	32	27	18	5.8
<b>9</b>	b	6.7	21	32	39	21	39	32	21	6.6
	t	6.7	21	32	39	21	39	32	21	6.6
<b>10</b>	b	8.1	25	36	58	28	58	36	25	8.1
	t	8.1	25	40	59	28	59	40	25	8.1
<b>11</b>	b	11	32	45	130	47	130	45	32	11
	t	11	32	53	136	47	136	53	32	11
<b>12</b>	b	22	54	47	292	79	292	47	54	22
	t	22	46	85	174	128	174	85	46	22

	15	59	-5	7	-24	7	-25	28	14	
→	15	36	-6	56	-95	9	-49	22	24	
→	43	39	-8	13	-108	7	-28	27	44	
→	49	36	-9	32	-115	61	19	24	74	
→	31	34	-10	51	-128	106	51	21	100	
→	17	32	-8	69	-141	135	81	18	121	
→	17	32	-5	89	-151	160	105	19	140	
→	17	30	-3	110	-156	178	128	19	157	
→	18	27	1	140	-157	191	148	20	176	
→	18	25	10	185	-149	200	167	20	201	
→	18	25	37	234	-126	208	184	20	233	
→	18	20	106	310	-96	198	172	19	282	
→										
□	TOTAL	275	390	101	1295	-1446	1460	953	258	1566
	ABS TOTAL	275	397	208	1295	1446	1460	1156	258	1569

Figure 6.10: Panel connection shears (in kips) at each interface for load case 5.

12	→	5	49	-23	1	-17	3	-21	33	3
		7	32	-23	2	-84	4	-42	24	12
11	→	10	40	-25	2	-101	4	-16	29	26
10	→	20	38	-27	2	-117	33	28	26	60
9	→	7	35	-27	4	-133	57	64	24	85
8	→	7	33	-28	7	-145	74	89	24	107
7	→	7	32	-28	14	-153	87	110	25	127
6	→	8	26	-27	19	-159	95	129	25	144
5	→	8	23	-26	31	-159	97	144	25	162
4	→	9	22	-25	62	-150	92	150	25	183
3	→	9	21	-23	123	-128	76	135	24	216
2	→	7	15	-3	216	-81	58	71	21	275
1	→									
TOTAL		102	364	-287	483	-1428	679	841	305	1399
ABS TOTAL		105	369	288	483	1428	679	999	306	1400

**Figure 6.11:** Panel connection shears (in kips) at each interface for load case 7.

## **CHAPTER 7**

### **CONCLUSION AND NEXT STEPS**

The study succeeded in proposing a simplified mechanistic design method including a new global overturning resistance system, as well as assessing the feasibility through the use of numerical modeling software. The global overturning system has potential based on the explainable results of the numerical analysis, however the potential is currently capped by the limits of numerical modeling software. The system level response seems reasonable, but the model does not fully capture the load resisting mechanism of the proposed system.

The most important part of the global overturning system is the use of a shear connection and CLT walls and panels to transfer the shear across the building. The small shear forces in the shear connections demonstrate that the shear connections are theoretically able to transfer the shear forces through every cross-section of the building, meaning ATS rods will only be necessary at the exterior of the building, thus showing the potential of a global overturning resistance system.

#### **7.1 Feasibility**

This study outlined a complete structural design process for a tall CLT building in a seismic region following the ASCE 7 ELFP method using an assumed R-factor. Numerically, the simplified design procedure was reasonable, including many conservative assumptions to ensure adequate strength and redundant load paths, however further experimental work such as large scale dynamic tests should be done to validate the design.

The fact that strength does not control gravity loading shows the strength of CLT in vertical loading applications, and the fact that vibration controls the floor design reinforces the idea of using CLT for primarily residential construction.

The use of an anchor tie-down system to resist global overturning, instead of the traditional stacked shear wall approach, will save money on material cost, construction time and complexity, and detailing and design time.

The design of a 12-story building for seismic coefficient as large as those present in Los Angeles is an ambitious goal, but the general feasibility of the design is even more promising for similar building in lower-seismic areas, or for high-seismic areas with lesser heights.

## **7.2 Drawbacks and Obstacles**

Realistically, a tall CLT building could not be built without approval from local jurisdiction. Currently there is no seismic force modification factor accepted in ASCE 7 for this type of construction. Lack of complete seismic design provision in the code framework remains the largest road block for CLT building seismic design. For its implementation, the fire regulation on tall timber buildings has not been developed yet. Currently, there are only two CLT manufacturers in the United States. Additionally, contractors, designers, and the public have less experience with CLT than other building materials, which makes it more difficult to take on projects. As CLT experience and usage continues to grow in the United States, as well as the rest of the world, the use of CLT will become a more viable option for residential construction than it already is. In order for CLT to continue to advance in the United States, however, regulations will have to be updated. Currently, many regulations regarding wood are done with timber framing in mind. Because timber framing has different strengths and drawbacks than CLT, CLT construction ends up being severely hindered in ways that don't make sense. CLT has recently been adopted into the NDS, which is an important step in developing separate regulations for CLT.

The U.S. Tall Wood Building Competition will serve as a pioneer effort for introducing this new construction practice in the U.S. Although the buildings selected for the competition are likely not going to have similar floorplan configurations as this study, the current study marks the first attempt to design a tall platform CLT building in the U.S. using ASCE 7 methodology.

## REFERENCES CITED

- [1] Green, Michael. "Why We Should Build Wooden Skyscrapers." *TED*. TED Talks, Feb. 2013. Web. Sept 2014.
- [2] *Summary Report: International Tall Wood Buildings*. Issue brief. Comp. Forestry Innovation Investment. Comp. Binational Softwood Lumber Council. May 2014.
- [3] "Technology of CLT-based Wooden Construction." *Lesoteka Hiše*. 2013. Web. 01 Oct. 2015.
- [4] Thompson, Henrietta. *A Process Revealed = Auf Dem Holzweg*. London: Murray & Sorrell, 2009. Print.
- [5] Stone, Jeffrey B., Ph.D., and David P. Tyree, PE, CBO. "Designing for Fire Protection." *ENR* (2015): n. pag. 1 Aug. 2015. Web. 20 Aug. 2015.
- [6] Patterson, Daryl. "Forte - Creating the World's Tallest CLT Apartment Building." *YouTube*. Rethinkwood, 20 Sept. 2013. Web. 18 June 2015.
- [7] "Forte." Victoria Harbour. Dec. 2012. Web. 1 Oct. 2015.
- [8] "Stadthaus Murray Grove." *E-Architect*. 2015. Web. 5 Oct. 2015.
- [9] "Wood Innovation Design Centre / Michael Green Architecture." *ArchDaily*. 19 May 2015. Web. 27 Aug. 2015.
- [10] "Winners Revealed - U.S. Tall Wood Building Prize Competition." *U.S. Tall Wood Building Prize Competition*. ReTHINK WOOD, 17 Sept. 2015. Web. 17 Sept. 2015.
- [11] Ceccotti, Ario, Carmen Sandhaas, Minoru Okabe, Motoi Yasumura, Chikahiro Minowa, and Naohito Kawai. "SOFIE Project - 3D Shaking Table Test on a Seven-storey Full-scale Cross-laminated Timber Building." *Earthquake Engng Struct. Dyn. Earthquake Engineering & Structural Dynamics* 42.13 (2013): 2003-021. Web.

- [12] Pei, S., J. W. Van De Lindt, M. Popovski, J. W. Berman, J. D. Dolan, J. Ricles, R. Sause, H. Blomgren, and D. R. Rammer. “Cross-Laminated Timber for Seismic Regions: Progress and Challenges for Research and Implementation.” *Journal of Structural Engineering J. Struct. Eng.* (2014). Web.
- [13] *SCE / SEI 7-10 Minimum Design Loads for Buildings and Other Structures*. Reston, VA: American Society of Civil Engineers/Structural Engineering Institute, 2013. Print.
- [14] Gagnon, Sylvain, and Ciprian Pirvu. *CLT Handbook: Cross-laminated Timber*. Québec: FPInnovations, 2011. Print.
- [15] “National Design Specification for Wood Construction.” *American Wood Council*. Nov. 2014. Web.
- [16] *AxisVM*. Computer software. *AxisVM*. Vers. 13. 2015. Web.
- [17] “Subject: Connectors for Cross-Laminated Timber Construction.” (n.d.): n. pag. *Strongtie.com*. Simpson Strong Tie Company, Inc, 1 Jan. 2015. Web. 16 Jan. 2015.
- [18] Simpson Strong Tie. *Strong-Rod Systems*. N.p.: Simpson Strong Tie, n.d. *Strongtie.com*. Simpson Strong-Tie, 2015. Web. 5 Oct. 2015
- [19] “ATS: Strong Rod.” *Strongtie.com*. Simpson Strong Tie, 2015. Web. 28 Sept. 2015.
- [20] “U.S. Seismic Design Maps.” *U.S. Seismic Design Maps*. United States Geological Survey, 12 June 2014. Web. 15 Oct. 2015.
- [21] “ANSI/APA PRG 320: Standard for Performance Rated Cross-Laminated Timber.” *ANSI/APA*. APA - The Engineered Wood Association, 2012. Web. 14 June 2015.
- [22] “National Design Specification Design Values for Wood Construction Supplement.” American Wood Council, Nov. 2014. Web. 28 Mar. 2015.
- [23] Ritter, Michael A. “Timber Bridges.” (2011): n. pag. *Woodcenter*. United States Department of Agriculture Forest Service, 1990. Web. Aug. 2015.

- [24] Porteous, Jack, and Abdy Kermani. *Structural Timber Design to Eurocode 5*. Oxford: Blackwell Pub., 2007. Print.